The Relationship Between Mineralogy, Groundwater Chemistry, and Groundwater Flow in the Moreno Hill Formation

Masters Thesis by

Cynthia P. Ardito

Submitted in partial fulfillment of the requirements

for the degree of

Master of Science in Geology

December 1987

New Mexico Institute of Mining and Technology

Socorro, New Mexico

Acknowledgements

Without the advice, assistance, encouragement, and support of many Socorrans whom I have been privledged to know, the completion of this thesis would not have been possible. I wish to thank my advisory committee for their technical assistance, as well as the State Mining and Mineral Resource Institute for their financial support.

As students of New Mexico Tech, we are fortunate to have the New Mexico Bureau of Mines and Mineral Resources available to broaden our educational experience. Indeed, I have benefited from this relationship. My sincerest thanks and warmest regards are extended to Frank Campbell, Lynn Branvold, her staff, and George Austin for helping with all my analytical work.

The Salt River Project has been helpful in providing some essential water-quality data for this study, and I would like to especially thank Marcie Greenburg. Bob Myers of New Mexico State University also sent much needed water-quality data which is appreciated. Brian McGurk deserves a special thank you for being a delightful field partner as well as for completing his independent study upon which this thesis is based.

Finally, Tony Zimmerman has been, and continues to be, an essential ingredient in my life. His boundless patience and optimism has proved invaluable in the completion of this study.

ABSTRACT

The Moreno Hill Formation (Cretaceous) is the coal-bearing sedimentary strata of the Salt Lake Coal Field located in west-central New Mexico. The formation is defined by a series of fluvial channels, crevasse-splays, and floodplain deposits expressed as interbedded sandstones, mudstones, and coals.

The effect of weathering on these continental-sedimentary deposits is investigated by comparing differences in the mineralogy of surface and subsurface samples. Results of a point-counting study of the sandstones reveal that surface samples have more total feldspar and porosity while subsurface samples have comparably more epimatrix. Pervasive carbonate cement is characteristic of a few samples. SEM analysis demonstrated that the epimatrix material is composed mainly of kaolinite. The plagioclase feldspars are albite (no calcium (or anorthite component) detected), and many exhibited distinctive dissolution textures. Semi-quantitative analysis in the mudstone samples indicate that Na-smectite and kaolinite are the dominant clay groups. Kaolinite is more abundant in the subsurface mudstone samples located above the coal zones.

Groundwater chemistry analyses are compared to distances along a flowpath (DAF). Sodium and bicarbonate concentrations increase with DAF, and these data are

strongly correlated. Calcium and magnesium concentrations decrease and sulfate concentrations increase with DAF, but correlation is poor. The concentration of dissolved silica is quite variable, yet samples in a recharge area had the highest values for this constituent.

Based on available mineralogic data and observable trends in groundwater chemistry evolution, governing reactions are assumed and applied to a geochemical reaction model employing the mass balance approach developed by Plummer (1984). Mass transfer calculations were performed using the computer program BALANCE (Parkhurst, et al., 1982). Speciation data were obtained from WATEQF (Plummer, et al., 1984). Results of the reaction modeling predict precipitation of calcite, dissolution of dolomite and gypsum, cation exchange, and an increase in dissolved carbon dioxide. The effects of feldspar weathering on the evolution of groundwater in this system are not adequately addressed by the mass balance approach.

A conceptual geochemical model is developed which describes the various pathways towards evolution of Na-HCO_3 groundwater in the Moreno Hill Formation. Governing reactions in this system include albite weathering to kaolinte, the breakdown of organic material to produce carbon dioxide, cation exchange, dissolution of gypsum formed by the oxidation of pyrite, and carbonate mineral equilibria. The weathering of feldspars is the dominant pH-controlling reaction in the system.

TABLE OF CONTENTS

Plates and Figures

Tables

INTRODUCTION

Weathering, in the strict sense of the word, constitutes the combined effects of the atmosphere, hydrosphere, and the bioshpere on rock or earth materials at or near the surface of the earth. This study explores a specific aspect of this geologic phenomenon, namely rock-water interactions and their combined effects on the evolution of groundwater chemistry. By studying the relationship between the mineralogy of surface and subsurface rock samples from comparable units within the same formation, and sampling groundwater at various points along an interpreted flowpath in order to compare major ion chemistries, it is possible to gain partial understanding of these processes. Major areas of interest to which this research is aimed, in an attempt to gain better understanding of extremely complicated and multivariant natural processes, include the following:

1) The effects the processes of weathering have on the the composition of sandstones, mudstones, and coals.

2) Water-rock interactions and how these processes are reflected in the natural environment, specifically with respect to changes in mineralogy and

groundwater chemistry.

3) The relationship between groundwater chemistry and groundwater flow.

The ultimate goal of this study is to define a geochemical model which integrates the above concepts into a description of the evolution of groundwater chemistry in the Moreno Hill Formation as a result of weathering processes.

METHODS OF INVESTIGATION

Drilling, lithologic core recovery, and ultimate coal analysis have been completed by the New Mexico Bureau of Mines and Mineral Resources (NMBM&MR) in 18.25-mi^2 of the Salt Lake Coal Field, west-central New Mexico (Figure 1). The coal-bearing lithologic unit in this area is the Moreno Hill Formation (Cretaceous). Cores which bound and include coal seams within this formation were available for study. Seventeen samples of this core, taken above, below, and within the coal zones, were obtained for compositional analysis. A comparable number of surface samples was collected at sites of coal-seam outcrops from stratigraphically related positions. In areas where core was available, but there are no surface exposures of coal, samples of sandstones and shales were collected to assess lateral variations within the formation, and possible geochemical effects on mineralogy resulting from the presence or absense of coal. The lack of continuous

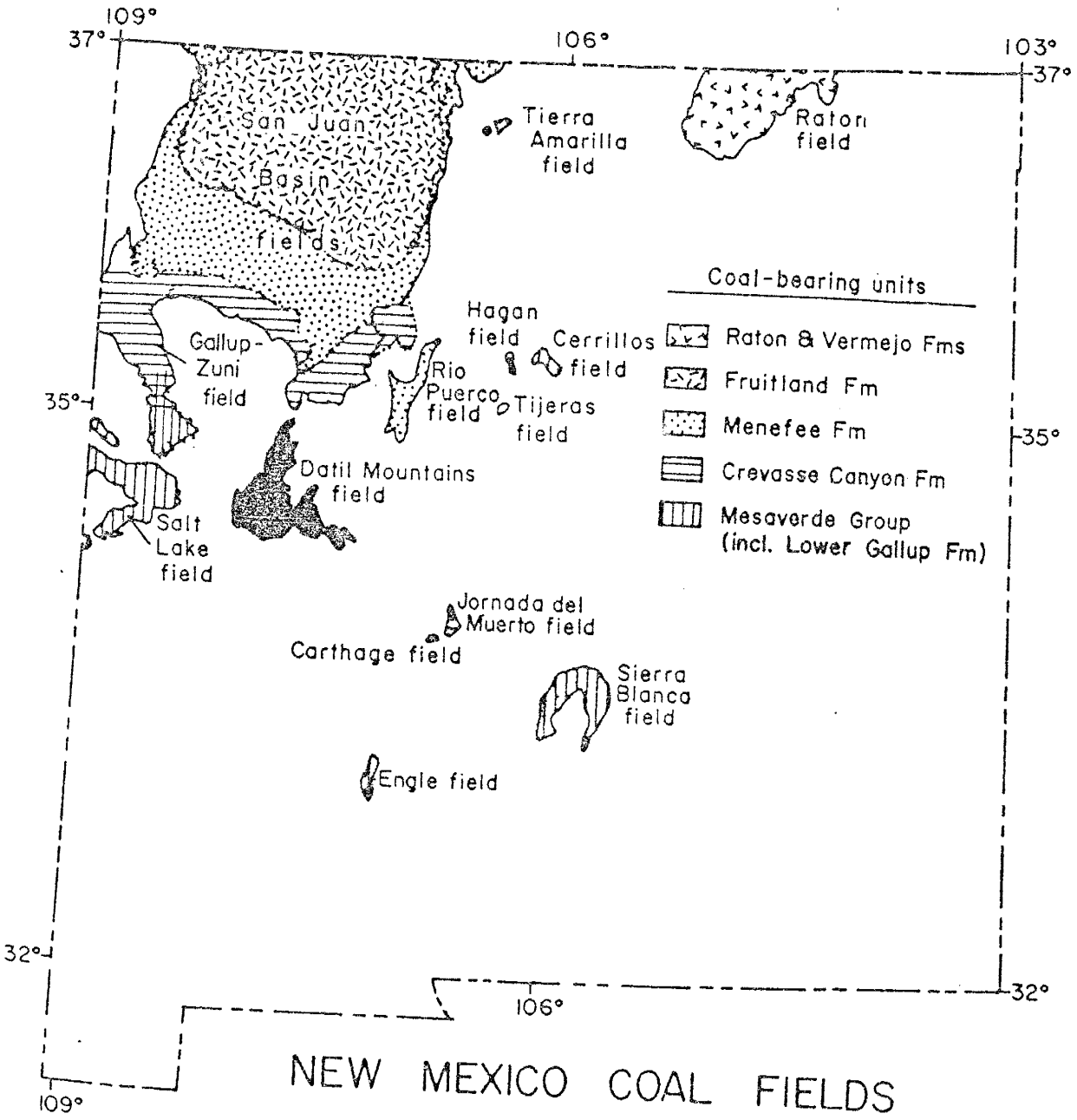

Figure 1. Location map for the Salt Lake Coal Field

RM-10. Coal fields and mines of New Mexico by D. E. Tabet and S. J. Frost, 1978, scale 1:1,000,000

sections of core placed limits on the total number of samples available for analysis.

Standard methods were employed for the compositional analysis of stratigraphic units within the Moreno Hill Formation. The relative proportion of clay mineral groups in the clay size fraction of the mudrocks is based on X-ray diffraction analyses. The diffractograms were analyzed following a method developed by George Austin of the NMBM&MR which is described in Chapter 3. Thin sections of surface and subsurface sandstone samples were counted until 400 grains had been identified. In this way, variations in grain mineralogies, cement mineralogies and textures, matrix types, and pore types and their origins are reliably estimated. Details of this aspect of the study are discussed in Chapter 3.

Water-chemistry data were obtained from the United States Geological Survey (USGS), the NMBM&MR, and the Salt River Project (SRP) of Phoenix, Arizona. During a routine monitor well sampling by SRP in August, 1986, nine wells were split-sampled for major ion chemistry. The analyses were performed at New Mexico Institute of Mining and Technology (NMIMT) under the guidance of Lynn Branvold. All water-chemistry analyses selected for use in this study had the same characteristics: 1) samples are from wells completed in the Moreno Hill Formation, 2) samples are from wells located witin the bounds of the study area, and 3)

samples have ion balances with less than 5% analytical error. A few samples were included from wells completed in the alluvium. Water-chemistry data are discussed in Chapter 4.

Geochemical reaction modeling is presented in Chapter 5. Through the use of the computer models WATEQF (Plummer, et al., 1984), which performs speciation calculations, and BALANCE (Parkhurst, et al., 1982), which performs mass transfer calculations, a reaction model was developed. This model is supported and challenged based on the mineralogy of the Moreno Hill Formation.

As discussed in Chapter 2, hydrogeologic data for the Moreno Hill Formation were obtained from McGurk and Stone (1986). Their study provided the background information necessary for conceptualization of groundwater chemistry evolution.

PREVIOUS WORK

Background data necessary for the developement of this study involve information gained from three separate disciplines; mineralogy, hydrology, and low-temperature geochemistry. An attempt to try and cover relevant previous work in all three of these fields is impossible; however, reports on studies similar to this one were consulted:

Foster (1950) studied the origin of Na-bicarbonate waters in the Atlantic and Gulf Coastal Plains. The intent

of her study was to find an explanation for the high concentrations of bicarbonate charateristic of deeper waters. Ms. Foster found that shallow waters in the water-bearing sands of the coastal plains were composed predominately of calcium and bicarbonate, while deeper waters in the same formation had sodium and bicarbonate as major dissolved constituents. The presence of base-exchange minerals and the process of cation exchange were used to explain the differences in cation composition between the shallow and deep waters; however, an explanation for bicarbonate concentrations of up to several hundred parts per million in the deep water samples remained a problem.

As is well known, $_{C}aCO3$ is much more soluble in the presence of CO_2 owing to the formation of bicarbonate. Foster (1950) reasoned that one source of high CO_2 in this area could be the chemical or biochemical reduction of sulfate by carbonaceous material which causes the liberation of carbon dioxide. However, all waters tested were low in sulfate and there was no noticeable increase in sulfate with lower bicarbonate content. Therefore, a conclusion was drawn that the high CO2 content in these waters stemmed from dynamochemical processes (or the progressive elimination of volatiles from coal by chemical and physical changes such as shear stress). Organic materials consist of large unstable molecules which are easily affected by natural processes. From peat and lignite, the dominant gases evolved are the

oxides, water, and carbon dioxide. As this process would indeed contribute high concentrations of CO_2, and as Ca is removed in exchange reactions with Na, excessive bicarbonate could remain in solution.

Laboratory tests were conducted which illustrated that in order to produce waters of high Na-HCO3 content from waters of high Ca-HCO3 content three parameters are necessary; 1) the presence of CaCO3, 2) base-exchange minerals, and 3) carbonaceous material.

Bricker and Garrals (1967), presented an interesting study of the relationship between mineralogy and natural-water equilibria. Most important to this study is their discussion of the silicate mineral phase and its control on the equilibrium of several important dissolved constituents. The foundation of their conclusions is based on the assumption that silicate minerals, considered as bulk phases, are rapidly reactive.

Mass balance calculations illustrated the liklihood that the silica content of most natural waters is derived from the weathering of silicate minerals, chiefly the feldspars, and not from quartz or amorphous silica as might be expected. Bricker and Garrels (1967) conceptulaized th process of feldspar weathering. When waters high in CO2, but low in cations and silica, encounter silicate minerals, both these consituents are leached and aluminosilicate residue, such as kaolinite, is left behind. As these waters

continue to alter the mineral, the pH of the solution rises, the concentrations of cations and silica increase, and kaolinite is precipitated. When concentrations of silica (silica saturation in natural waters occurs at 60 mg/l; Hem, 1985) and cations become very high, then montmorillinite begins to form.

Bricker and Garrels (1967) concluded that at any stage in the weathering of a feldspar grain, the solution is in equilibrium with kaolinite or montmorillonite, and not feldspar. Reactions of feldspars with water are so fast that near-equilibrium with one or more silicate phases is at all times achieved. Silica concentrations plotted against ratios of cations to H+ were shown to have certain genetic patterns due to the control of silicate minerals on equilibrium states of some constituents.

Finally, Bricker and Garrels (1967) concluded that, as the weathering of feldspars consume CO_2, and because reduction of CO_2 concentration is the chief buffering process of many natural waters, silicate minerals as well as carbonate equilibria must be considered in terms of controls on the chemistry of natural waters.

In a later study by Bricker and Godfrey (1968), this emphasis on silicate equilibria was taken to the field to study the concept of groundwater evolution. As silicate minerals consitute approximately 95% of the earth's crust, they concluded that most natural waters will, during the

course of the hydrologic cycle, react with silicate minerals resulting in alteration or transformation of these minerals. Water is the primary agent of rock weathering, and silicate minerals are shown to play an important role governing the composition of natural waters.

To illustrate these ideas, Bricker and Godfrey (1968) chose a small wooded watershed where they were able to have tight control on the process of groundwater evolution. Most importantly, all waters draining this small basin, were known to originate as precipitation in the watershed. The bedrock in the area is pelitic schist which consists predominately of silicate minerals. The overall weathering relationship for the chosen system was illustrated as follows:

Primary alumino-silicates + H_2O + CO_2 = Aluminum-rich solids + Alkali cations + Alkaline earth cations + $HCO_3^-(aq)$ + $H_4SiO_4(aq)$

Bricker and Godfrey (1968) completed chemical analyses of rain, stream, and soil-water samples. It was observed that the chemical composition of the stream varied little over the course of a year. No aluminum was found in the rain water samples and little was found in the stream samples. The Al/SiO_2 ratio was 5.0E10-03. Because of this it was assumed that aluminum remained conserved as a solid

pahse in all weathering reactions. Their data showed that kaolinite was the stable weathering product in all samples analyzed as illustrated through stability diagrams.

Because of the small magnitude and short duration of the compositional variation of the stream samples in flood and baseflow stages, the authors concluded that water-silicate reactions are quite rapid. Through back-reactions and mass balance calculations, they found that the weathering of oligoclase was the source of most of the dissolved constituents in stream waters. Biotite was shown to contribute some of the silica, potassium, and magnesium.

Garrels and MacKenzie (1967) studied the composition of ephemeral and perennial springs in the Sierra Nevada. Many of the conclusions they arrived at are similar to the studies previously described. Having great success in reconstructing original mineral compositions form observed water compositions, their conclusions are summarized as follows:

1) Dissolved silica in the groundwater comes from the breakdown of silicates with minor amounts coming from the direct solution of quartz. The silica in the water represents CO_2 changed to HCO3 through the process of weathering.

2) Waters gain much of their dissolved silica in the first few feet of travel along a flowpath.

Aggressive waters with high dissolved CO_2 content cause the alteration of feldspars and the production of kaolinite. Rock minerals react continuously to produce kaolinite which in turn controls the composition of water by its presence.

3) 80% of the rock-derived constituents in natural water samples can be accounted for by the breakdown of plagioclase alone.

4) High sodium to potassium ratios in chemical analyses are related to differential weathering of Na-feldspars as compared to K-feldspar rather than to K^+ adsorption. Residual minerals resulting from rock-water interactions are a mixture of quartz, K-feldspar, and kaolinite.

Garrels and MacKenzie (1967) plotted the equilibrium constant of the reaction between montmorillonite and kaolinite vs Na (mg/l). Here it was shown that in deeper circulating waters, montmorillonite will begin to form as these waters will have gained high concentrations of the necessary constituents due to the longer residence time of these waters.

In three separate studies of the geology, hydrology, and hydrochemistry of lignite deposits in North Dakota the

relationship between mineralogy and groundwater chemistry was explored (Moran, et al., 1978a, 1978 and Groenwold, 1981). Since all of these studies are very similar in content to the investigation described in the forthcoming chapters, details of these works will be reserved for comment until Chapter 6 at which point the conceptual geochemical model of groundwater evolution is discussed.

Thorstenson et al. (1979), investigated the geochemistry of the Fox Hills aquifer and attempted to relate the relevant geochemical data to observed groundwater flow in the area. The Fox Hills Sandstone is composed of a lithologic sequence which is quite similar to that of the Moreno Hill Formation. Due also to the many parallels that can be drawn between Thorstenson's paper and this study, further comment is reserved for Chapter 6.

Galen (1982) from the University of Wisconsin described groundwater geochemical evolution in a silicate aquifer. He concluded that groundwater chemistry evolution is governed by three processes; 1)residence time, 2) relative rates of silicate mineral dissolution, and 3) the presence or absence of carbonate minerals.

Chapelle (1982) studied the geochemical evolution of groundwater in the Aquia Aquifer of Maryland. This aquifer consists of glauconitic quartz sandstone. He constructed stoichiometric chemical models for three regions of this aquifer where water chemistries appeared to be very

different.

Through mass balance calculations, Chapelle (1987) hoped to predict where calcite was likely to occur in the system. Using the same computer programs employed for this study, WATEQF and BALANCE, he showed that mass balance calculations were able to accurately predict where calcite would tend to dissolve or precipitate in the system. The calculations were tested by correlation with the saturation indices for this mineral, and by field observation of calcite in the formation.

Powell and Larson (1985) described the relationship between groundwater quality and mineralogy in a coal-producing formation. The Norton Formation of Buchanan County, Virginia consists of flat-lying beds of sandstone, siltstone, shale, clay, and coal, very similar to the Moreno Hill Formation. Powell and Larson discussed in greater detail, relative to other studies, the geochemical modeling aspects of groundwater chemistry evolution. Many parallels may be drawn between their approach and this one.

Velbel (1985) provided a particularly interesting look at groundwater chemistry evolution through the use of activity diagrams. In his paper, he suggested that the composition of deep weathering waters are not controlled by equilibrium achieved between groundwater and the weathering products of minerals, but by the relative rates of dissolution, precipitation, and water movement through the

deep weathering zone. In effect, his is a nonequilibrium, kinetic approach to groundwater chemistry evolution.

Velbel's study was conducted in the forested watersheds of the southern Blue Ridge Mountains. Both major lithostratigraphic units in this area are dominately metagraywackes with pelitic schists and metavolcanic rocks. Velbel found, when parameters from water smaples of the same area were plotted over time, there were increases in average pH and concentrations of most major cations in concert with an increase in average discharge rate. These trends suggested to Velbel that, as more water is flushed through a unit volume of watershed per unit time, the chemical weathering reactions by which cations are added to solution do not proceed as far. In other words, there seemed to be an important relationship between rates of percolating solutions and weathering reactions.

Velbel described groundwater chemistry evolution as "a dilute solution acquiring solutes by the weathering of primary silicate minerals would evolve toward thermdynamic equilibrium by acquiring alkalis, alkaline earths, and silica, and losing hydrogen". This evolution was illustrated by an activity/activity diagram on which a path from the lower left (dilute, acidic) to the upper right (cation-rich, acid-depleted) section of the diagram is shown. When he plotted his data an activity/activity diagram, it was evident that slowly-flushed systems are able

to evolve to a state closer to thermodynamic equilbrium than rapidly flushed systems. Velbel's paper emphasized the importance of reaction rates to the understanding of groundwater chemistry evolution.

A classic paper by Palmer and Cherry (1984/85) presents concepts fundamental to the study of rock-water interactions and the geochemical evolution of groundwater. They focused their research for this paper on changes occurring in groundwater chemsitry as a flowpath is lengthened an as variuos mineralogies are encountered. Their use of a variety of hypothetical examples involving differing stratigraphic sequences illustrates the importance of the sequence of minerals encountered by groundwater as it moves along a flow path.

Palmer and Cherry (1984/85) introduce their ideas by pointing out that, traditionally, hydrogeologists regard the major-ion chemistry of groundwater as being controlled primarily by time and distance traveled as illustrated by Chebatorev (1955). Here it is shown that as groundwater chemistry develops, the relative abundance of anions evolve according to the following sequence:

$$HCO_3^- = HCO_3 + SO_4^{2-} = SO_4^{2-} + HCO_3^- = SO_4^{2-} + Cl^- = Cl^-$$

Palmer and Cherrys (1984/85) showed that this relationship is not always valid.

Palmer and Cherry used a geochemical mass transfer model, WATEGM-SE, to illustrate hypothetical examples of how groundwater chemistry evolves along a flowpath through differing sequences of sedimentary rocks. Their emphasis was on how certain parameters, such as temperature, pressure, soil gas, and the sequence of mineral assemblages encountered, can affect the geochemistry of groundwater.

The results of their study clearly indicate that the anion compostition of groundwater will not always follow the Chebatorev sequence described earlier. Their simulations illustrated the importance of considering mineral assemblages and the order the assemblages are encountered. Though their hypothetical examples and the conclusions they draw about specific sequences can not be directly transferred to a field situation, the excercise serves to point out the importance of undertstanding the mineralogy of the aquifer when trying to draw conclusions about groundwater chemistry evolution.

The problems encountered when trying to translate their work to a field situation are instructive. Two assumptions used in their work, instantaneous reaction-rate equilibria and pure mineral assemblages, are not realistic when considering the natural environment. As they point out, solution equilibria with calcite can be as long as 16 days while reaction rates of silicate minerals can be even slower or never achieved due to the formation of secondary

minerals. They suggested that these secondary minerals tend to isolate the priamry mineral from solution. Also, reactive minerals, that may have a very important influence on the geochemical evolution of groundwater, may only constitute a small portion of the total rock mass. For example, only 0.13 wt.% is required to cause saturation of water initially devoid of calcium and sulfate, while only 1 wt.% calcite is needed to saturate water under a constant p_{CO2} of 10^{-2} bar.

Palmer and Cherry concluded that though there are serious limitations (many of which are not discussed here) to this approach, equilibrium-based mass transfer models offer a means fro evaluating hyptheses pertaining to the geochemical evolution of groundwater along a flowpath. Most importantly, the sequence of minerals encountered by groundwater as it moves through the system can have a profound effect on the resulting chemistry of discharge waters.

REGIONAL SETTING

The topography of the study area consists of broad, flat alluvial valleys occasionally separated by mesas with gently sloping tops and areas of rugged upland country (Plate 1). Steep escarpments rise abruptly from the alluvial floor to heights of as much as 400 ft. Generally, the land surface rises gradually in an easterly direction.

The climate in this area is arid to semiarid with annual precipitation at Quemado and Fence Lake usually varying between 9 and 15 inches (McGurk and Stone, 1986). Up to half of this precipitation occurs in thunderstorms during the summer months. The annual precipitation increases approximately 4 inches for every 1000 ft of elevation. Potential evapotransporation can be as much as 3 times the annual precipitation at 31.04 inches.

MORENO HILL FORMATION

The Moreno Hill Formation (Cretaceous) consists of coal-bearing continental sedimentary rocks. A series of fluvial channel-fills, crevasse splays, and floodplain deposits compose the strata of this formation which has been subdivided into three informal members: the lower, middle, and upper. The type section for this unit is located in Sec. 7, T4N, R18W (Campbell and Roybal, 1984).

The lower member of the Moreno Hill Formation is

dominated by fluvial sandstones and associated crevasse-splay deposits, dark-gray mudstones, claystones, and coal seams. Sandstone units are not correlative between well logs, but are present in all wells that have penetrated this lower member. Campbell and Roybal (1984) concluded that this laterally discontinuous distribution of sandstones is indicative of a meandering stream deposit. Mineable coal seams are found in two zones. The Rabbit Zone is located approximately 60 ft below the base of the middle member. The Cerro Prieto Zone lies roughly 150-200 ft below the Rabbit. The lower member can be as thick as 440 ft. Sedimentary and groundwater samples analyzed and discussed in this study are all from this member.

The middle member consists of a sandstone sequence with coarse sands which are friable, have little matrix, and a grain-supported texture. This member is distinguishable, and therefore serves as an excellent marker bed, because of its pinkish-yellow color and its erosion-resistant, ledge-forming morphology. Sedimentary structures include trough and planar crossbeds. Thickness of this unit ranges from 28 to 80 ft.

The upper member consists of greenish-yellow to light gray mudstones and claystones with a few channel sandstones. There are carbonacous shale beds and a few thin coal seams. The few sandstone beds have high silt and clay contents, are poorly cemented, and are easily erodable. The thickness of

this member varies from 250 to 761 ft.

The contact of the Moreno Hill Formation with the underlying Atarque Formation is sharp. The Atarque Sandstone is a regressive marine strandline deposit. The lower portion of the Atarque has a higher silt and clay content than the rest of the formation. The Atarque is in turn underlain by a thick marine deposit, the Mancos Shale.

Unconformably overlying the Moreno Hill Formation in the Fence Lake area is the Fence Lake Gravel (Tertiary). It consists mainly of lenses of calcareous sandstone and conglomerate. The formation conspicuously caps the higher mesas and ridges. Its contact with the underlying Moreno Hill Formation is sharp.

The Moreno Hill Formation has experienced little in the way of structural deformation. Major features consist of regional and local faulting. A few major faults have been mapped in the vicinity of State Highway 32 (Campbell and Roybal, 1984). Regional displacement is on the order of a few feet while the regional dip is 3 to 5 degrees to the southeast. These strata were uplifted slightly during the Laramide Orogeny (Cather and Johnson, 1984) and the gentle dips are locally interrupted by folds and flexures associated with Cenozoic volcanism. Cerro Prieto, a prominant land feature, is a volcanic dome originating during this period of volcanism; other similar domes exist in the area.

One interesting feature in this area is a northeast trending zone of high-angle normal faults and volcanic structures located in the south central portion of the Nation's Draw area (Plate 1) (McGurk and Stone, 1986). This feature has been named the Tejana Mesa Fault Zone and has been structurally related to the Jemez lineament described by A. W. Laughlin et al, 1979. A major fault in this zone extends from Tejana Mesa northeast across Hubbel Draw to Section 28, T4N, R15W. It is responsible for up to 250 ft. of stratigraphic displacement. There may be other faults associated with this system. The Nation's Draw valley may be the surface expression of this faulting. In this area, groundwater flow may be structurally controlled.

HYDROGEOLOGY

The study area is part of the Carrizo Wash watershed which feeds into the Little Colorado River north of St. John's Arizona (McGurk and Stone, 1986). Surface flow in this area is in the form of intermittent streams. Domestic and stock water come primarily from groundwater in the alluvial fill of the valleys and from the Moreno Hill Formation. Perched aquifers occur in the mesas and provide a limited source of water from springs and wells. The regional water table ranges in depth from 20 ft, in the western valleys of the major draws, to as much as 900 ft, as measured in wells located on the Mariano and Tejana

Mesas.

Though the Moreno Hill Formation does not constitute a confined aquifer, hydraulically isolated from other water-bearing formations, the following discussion of hydrogeology and hydrogeochemistry will focus on this formation due to a lack of hydrologic and hydrochemical data for the other formations. For reasons which will be given later, it is believed that the hydrogeochemical processes at work within the lower member of the Moreno Hill Formation exert a dominant control on the groundwater chemistry as a result of water-rock interactions within this formation. The upper and middle members of this formation are above the regional water table in the study area.

Hydraulic conductivity and transmissivity measurements estimated by various pumping and slug test methods for the alluvium and the Moreno Hill Formation were tabulated by McGurk and Stone (1986). These data are quite variable for the alluvium, with hydraulic conductivities ranging from 0.32 ft/day to 19.45 ft/day, and averaging 9.37 ft/day. For the coal units within the Moreno Hill Formation, hydraulic conductivities range from 0.2 ft/day to 4.7 ft/day, averaging 1.6 ft/day. Values for sandstone units above the coal beds range from 0.02 ft/day to 22.4 ft/day, averaging 4.23 ft/day. For sandstone units below the coal these values range from 0.1 to 13.4 ft/day.

By gathering a multitude of water level measurements

and drawing a contour map of these data, McGurk and Stone (1986) demonstrated that the potentiometric surface mimics the topography in this area. The shallow groundwater flow pattern follows the surface drainages and divides with groundwater flow being towards the major draws. Recharge areas are located along slopes, in the upper reaches of arroyos, and on the mesas. Discharge areas occur in the downstream portions of major draws and in localized areas where permeability variations influence flow conditions, such as in areas of perched aquifers. The Nation's Draw and Largo Creek Draw are considered to be two separate groundwater basins.

Areal recharge rates are very low due to fine-grained deposits, low annual rainfall, and high evaporation rates (Stone, 1984). These rates are estimated to be 0.05 in/yr in the alluvium and 0.08 in/yr in the bedrock. Estimates for soil-water age at the base of the unsaturated zone are on the order of thousands of years.

Figure 2 depicts the generalized flow pattern for the area where groundwater chemistry evolution is examined. Actual flow patterns in the Moreno Hill Formation are much more complex due to the extreme heterogeneity of the formation. However, upward flow from underlying formations is not a complicating factor due to the extremely low permeability and thickness of the Mancos Shale Formation which lies below the Moreno Hill. Lenses of higher

hydraulic conductivity within the formation do cause localized areas to have vertical flow components.

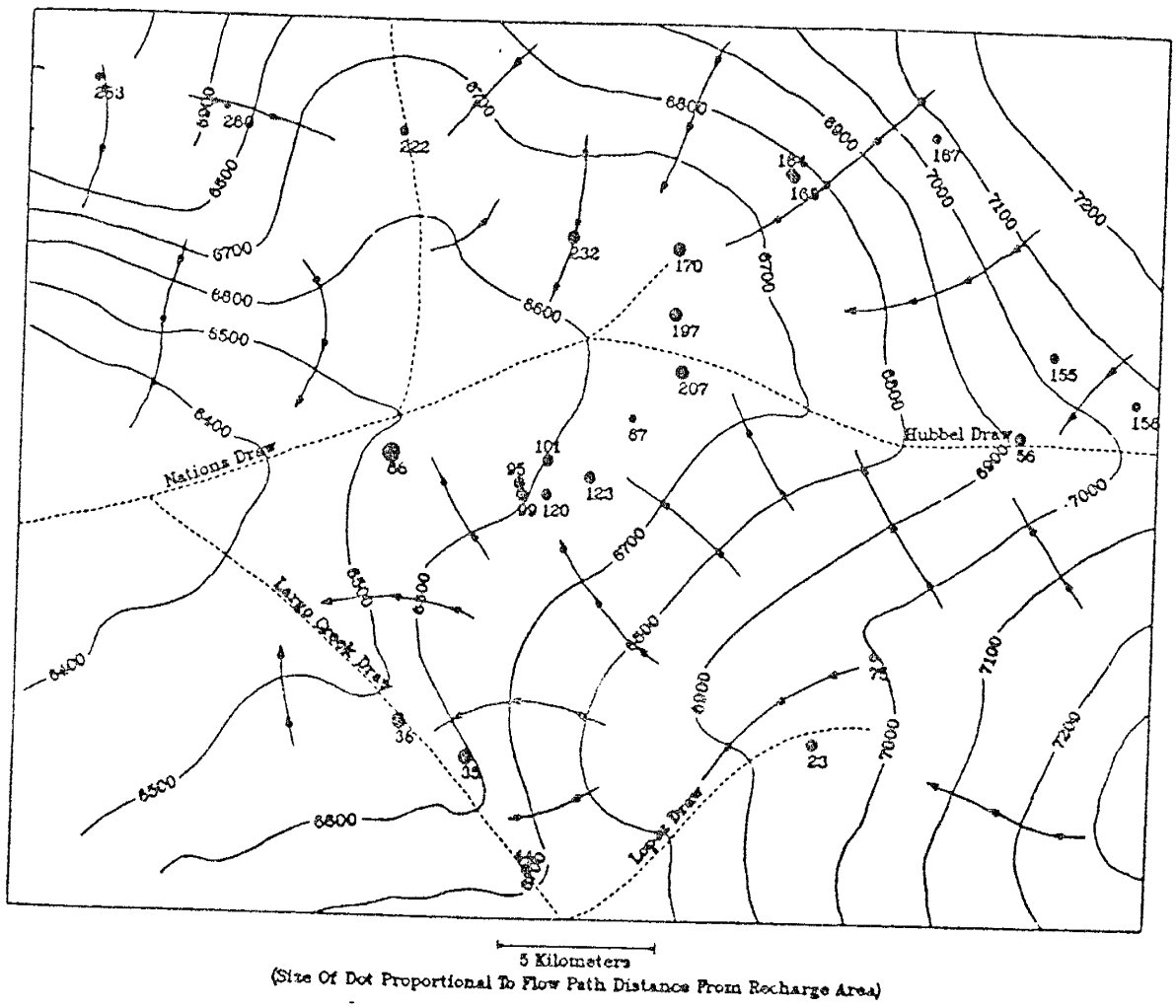

Figure 2. Water table elevation map showing groundwater sampling localities. (Distance along flowpath is based on simplified model of groundwater flow with recharge in higher elevations, and discharge in lower reaches of major draws).

MINERALOGY OF THE MORENO HILL FORMATION

Plate 1 illustrates locations for surface and subsurface samples of lithologic units within the lower Moreno Hill Formation. Sample location identifiers were assigned on the basis of township, range, and section (the section number is separated by a hyphen). For the surface samples, the letter at the end of the ID number is based on stratigraphic position. A few sandstones units were randomly sampled; they are represented by an "SS" followed by a number. For the subsurface samples the third number represents the depth (in feet) below ground surface at which the core was taken.

Only limited sections of core were retained by the NMBM&MR drilling project for further study. Most of the cores contained coal zones with bounding lithologies. Samples of each zone were obtained for analysis. Surface lithologic sampling localities were chosen, when possible, where outcrops of lignite occur in the vicinty of NMBM&MR drilling sites. Care was taken to sample mudstones and siltstones above and below lignite zones as well as capping sandstones in order to have some correlation with subsurface samples. Sites 416-31 and 416-32 were drilled and cored for a recharge study by the NMBM&MR (Stone, 1984). The core from these drilling sites consists mainly of

sandstones units. Surface sandstone samples (SS-1 through 5) were taken from localities without coal outcrops to correspond to those cores. Therefore, though exact stratigraphic relationships were impossible to establish between surface and subsurface samples, due to a lack of complete cores, all samples originated in similar sedimentary environments, and were obtained from corresponding positions in the stratigraphic sequence.

SANDSTONE MINERALOGY

Sandstone samples from the lower Moreno Hill Formation are generally buff to light brown, locally stained with iron in the form of Liesegang rings, fine-grained, subangular to subrounded, and poorly to moderately sorted. If not tightly cemented with carbonate minerals, the samples are extremely friable with abundant clay matrix. Appendix 1 gives hand sample descriptions and petrographic observations for these samples.

Point-counting Methodology

Thirty-four samples (17 surface and 17 subsurface) were sent to Pioneer Thin Section in Draper, Utah. The samples were impregnated with blue epoxy and stained for potassium feldspar. In all samples 400 grains were counted to ensure a 95% confidence limit. This is based on a precision estimate of $\pm$5%, for minerals 50% in abundance, to $\pm$2%, for

minerals 5% in abundance (van der Plas and Tobi, 1965).

Important to the applicability of any point-count exercise is the establishment of parameters which will provide a strong basis for interpretations with the intent of the investigation. An admittedly surficial perusal of recent literature reveals that the intent of most point-counting exercises is to establish provenance through the relative abundance of certain types of grains such as quartz and particularly lithic fragments. The intent of this study is quite different as it attempts to establish how the weathering process manifests itself through the alteration of primary minerals at the surface and in the subsurface. Though many petrographers would wish to see through the mask of grain alteration and establish original grain type, for this study, what is most important is to recognize alteration products and quantify them as such.

Results of Point-counting

Table 1 gives a brief description of the 15 parameters chosen to be quantified. Following is a more in depth discussion of these parameters which focuses on specific observations and problems encountered with their use in this exercise. In general, the finer-grained samples (.1mm-.3mm) were more difficult to count as the grains were often impossible to identify. Therefore, less weight can be given to the associated results. Point-counting data are found in

Parameter	Description
Qm	Monocrystalline quartz
Qp	Polycrystalline quartz
Fk	Potassium feldspar
Fp	Plagioclase feldspar
L	Lithic fragments
Mg	Magnetite
Mm	Muscovite mica
Mcb	Chlorite/biotite mica
Mo	Orthomatrix
Me	Epimatrix
Mp	Pseudomatrix
Cq	Quartz cement
Cc	Carbonate Cement
Cf	Hematite cement
P	Porosity

Table 1. Point-counting parameters

Tables 2 through 5. Some major differences between the mineralogy of surface and subsurface samples are immediately obvious when mean percentage values are compared (Table 6).

Monocrystalline (Qm) and polycrystalline (Qp) quartz were counted separately to check for any major differences between the two sets of samples. As expected, little difference was observed other than slightly more Qm and slightly less Qp in the subsurface samples. It is concieveable that Qp grains are more susceptable to alteration by deformation and/or rock-water interactions. Quartz grains often showed dissolution textures in subsurface samples. These grains are optically very easy to identify, therefore the data for this parameter is likely the most reliable.

Plagioclase feldspar (Fp) and potassium feldspar (Fk) were easily distinguished, as staining turns Fk grains a distinct yellow color. Occasionally, a grain was observed which was incompletely stained and exhibited albite polysynthetic twinning, characteristic of Fp. This phenomenon can either be explained by incomplete staining, replacement textures, or antiperthites. Antiperthites with Fk as the host mineral, is the most logical of the three choices based on textural evidence. These grains were counted as Fk (Figure 3, 417-3-37). An interesting characteristic of Fp grains is that often they contained

SURFACE SAMPLES

SAMPLE	417-3 SS-B	417-3 SS-G	416-17 SS-2	416-17 SS-3	416-32 SS-4	416-32 SS-5	417-24 SS-6	416-31 SS-F	416-31 SS-I	417-25 SS-1	418-7 SS-1	418-7 SS-F3	418-7 SS-F2	219-26 SS-B	219-26 SS-D	219-26 SS-F	119-17 SS-1
Qm	282	197	338	205	131	113	250	225	268	189	186	210	214	195	195	217	227
Qp	22	10	10	34	61	53	26	20	10	33	46	41	29	16	10	22	18
Fk	62	103	27	103	103	127	82	89	74	100	102	80	86	81	113	94	94
Fp	24	50	13	34	18	30	19	47	31	20	27	35	35	19	23	37	54
Ft	86	153	40	137	121	157	101	136	105	120	129	115	121	100	136	131	148
L	3	27	12	24	70	75	15	5	9	22	39	32	30	17	37	30	4
Mg	0	0	0	0	13	0	1	4	0	23	0	1	2	37	0	0	0
Mm	6	10	0	0	3	0	7	7	7	13	0	0	0	8	3	0	3
Mcb	1	3	0	0	1	2	0	3	1	0	0	1	4	27	19	0	0
Mo	0	0	0	0	0	0	0	0	0	0	0	0	0	0	0	0	0
Me	60	56	30	9	40	0	51	66	50	29	60	36	54	82	184	48	31
Mp	43	108	19	8	26	19	42	48	63	31	53	54	59	127	117	36	47
Cq	0	7	0	0	69	0	0	0	0	34	0	0	0	8	19	0	0
Cc	0	0	0	0	1	287	0	6	0	0	0	0	0	0	0	0	27
Cf	74	52	39	0	29	2	36	35	20	88	48	61	13	59	6	26	12
P	71	49	129	168	64	5	82	37	88	76	132	116	110	0	22	56	136
TOTAL	648	672	617	585	629	713	611	592	621	658	693	667	636	676	748	566	653
AVE GRAIN(mm) SIZE	0.3	0.2	1.0	0.8	0.7	0.3	0.6	0.1	0.2	1.0	0.4	0.3	0.5	0.1	0.1	0.2	0.4

Table 2. Raw data from point-counting surface sandstone samples.

SURFACE SAMPLES

SAMPLE	417-3 SS-B	417-3 SS-G	416-17 SS-2	416-17 SS-3	416-32 SS-4	416-32 SS-5	417-24 SS-6	416-31 SS-F	416-31 SS-I	417-25 SS-1	418-7 SS-1	418-7 SS-F3	418-7 SS-2	219-26 SS-B	219-26 SS-D	219-26 SS-F	119-17 SS-1
Qm	43.5%	29.3%	54.8%	35.0%	20.8%	15.8%	40.9%	38.0%	43.2%	28.7%	26.8%	31.5%	33.6%	28.8%	26.1%	38.3%	34.8%
Qp	3.4%	1.5%	1.6%	5.6%	9.7%	7.4%	4.3%	3.4%	1.6%	5.0%	6.6%	6.1%	4.6%	2.4%	1.3%	3.9%	2.8%
Fk	9.6%	15.3%	4.4%	17.6%	16.4%	17.8%	13.4%	15.0%	11.9%	15.2%	14.7%	12.0%	13.5%	12.0%	15.1%	16.6%	14.4%
Fp	3.7%	7.4%	2.1%	5.8%	2.9%	4.2%	3.1%	7.9%	5.0%	3.0%	3.9%	5.2%	5.5%	2.8%	3.1%	6.5%	8.3%
Ft	13.3%	22.8%	6.5%	23.4%	19.2%	22.0%	16.5%	23.0%	16.9%	18.2%	18.6%	17.2%	19.0%	14.8%	18.2%	23.1%	22.7%
L	0.5%	4.0%	1.9%	4.1%	11.1%	10.5%	2.5%	0.8%	1.4%	3.3%	5.6%	4.8%	4.7%	2.5%	4.9%	5.3%	0.6%
Mg	0.0%	0.0%	0.0%	0.0%	2.1%	0.0%	0.2%	0.7%	0.0%	3.5%	0.0%	0.1%	0.3%	5.5%	0.0%	0.0%	0.0%
Mm	0.9%	1.5%	0.0%	0.0%	0.5%	0.0%	1.1%	1.2%	1.1%	2.0%	0.0%	0.0%	0.0%	1.2%	0.4%	0.0%	0.5%
Mcb	0.2%	0.4%	0.0%	0.0%	0.2%	0.3%	0.0%	0.5%	0.2%	0.0%	0.0%	0.1%	0.6%	4.0%	2.5%	0.0%	0.0%
Mo	0.0%	0.0%	0.0%	0.0%	0.0%	0.0%	0.0%	0.0%	0.0%	0.0%	0.0%	0.0%	0.0%	0.0%	0.0%	0.0%	0.0%
Me	9.3%	8.3%	4.9%	1.5%	6.4%	0.0%	8.3%	11.1%	8.1%	4.4%	8.7%	5.4%	8.5%	12.1%	24.6%	8.5%	4.7%
Mp	6.6%	16.1%	3.1%	1.4%	4.1%	2.7%	6.9%	8.1%	10.1%	4.7%	7.6%	8.1%	9.3%	18.8%	15.6%	6.4%	7.2%
Cq	0.0%	1.0%	0.0%	0.0%	11.0%	0.0%	0.0%	0.0%	0.0%	5.2%	0.0%	0.0%	0.0%	1.2%	2.5%	0.0%	0.0%
Cc	0.0%	0.0%	0.0%	0.0%	0.2%	40.3%	0.0%	1.0%	0.0%	0.0%	0.0%	0.0%	0.0%	0.0%	0.0%	0.0%	4.1%
Cf	11.4%	7.7%	6.3%	0.0%	4.6%	0.3%	5.9%	5.9%	3.2%	13.4%	6.9%	9.1%	2.0%	8.7%	0.8%	4.6%	1.8%
P	11.0%	7.3%	20.9%	28.7%	10.2%	0.7%	13.4%	6.3%	14.2%	11.6%	19.0%	17.4%	17.3%	0.0%	2.9%	9.9%	20.8%
TOTAL	100.0%	100.0%	100.0%	100.0%	100.0%	100.0%	100.0%	100.0%	100.0%	100.0%	100.0%	100.0%	100.0%	100.0%	100.0%	100.0%	100.0%

Table 3. Percentages of point-counting parameters for surface sandstone samples.

SUBSURFACE SAMPLES

SAMPLE	417-3 34	417-3 36	417-3 37	416-32 38	416-32 40	416-32 42	416-32 44	416-31 44	416-31 48	416-31 65	416-31 70	518-17 221	518-17 226	519-20 285	519-20 275	519-20 281	119-8 104
Qm	266	296	269	197	179	180	124	226	240	375	321	293	308	307	307	301	201
Qp	17	14	55	37	41	47	41	17	6	10	8	21	28	9	10	15	9
Fk	78	53	58	66	93	95	128	119	101	2	63	28	52	53	64	31	121
Fp	33	27	18	39	35	26	36	27	9	0	1	10	4	6	12	38	31
Ft	111	80	76	105	128	121	164	146	110	2	64	38	56	59	76	69	152
Mg	3	0	0	3	0	0	5	0	35	0	0	0	3	0	0	2	0
L	2	0	0	57	52	52	54	11	3	0	7	11	0	25	5	11	25
Mm	1	2	0	1	0	0	8	0	0	0	0	2	5	0	0	0	2
Mcb	0	8	0	0	0	0	4	0	6	13	0	35	0	0	2	2	11
Mo	0	379	80	0	0	0	151	0	0	0	0	0	0	0	0	0	0
Me	70	18	8	109	130	100	79	162	202	243	271	163	154	143	162	234	360
Mp	12	4	3	79	78	47	10	84	43	6	12	16	143	29	36	20	62
Cq	0	0	0	4	3	8	0	0	0	4	0	1	0	6	0	3	1
Cc	0	0	1	1	1	2	0	7	136	1	1	3	0	0	0	0	0
Cf	35	37	5	44	17	74	80	140	31	31	15	3	3	10	24	102	0
P	70	6	68	38	50	30	41	17	3	67	104	26	11	46	35	11	4
TOTAL	587	844	565	675	679	661	761	810	815	752	803	612	711	634	657	770	827
AVE GRAIN(mm) SIZE	1.0	1.0	2.0	0.6	0.4	0.4	0.2	0.3	0.2	0.1	0.3	0.1	0.1	0.7	0.3	0.4	0.3

Table 4. Raw data from point-counting subsurface sandstone samples.

SUBSURFACE SAMPLES

SAMPLE	417-3 34	417-3 36	417-3 37	416-32 38	416-32 40	416-32 42	416-32 44	416-31 44	416-31 48	416-31 65	416-31 70	518-17 221	518-17 226	519-20 285	519-20 275	519-20 281	119-8 104
Qm	45.3%	35.1%	47.6%	29.2%	26.4%	27.2%	16.3%	27.9%	29.4%	49.9%	40.0%	47.9%	43.3%	48.4%	46.7%	39.1%	24.3%
Qp	2.9%	1.7%	9.7%	5.5%	6.0%	7.1%	5.4%	2.1%	0.7%	1.3%	1.0%	3.4%	3.9%	1.4%	1.5%	1.9%	1.1%
Fk	13.3%	6.3%	10.3%	9.8%	13.7%	14.4%	16.8%	14.7%	12.4%	0.3%	7.8%	4.6%	7.3%	8.4%	9.7%	4.0%	14.6%
Fp	5.6%	3.2%	3.2%	5.8%	5.2%	3.9%	4.7%	3.3%	1.1%	0.0%	0.1%	1.6%	0.6%	0.9%	1.8%	4.9%	3.7%
Ft	18.9%	9.5%	13.5%	15.6%	18.9%	18.3%	21.6%	18.0%	13.5%	0.3%	8.0%	6.2%	7.9%	9.3%	11.6%	9.0%	18.4%
Mg	0.5%	0.0%	0.0%	0.4%	0.0%	0.0%	0.7%	0.0%	4.3%	0.0%	0.0%	0.0%	0.4%	0.0%	0.0%	0.3%	0.0%
L	0.3%	0.0%	0.0%	8.4%	7.7%	7.9%	7.1%	1.4%	0.4%	0.0%	0.9%	1.8%	0.0%	3.9%	0.8%	1.4%	3.0%
Mm	0.2%	0.2%	0.0%	0.1%	0.0%	0.0%	1.1%	0.0%	0.0%	0.0%	0.0%	0.3%	0.7%	0.0%	0.0%	0.0%	0.2%
Mcb	0.0%	0.9%	0.0%	0.0%	0.0%	0.0%	0.5%	0.0%	0.7%	1.7%	0.0%	5.7%	0.0%	0.0%	0.3%	0.3%	1.3%
Mo	0.0%	44.9%	14.2%	0.0%	0.0%	0.0%	19.8%	0.0%	0.0%	0.0%	0.0%	0.0%	0.0%	0.0%	0.0%	0.0%	0.0%
Me	11.9%	2.1%	1.4%	16.1%	19.1%	15.1%	10.4%	20.0%	24.8%	32.3%	33.7%	26.6%	21.7%	22.6%	24.7%	30.4%	43.5%
Mp	2.0%	0.5%	0.5%	11.7%	11.5%	7.1%	1.3%	10.4%	5.3%	0.8%	1.5%	2.6%	20.1%	4.6%	5.5%	8.6%	7.5%
Cq	0.0%	0.0%	0.0%	0.6%	0.4%	1.2%	0.0%	0.0%	0.0%	0.5%	0.0%	0.2%	0.0%	0.9%	0.0%	0.4%	0.1%
Cc	0.0%	0.0%	0.2%	0.1%	0.1%	0.3%	0.0%	0.9%	16.7%	0.1%	0.1%	0.5%	0.0%	0.0%	0.0%	0.0%	0.0%
Cf	6.0%	4.4%	0.9%	6.5%	2.5%	11.2%	10.5%	17.3%	3.8%	4.1%	1.9%	0.5%	0.4%	1.6%	3.7%	13.2%	0.0%
P	11.9%	0.7%	12.0%	5.6%	7.4%	4.5%	5.4%	2.1%	0.4%	8.9%	13.0%	4.2%	1.5%	7.3%	5.3%	1.4%	0.5%
TOTAL	100.0%	100.0%	100.0%	100.0%	100.0%	100.0%	100.0%	100.0%	100.0%	100.0%	100.0%	100.0%	100.0%	100.0%	100.0%	100.0%	100.0%

Table 5. Percentages of point-counting parameters for subsurface sandstone samples.

	SURFACE		SUBSURFACE	
Point	MEAN	STD DV	MEAN	STD DV
P	12.5	7.8	5.4	4.2
Ft	18.6	4.4	12.9	5.8
Fp	4.8	1.9	2.9	2.0
Fk	13.9	3.3	9.9	4.5
Me	7.9	5.3	21.0	11.0
Mp	8.1	4.8	5.6	5.3
Qm	33.5	9.3	36.7	10.4
Qp	4.2	2.4	3.3	2.6
%GRAINS	62.2	4.5	56.6	7.3
GRAIN SIZE (MM)	0.42	0.3	0.49	0.5

Table 6. Means and standard deviations (STD DV) for selected point-counting parameters.

small black inclusions with an unidentified composition (Figure 4, 416-31-SS-I, notice the extremely altered grains and dissolution textures). This phenomenon was also observed in the epimatrix, a parameter to be discussed later in this section. Possible explanations for the composition of these inclusions include magnetite grains or organic material. It would be impossible for the latter to be inclusions in the plagioclase crystals unless mobilized organic detritus was deposited in the voids of extremely altered crystals. Sericitic alteration of Fp grains and intergrowths of quartz and feldspar were observed in all samples.

Lithic fragments (L) in all samples were extremely altered and, therefore, it was often impossible to precisely identify their original lithology. Microlitic textures characteristic of volcanic rocks were occassionally observed (Figure 3 , 417-3-37), volcanic fragment in upper right corner). Laminations indicating a sedimentary origin for some lithic fragments were found in a few of the grains. However, when samples are fine-grained and extremely altered, a lithic fragment could have been mistaken for an altered plagioclase grain and vice versa. However, it is felt that misidentification of grains is relatively minor considering the amount of data accumulated with confidence, and that the conclusions are drawn from averages of data.

Magnetite (Mg) proved to be an insignificant parameter

Figure 3. Subsurface sandstone sample, 417-3-37, with antiperthite texture and volanic lithic fragment (MAG. 25x, 0.65FW).

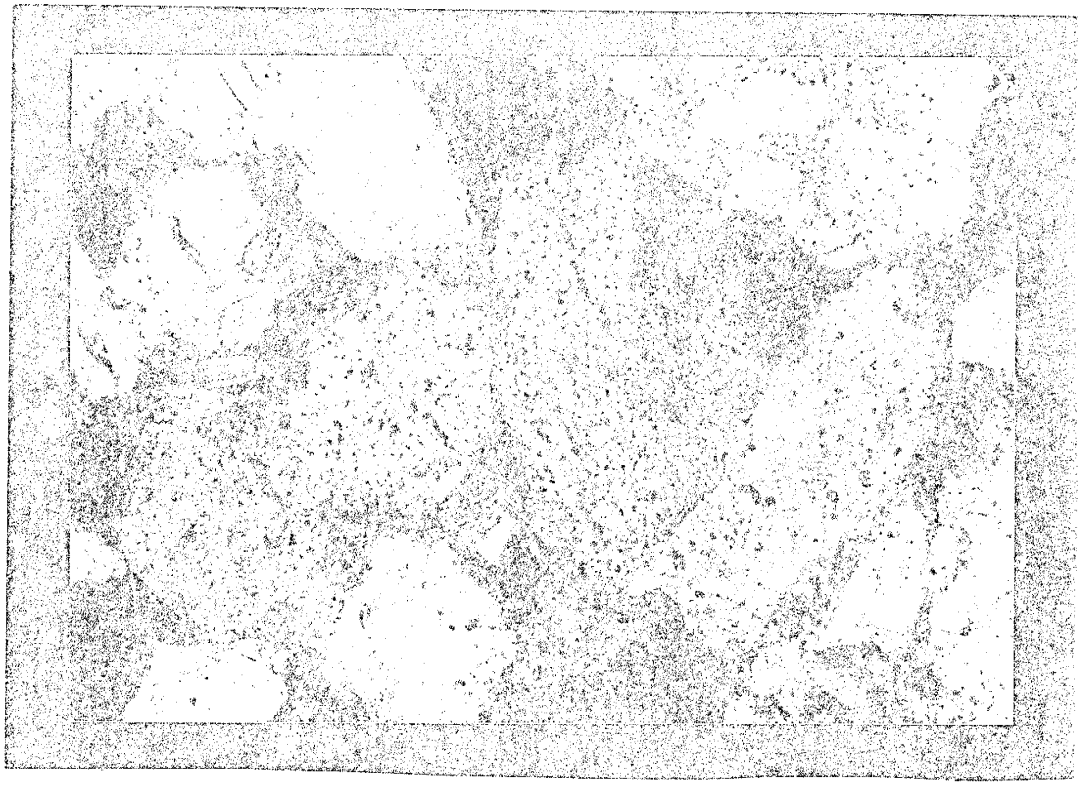

Figure 4. Surface sandstone, 416-31-SS-I, sample with extremely altered plagioclase and black inclusions (MAG. 50x, 0.65FW).

and could easily have been omitted from the point-counting study without altering any conclusions reached. A more useful parameter for the study would have been organic material, which was quite abundant in some samples (Figure 5, 416-31-70 and Figure 6, 416-32-44, the dispersed black material in this sample could be organic in origin).

Chlorite, biotite (Mcb), and muscovite (Mm) are present as a minor constituent of most of these samples. Biotite was often altered to chlorite, at least partially; therefore, these parameters were grouped together. Many of the mica grains were actually altered to pseudomatrix (discussed below) and were counted as such.

Dickinson (1970) developed a classification scheme based on origin for the different types of matrix encountered in sandstone. Briefly, orthomatrix refers to recrystallized "lutum" or protomatrix (almost never observed in thin section, according to Dickinson, and protomatrix is defined as the original, unaltered matrix), with relict clastic texture, and an inhomogeneous composition. The framework of the rock imperceptibly grades into this detrital "paste" termed orthomatrix. Pseudomatrix refers to a discontinuous interstitial "paste" which is created through the deformation of weak grains, most commonly argillaceous lithic fragments, but also minerals from the mica group. Epimatrix, a parameter which is significant to this study, refers to inhomogeneous interstitial material

Figure 5. Subsurface sandstone sample, 416-31-70, dispersed organic material (MAG. 50x, 0.65FW).

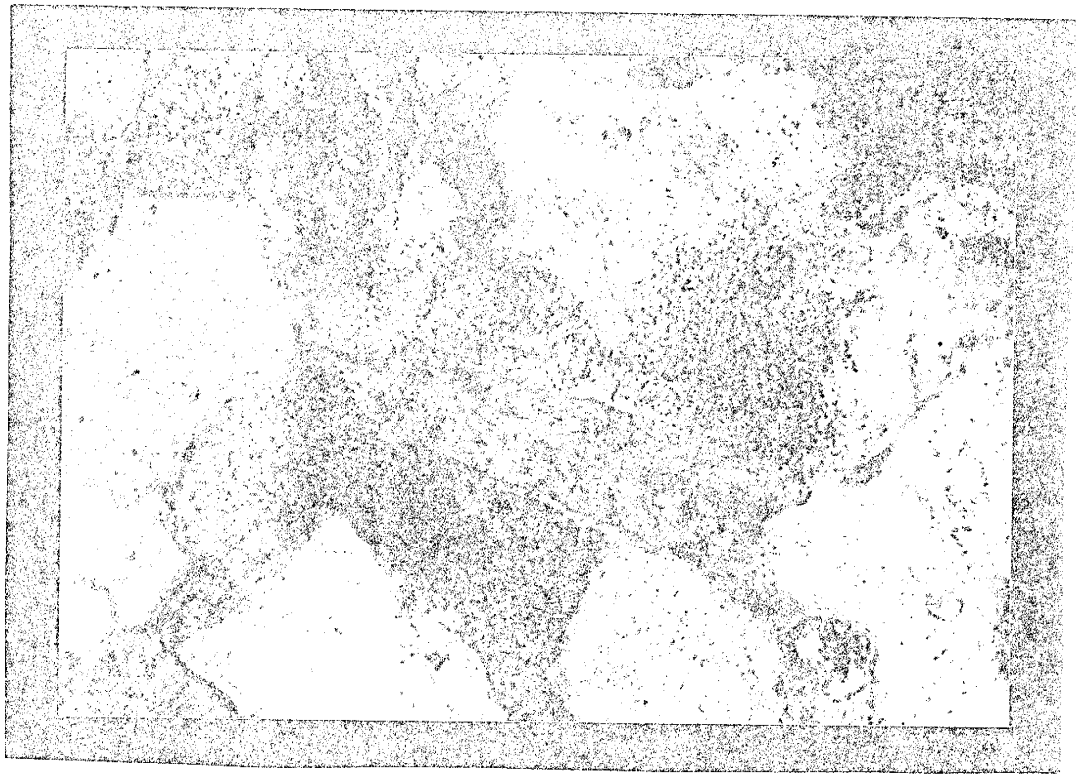

Figure 6. Subsurface sandstone sample, 416-32-44, dispersed organic material associated with hematite cement (?) (MAG. 50x, 0.65FW).

grown in originally open interstices during the process of diagenesis. This type of matrix lacks the homogeneity and textural evidence of pore-filling phenomenon, and the two are easily distinguished. The latter can be classified as a phyllosilicate cement.

Orthomatrix (Mo) was only observed as a significant component in one sample, 417-3-36, where it was found to comprise 45% of the rock. Pseudomatrix (Mp) was found occurring mostly as deformed mica grains or extremely altered and deformed plagioclase (Figures 7, 417-3-37 and 8, 416-32-SS-5, notice the black inclusions in albite grains). The grains were recognized as Mp as they tended to wrap around the rigid form of unaltered grains. Epimatrix (Me) was observed in all samples as a significant constituent. Often relic grain boundaries, most likely that of plagioclase, were observed as textural features within the epimatrix. As described earlier when discussing the feldspars, tiny (<.03mm) black inclusions were found in the epimatrix as well as the plagioclase feldspars (Figure 6, 416-32-44).

Several different types of cement occur in these sandstones, namely quartz (Cq), carbonate (Cc), and what was identified as iron cement (Cf), or, perhaps more accurately, hematite cement. Cq was often in the form of overgrowths on grains, but also occurs as a void-filling constituent with a crptocrystalline texture. Though never extremely abundant,

Figure 7. Subsurface sandstone sample, 417-3-37, pseudomatrix, (deformed plagioclase with black inclusions in center of photograph) (MAG. 25x, 1.3FW).

Figure 8. Surface sandstone sample, 416-32-SS-5, psedomatrix (deformed biotite in center of photograph) (MAG. 25x, 1.3FW)

Cq was found as a component of nearly all samples. Carbonate cement, on the other hand, is extremely localized yet pervasive when it occurs in these samples (Figure 9, 416-32-SS-5). Cf was found to be in greatest abundance as a cementing agent for these rocks, yet the exact composition of this cement is unknown. Cf and organic material were often observed together and may be genetically related. This cement was distinguished by its rusty iron color and opaqueness. Most samples are extremely friable and poorly cemented.

Though there are many different types of porosity, this parameter was not broken into categories as, initially, it was felt that intergranular porosity was by far the most significant. However, though not extremely abundant, moldic porosity was observed in some of the surface samples, and, in retrospect, it may have proved useful to quantify this parameter (Figure 10, 416-31-SS-I). Most important to the conclusions reached in this study, is the fact that moldic porosity was not found to occur in the subsurface samples. Some of the surface samples have up to 21% porosity and much of this is believed to be attributable to alteration and dissolution of albite grains (Figure 11, 416-17-SS-2, grain in center of view partially dissolved). The subsurface samples have a maximum of 12% porosity.

Table 5 illustrates a mean percentage comparison of significant parameters; important conclusions reached in

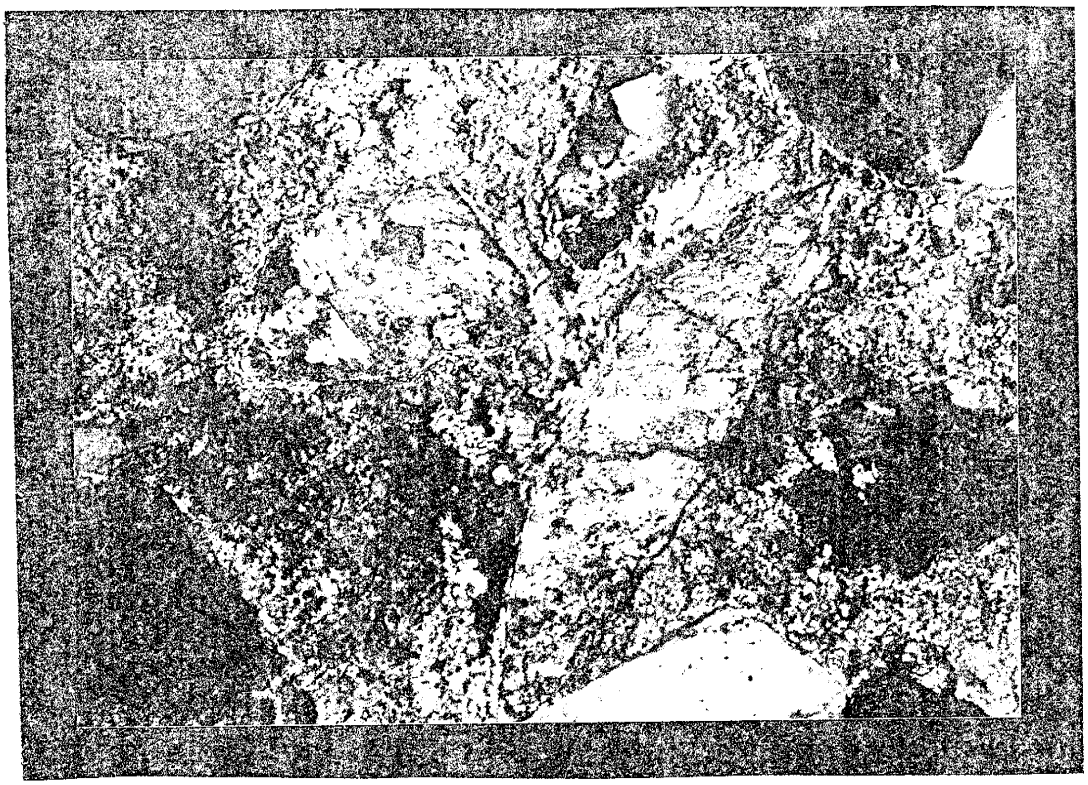

Figure 9. Surface sandstone sample, 416-32-SS-5, carbonate cement surrounding potassium feldspar (MAG. 50x, 1.3FW).

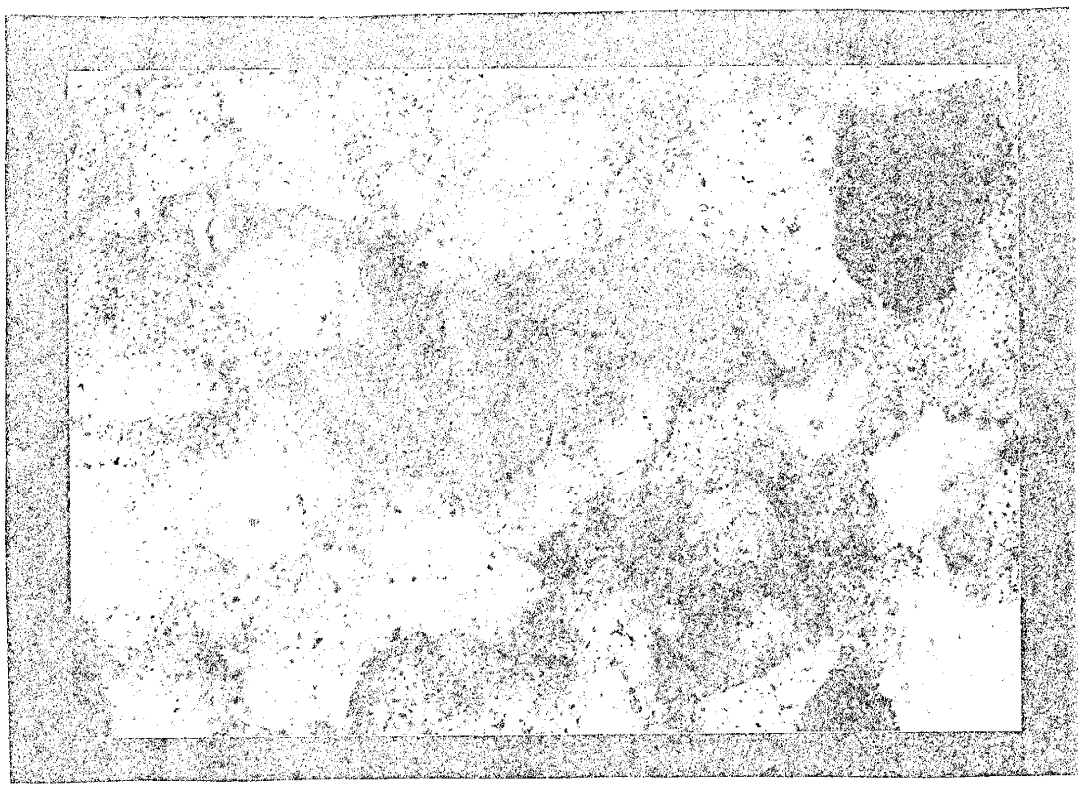

Figure 10. Surface sandstone sample, 416-3-SS-I, moldic porosity (relic grain boundary) (MAG. 50x, 1.3FW).

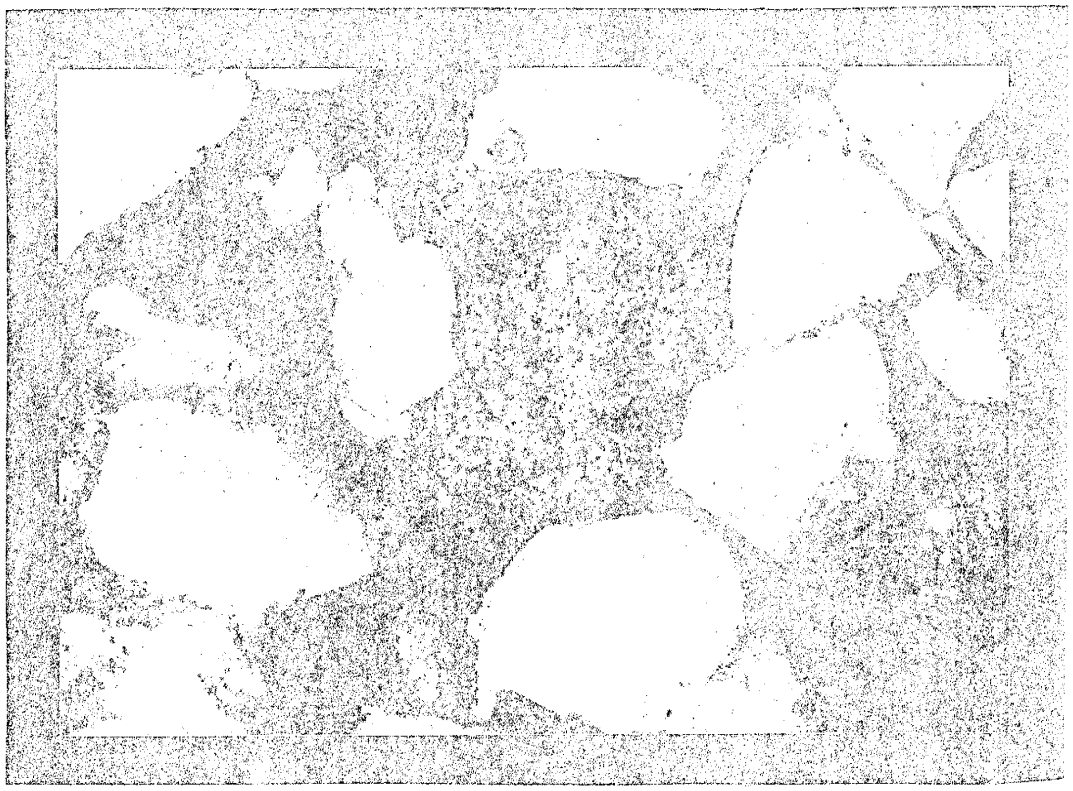

Figure 11. Surface sandstone sample, 416-17-SS-2, abundant porosity, extremely altered plagioclase in center of photograph (MAG. 25x, 0.65FW).

review of these data include the following:

1. Surface sandstone samples have a combined mean percentage value for total feldspar and porosity which is 12.8% greater than the same parameters averaged for the subsurface samples.

2. Subsurface samples have a mean percentage for epimatrix which is 13.1% greater than surface samples (Figures 10, 416 -31-SS-I and 5, 416-31-70, for a comparison of surface and subsurface samples from the same general stratigraphic position. Figure 12 depicts percent epimatrix vs depth for subsurface samples. Though there is some scatter in the data, clearly all samples from the deeper zones had the highest values for epimatrix. Groundwater depth in this area is, on the average, approximately 50 feet except on the high mesas. A maximum value for epimatrix percentage is reached at approximately 70 feet. More data is needed to fully establish this relationship.

3. Both polycrystalline and monocrystalline quartz values remain fairly constant in both sets of samples.

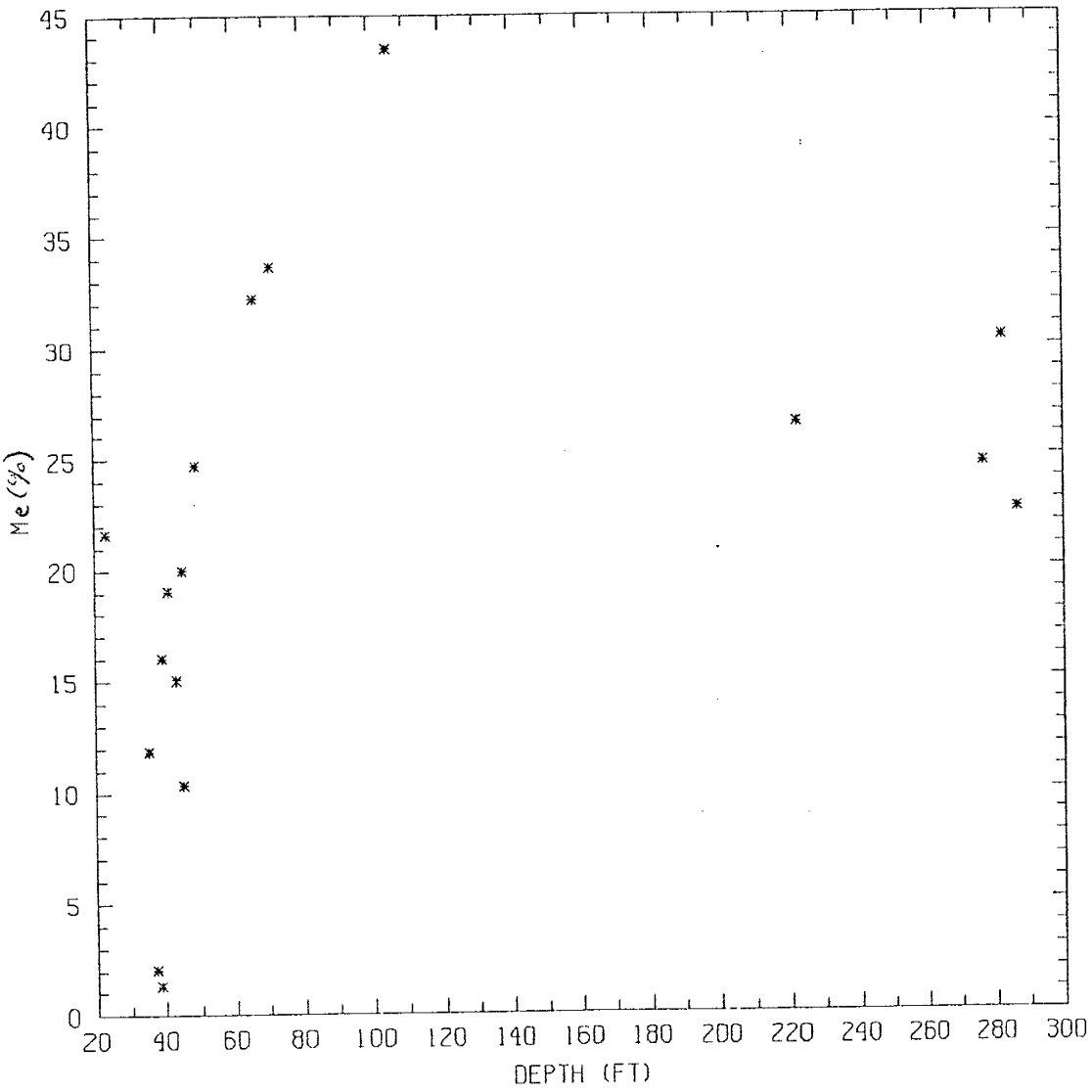

Figure 12. Percent epimatrix vs depth of sandstone sample in feet below the surface.

4. The mean percentage of total grains in the surface samples is 5.6% greater than in the subsurface samples (although this difference between sample means occurs within the standard deviations about those means).

Scanning Electron Microscope Analysis

An attempt was made to qualify the chemical character and clay mineral type of the epimatrix material through the use of a scanning electron microscope (SEM) at NMIMT. Also, it was hoped that the chemical character of the small black inclusions in the epimatrix and plagioclase grains described earlier could be determined. Unfortunately, funding was limited at this point in the study and only a few hours of time on the SEM were possible. As a result of petrographic work, two samples were found which contain excellent examples of epimatrix and pervasively altered plagioclase grains (416-32-44 and 417-3-34), and they were chosen for the study.

One of the limitations of SEM investigations is the inability to pinpoint exact locations for analysis in a sample chip. Since all thin sections had cover slips epoxied to their surfaces, they could not not be used for this part of the study. Greater accuracy in locating a particular spot for analysis is possible with the use of uncovered thin sections. Epimatrix is so pervasive in the

chosen samples that it was easy to find sections of the sample chip to analyze. One advantage of SEM techniques is the ability to identify clay minerals through the use of both crystal morphology and chemistry.

Albitization of plagioclase feldspars is pervasive in both of the samples. Chemical analyses of all plagioclase feldspars revealed predominant sodium, aluminum, and silica (no calcium was found in any of the feldspars tested); all epimatrix that was chemically analyzed consisted of Al and Si. Based on the chemistry and morphology of this substance, it is concluded that the epimatrix consisted predominantly of kaolinite. No significant iron oxide was detected in many attempts to analyze the chemistry of the sample, yet the plagioclase minerals and the epimatrix were seen in thin section to be riddled with black, opaque inclusions. This would favor the conclusion that these black inclusions, as it were, are organic in origin. These data do not support the conclusion that hematite is the most common form of cement in these samples. It is possible that the organic material present is acting as a cementing agent.

A few selected photographs were retained for illustration of pertinent alteration effects. In Figure 13, (416-32-44), an albite grain exhibits dissolution textures. Figures 14 and 15, (417-3-34) depict potassium feldspar and plagioclase grains surrounded by kaolinite. In fact, kaolinite was found to blanket most of the grains in these

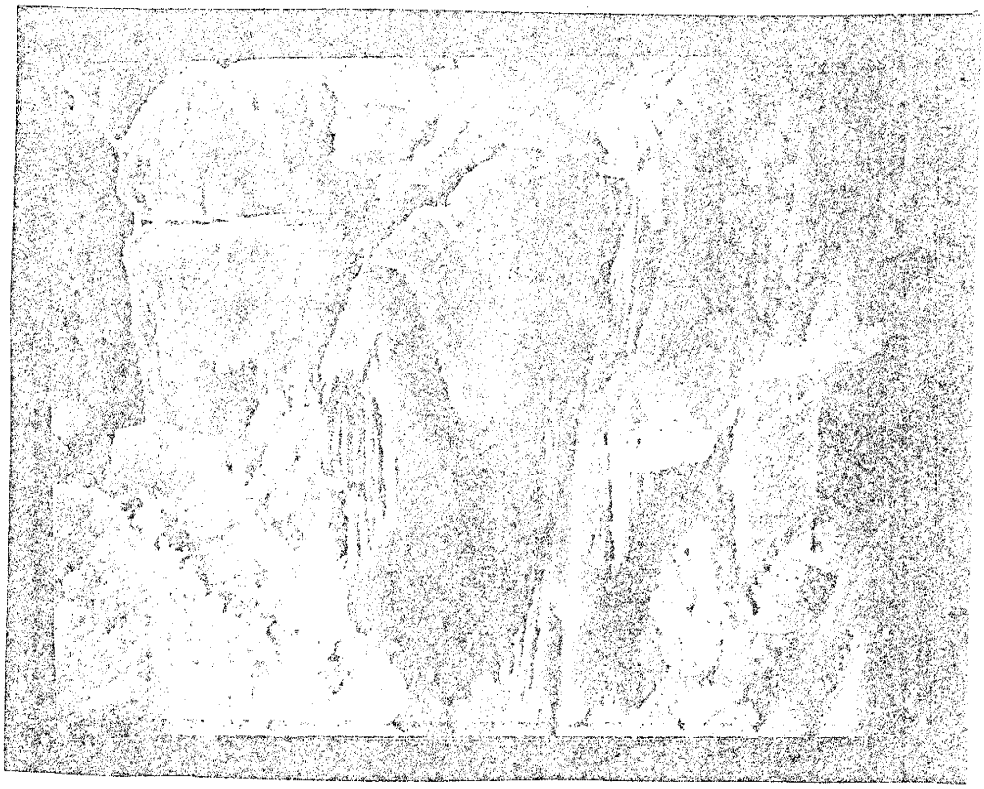

Figure 13. Subsurface sandstone sample, 416-32-44, albite with dissolution textures (etch pits) (MAG. 1000x).

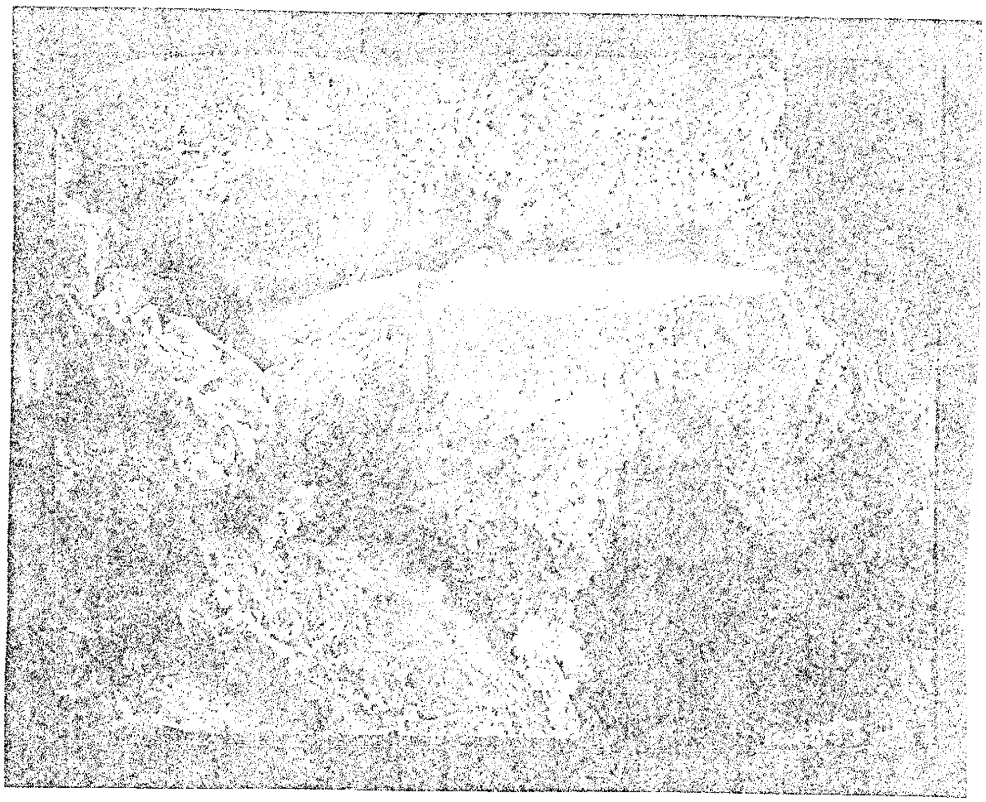

Figure 14. Subsurface sandstone sample, 417-3-34, potassium feldspar surrounded by altered plagioclase and kaolinite (MAG 270x).

Figure 15. Subsurface sandstone sample, 417-3-34, altered albite with dissolution textures (MAG. 350x).

samples.

It is generally accepted that the mechanism for feldspar weathering is for cations at the surface of the mineral to be leached away leaving behind an Al-Si rich material (Berner and Holdren, 1979). This protective coating serves ultimately to inhibit water-rock reactions which are initially very rapid. This blanket of kaolinitic material serves to isolate the primary grain from the pore fluids. In Chapter 6, this theory will be challenged, and the weathering of feldspars will be discussed as being a surface-controlled process (Holdren, G. R. and R. A. Berner, 1979).

In Figure 16, (416-32-44), a euhedral quartz grain, most likely having precipitated from solution, is surrounded by quartz grains whose surfaces appear to be etched. This could be caused by the weathering of feldspar minerals which liberates orthosilicic acid. This acid, produced in great quantities, could cause the partial dissolution of quartz grains.

CLAY MINERALOGY

X-ray diffraction (XRD) analyses were obtained from 37 samples (19 subsurface and 18 surface). The relative proportions of major clay mineral groups in the clay size fraction of mudrocks (shales, siltstones, and mudstones) were determined from the diffractograms following a method

Figure 16. Subsurface sandstone sample, 416-32-44, euhedral quartz grain with etched surface (MAG. 2250x).

developed by George Austin of NMBM&MR (personal communication, 1985).

Analytical Methods

Approximately 140 grams of crushed mudrock were added to 0.95 liters of distilled water and agitated for 3-5 minutes in a conventional blender until all of the rock material had been dispersed. Silt and sand-sized grains were allowed to settle out for one minute, and the mixture was decanted into polyethylene containers. The samples were then stored for 24 hours. If the clay minerals were observed to flocculate (complete separation from the distilled water), than the water was decanted, more distilled water was added, and the samples were manually agitated. This process was repeated until the samples remained deflocculated for a minimum of 24 hours.

Once the sample was prepared, it was manually reagitated and allowed to remain undisturbed for 10 minutes. An eye-dropper was touched to the surface of the suspension, a portion was drawn off, and it was applied to a glass slide. An assumption is made that this decanted portion contains, predominantly, the less than 2 micrometer-sized particles. The slides were then allowed to air-dry. Occasionally, during this drying process, a sample was found to have cracked and curled on the slide and had to be remade. Most likely, the cause of this cracking is the

fact that clay minerals of different morphologies and moisture retentions mixed together in the same sample can cause an imbalance of electrostatic forces which leads to cracking and bending (George Austin, personal communication, 1985). Another possibility is that the liquid sample which was too concentrated with clay material. Repeated attempts to prepare a slide from sample 219-26-A were unsuccessful.

This procedure for the preparation of clay slides to be used for XRD analysis, yields a strongly oriented sample with the c-axes perpendicular to the slide's surface. This allows for strong basal x-ray reflections and clear peaks which are relatively easy to interpret from the diffractograms.

Semi-quantitative Analysis

Each oriented clay slide was run on the XRD three times as required by the semi-quantitative clay analysis method (George Austin, personal communication, 1986) These three runs include: 1) simple oriented; 2) a second analysis after treatment of the sample in an ethylene glycol atmosphere which induces complete expansion of expandable clay minerals; and, 3) a third analysis after heating to 350°C-400°C for at least 30 minutes. For the heat-treated slide, the trace of the XRD must pass over the 10A peak while the slide is still hot. This proved to be one of the most difficult parts of the procedure to accomplish as the slide

must be transferred to the XRD immediately after removal from the oven.

After all the diffractograms have been produced, the patterns are analyzed by employing the following equations (subscripts indicate the order of the peak, such as first order illite would be I_1):

$$T = \text{heated 10A peak} + K_1 \qquad 1)$$

$$\text{Illite} = \frac{\text{glycolated } I_1}{T} * 10 \qquad 2)$$

$$\text{Kaolinite} = \text{oriented } \frac{K_1}{T} * 10 \qquad 3)$$

$$\text{Smectite} = \frac{\text{glycolated } .25S_1}{T} * 10 \qquad 4)$$

$$\text{Mixed-layer Illite and Smectite} = \qquad 5)$$

$$\frac{\text{Heated 10A} - (.25S_1 + \text{glycolated } I_1)}{T} * 10$$

The above calculations (equations 1-5)produce what is termed a "parts in ten" analysis for the major clay groups: Illite, Kaolinite, Smectite, and Mixed Layer.

Results of Semi-quantitative Clay Analysis

Tables 7 and 8 give the results of this semi-quantitative clay analysis. By far the most dominant clay mineral groups in these samples are kaolinite and Na-smectite with minor mixed-layer clay and illite. No Ca-smectites were found in either the surface or the subsurface samples. Unfortunately, the data did not provide for any

Clay Mineralogy of Surface Samples

Sample	Illite	Kaolinite	Smectite	Mixed-layer
219-26-C (NC)	1	6	2	1
219-37-A (BC)	0	8	2	0
219-37-C (AC)	2	5	3	0
416-31-B (BC)	1	4	3	2
416-31-D (AC)	1	3	3	3
416-31-E (AC)	1	8	1	0
416-31-G (BC)	1	4	2	3
417-3-C (BC)	2	7	1	0
417-3-E (AC)	1	5	2	2
417-3-F (AC)	1	3	5	1
417-24-A (AC)	1	6	2	1
417-24-B (AC)	1	7	1	1
417-24-E (BC)	1	8	1	0
417-24-F (BC)	1	4	3	2
418-7-A (BC)	1	3	4	2
418-7-B (BC)	0	6	2	2
418-7-D (AC)	1	5	2	2
418-7-E (AC)	1	2	4	3

(numbers represent "parts in ten", BC = below coal, AC = above coal, and NC = no coal)

Table 7. Semi-quantitative analysis of major clay groups for surface mudstone samples.

Clay Mineralogy of Subsurface Samples

Sample	Illite	Kaolinite	Smectite	Mixed-layer
119-8-106 (BC)	1	4	5	0
219-24-156 (AC)	1	4	3	2
219-54-165 (BC)	1	4	2	3
416-31-56 (BC)	1	5	3	1
416-31-60 (BC)	1	2	3	4
416-31-62 (BC)	1	4	3	2
416-32-19 (NC)	1	6	3	0
416-32-29 (NC)	1	3	4	2
416-32-31 (NC)	1	3	4	2
416-32-33 (NC)	1	5	4	0
417-3-41 (BC)	1	6	2	1
417-3-44 (BC)	1	6	1	2
417-3-134 (AC)	1	6	1	2
417-3-137 (BC)	1	7	1	2
417-14-135 (AC)	1	7	0	2
417-14-136 (BC)	1	5	2	2
517-1-22 (AC)	1	8	0	1
517-1-23 (BC)	1	5	0	4

(numbers represent "parts in ten", BC = below coal, AC = above coal, and NC = no coal)

Table 8. Semi-quantitative analysis of major clay groups for subsurface mudstone samples.

clear cut relationships between these sets of samples. Table 9 gives means and standard deviations for groups of samples taken above and below the coal zones. The kaolinite content of the subsurface samples above the coal seams is higher, by approximately two parts in ten, than the surface samples above the coal seams. This corresponds to a decrease by two parts in ten of Na-smectite in the subsurface samples which would indicate that this mineral is altering to kaolinite in the subsurface. Unfortunately, this same relationship could not be derived between sets of samples from below the coal seams.

The results of the clay analysis are probably the most disappointing of any achieved in this study. Several reasons are offered to explain this problem. First of all, clay minerals are extremely complex and heterogeneous. Indeed, many clay minerals formed by the processes of weathering and diagenesis are interstratified at the crystalline structure level (Wilson and Nadeau, 1985). It is concievable that the Austin method (Austin, G., personal communication, 1985), while applicable to some studies, may not be sensitive enough to reflect the subtle changes that are the result of weathering phenomenon. A potential source of error may lie in the fact that the core samples, which were retained from the NMBM&MR drilling operations, were not immediately preserved in plastic bags to isolate them from the environment. The samples were stored in NMBM&MR core

Sample	Illite		Kaolinite		Na-smectite		Mixed-layer	
	MEAN	STD DV	MEAN	STD DV	MEAN	STD DV	MEAN	STD DV
Subsurface (NC)	1.23	0.16	4.08	1.47	3.73	0.71	1.96	0.78
Subsurface (AC)	0.88	0.46	6.52	1.73	1.06	0.98	1.54	0.64
Surface (AC)	1.00	0.50	4.89	1.96	2.67	1.41	1.56	1.33
Subsurface (BC)	0.99	0.30	4.92	1.62	1.67	1.07	2.40	1.27
Surface (BC)	0.75	0.71	5.50	2.00	1.75	1.04	1.75	1.49

Table 9. Means and standard deviations (STD DV) for groups of mudstone samples with no coal (NC), above coal (AC), or below coal (BC).

shed for several months before the project started, after which they were prepared and analyzed.

Most important to this study is the fact that Na-smectite, which has a very high cation-exchange capacity, not Ca-smectite, was identified, and that there is abundant kaolinite in both sets of samples. The relevance of these data to groundwater chemistry will be discussed in below.

COAL CHEMISTRY

Ultimate coal analyses of surface and subsurface lignite and coal samples taken for this study are given in Tables 10 and 11. The most notable difference in these data sets are the BTU as received values. Subsurface samples have a mean of 9611 BTU with a standard deviation of 1644.5, whereas surface samples have a mean of 6786.5 BTU with a standard deviation of 1134.5. There was no overlapping of standard deviations around respective means. All surface samples can be classified as lignite, and most subsurface samples can be classified as coal (Bates and Jackson, 1980).

Total sulfur in the surface samples is somewhat less than in the subsurface samples. Some 26% of the sulfur in the subsurface samples occurs as pyrite while 5% occurs as sulfae. For the surface samples, these values are 11.9% and 17.4% respectively. These data reflect the effects of oxidation of minerals during the surface weathering process. Plates of selenite were observed in outcrops of coal.

SURFACE COAL CHEMISTRY

SAMPLE #	417-3-SCA	417-7-SCC	417-24-SCC	417-24-SCD	MEAN	STD DEV
VM	41.46	36.55	31.29	40.46	37.44	4.62
H20	8.87	10.79	7.87	9.21	9.19	1.21
ASH	28.83	21.73	29.09	12.47	23.03	1.82
CARBON	34.24	41.96	41.36	52.28	42.46	7.43
HYDROGEN	3.43	4.31	3.76	4.80	4.07	0.60
NITROGEN	0.91	1.14	1.04	1.28	1.09	0.15
SULFER	0.41	0.95	0.41	0.52	0.57	0.26
BTU	5931.00	6430.00	6328.00	8457.00	6786.50	1134.30
S (%PYRITE)	17.50	6.30	12.20	11.50	11.40	4.60
S(%ORGANIC)	82.50	48.40	87.80	88.50	76.80	19.10
S (%SO4)	0.00	45.30	24.40	17.40	21.80	39.20

Table 10. Coal chemistry data for surface samples, Frank Campbell, NMBM&MR, 1986

SUBSURFACE COAL CHEMISTRY

SAMPLE #	417-31-1	417-3-1	417-14-1	417-23-1	MEAN	STD DEV
VM	33.39	30.81	36.61	29.86	32.67	3.02
H20	10.86	10.24	8.62	6.67	9.10	1.87
ASH	11.47	27.91	9.87	32.36	20.40	11.40
CARBON	61.64	46.02	63.78	46.27	54.43	9.60
HYDROGEN	4.39	3.65	4.78	4.41	4.31	0.47
NITROGEN	1.12	0.97	1.35	0.93	1.09	0.19
SULFER	0.91	0.78	0.73	0.58	0.75	0.14
BTU	10739.00	8228.00	11303.00	8174.00	9611.00	1644.50
S (%PYRITE)	41.80	6.40	26.00	31.00	26.30	14.80
S(%ORGANIC)	58.20	73.10	74.00	69.00	68.60	7.20
S (%SO4)	0.00	20.50	0.00	0.00	5.10	10.30

Table 11. Coal chemistry data for subsurface samples, Frank Campbell, NMBM&MR, 1986

GROUNDWATER CHEMISTRY OF THE MORENO HILL FORMATION

Groundwater chemistry data were collected from a variety of sources for this study. Plate 1 gives the locations of all wells sampled. Different symbols were assigned to the nine wells which are part of the Salt River Project groundwater-monitoring system. Water-quality analyses for these nine wells were completed at NMIM&T during the summer of 1986.

Figure 2 illustrates water-quality sampling localities. The contour lines represent the water-table elevations in this area as derived from data that were compiled and interpreted by McGurk and Stone (1986). Arrows indicate generalized flow directions interpreted from the contour lines. The numbers next to the well locations are accession numbers which correspond to those used in the McGurk-Stone report. Symbol sizes correspond to distance along a flowpath (DAF) from an interpreted recharge area. Following is a discussion of data collection and groundwater chemistry analysis, graphical methods of data presentation, and trends in groundwater chemistry as a function of flowpath length in the Moreno Hill Formation.

Data Collection

A wealth of water quality data is available for the

Salt Lake Coal Field and surrounding areas from the United States Geological Survey (USGS), the National Uranium Resource Evaluation study (NURE), and the Salt River Project (SRP). NURE data were not included in this study as they were incomplete (Figure 2, 23, 35, 36, 44). The major criteria used to select data from these sources include; 1) less than 5% error for the cation-anion balance, and 2) samples had to be obtained from wells that were screened in the Moreno Hill Formation (mostly the lower member). There are two exceptions in the data set: samples 197 and 101 were obtained from wells screened in the alluvium overlying the Moreno Hill. These samples were used in the study as it was felt that the Moreno Hill Formation is the major source for alluvium in this area; therefore, the mineralogy for these two units is similar and water chemistry analyses from 197 and 101 are relevant to the study.

The USGS has performed extensive groundwater quality studies in Catron and Cibola Counties. This information is available from a computerized database called WATSTORE. Unfortunately, though hundreds of analyses were made available, only six of these met the criteria imposed by the study. These data are presented in Table 12.

The Salt River Project (SRP), 1982, was another source of groundwater chemistry data for this project. SRP has done an extensive water quality study spanning several years in certain parts of the study area. Through the use of

ACC#	164	165	222	232	260	263	123
SAMPLE	416-10 331A	416-10 331B	417-8 121	417-23 212	418-3 442	418-5 144B	317-12 314
DATE	12/17/80	12/17/80	10/14/80	1/22/86	10/31/80	10/30/80	5/22/84
LITHOLOGY	KMH	KMH	KHML	KHML	KHML	KMHM	KMHL
SOURCE	USGS	USGS	USGS	USGS	USGS	USGS	SRP
				CONSTITUENT (MG/L)			
CA	22.0	43.0	5.0	140.0	50.0	47.0	24.0
MG	5.0	11.0	0.0	27.0	32.0	8.0	4.0
NA	89.0	120.0	120.0	180.0	57.0	14.0	156.2
K	1.8	2.3	1.3	4.1	8.7	0.7	4.3
FE	0.0	0.0	1.0	0.1	0.0	0.0	0.0
HCO3	231.0	243.0	280.0	393.0	247.0	195.0	366.0
CO3	0.0	0.0	0.0	0.0	0.0	0.0	0.0
SO4	68.0	200.0	44.0	500.0	66.0	21.0	73.0
CL	5.7	9.5	10.0	6.4	63.0	15.0	9.6
F	0.7	0.6	0.6	0.2	0.6	0.7	1.5
NO3	0.0	0.0	0.0	0.1	4.2	1.8	0.0
SiO2	14.0	10.0	0.0	17.0	25.0	22.0	0.0
TDS	320.0	520.0	330.0	1034.0	460.0	230.0	462.0
EC (US/CM)	533.0	846.0	600.0	1480.0	795.0	418.0	730.0
PH	8.0	7.7	8.1	8.1	8.0	7.7	8.0
TEMP (C)	11.0	11.0	15.0	16.0	13.0	14.0	14.0
HYDROCHEM. FACIES	Na HCO3	Na HCO3-SO4	Na HCO3	Ca-Na SO4	Na-Ca-Mg HCO3-Cl	Ca HCO3	Na HCO3
DAF (km)	7.2	7.6	3.7	10.5	0.0	0.1	8.9

Table 12. Water quality data from the United States Geological Survey, (DAF = Distance Along Flowpath).

several dedicated monitor wells screened within the Moreno Hill Formation, water-quality data were collected and published in their 1982 report. The data from recent sampling and analysis of a number of these wells are presented in Table 13. Nine of SRP's wells, which are regularly monitored to date, were sampled in August, 1985 during one of their scheduled monitor well sampling trips. Major anion and cation analysis of these split samples was performed at NMBM&MR. The results of these analyses compared so closely with analyses performed by SRP in previous years that all obtainable data for these nine monitor wells were averaged. These data are presented in Table 14. Unique to this data set is the fact that the exact lithology of the screened interval was known for these wells and is presented in this Table as sandstone above coal (ssac), sandstone below coal (ssbc), alluvium (al), or coal.

Field Sampling Techniques

All of the nine monitor wells sampled were purged by dedicated submersible pumps before sampling until three well-bore volumes had been evacuated. A few of the wells went dry before this prescribed volume had been achieved. Sampling of these wells occurred after they had been allowed to recharge. For a couple of the wells, recovery took up to an hour.

ACC#	170	167	56	155	156	86
SAMPLE	416-19 24	416-12 221	315-5 413	415-33 114	415-34 324	317-8 314
DATE	5/29/86	5/28/86	5/28/86	5/28/86	5/28/86	7/79
LITHOLOGY	KMHL	KMH	KMH	KMH	KMH	KMHL
SOURCE			NMBM&MR			
			CONSITUENT (MG/L)			
CA	57.0	3.6	6.7	87.0	40.0	12.0
MG	17.0	0.5	1.0	18.0	10.0	2.8
NA	97.0	133.0	170.0	40.0	63.0	240.0
K	3.0	1.2	4.7	4.0	2.2	1.6
HCO3	353.0	339.0	413.0	360.0	285.0	536.5
CO3	0.0	0.0	0.0	0.0	0.0	0.0
SO4	125.0	0.0	40.0	58.0	28.0	180.0
CL	8.0	7.4	14.0	12.0	11.0	19.0
F	0.7	5.8	0.9	0.2	0.3	1.0
NO3	0.3	0.0	0.8	0.8	1.6	0.0
SiO2	7.4	4.4	5.4	8.7	7.9	10.0
TDS	489.0	323.0	447.0	406.0	304.0	677.0
EC(us/cm)	950.0	500.0	650.0	580.0	475.0	930.0
PH	7.1	8.2	8.1	7.1	7.6	8.0
HYDROCHEM FACIES	Ca-Na HCO3	Na HCO3	Na HCO3	Ca HCO3	Ca-Na HCO3	Na HCO3
DAF (km)	11.3	3.2	9.8	4.8	4.0	22.5

Table 13. Water-quality data from NMBM&MR (DAF = Distance Along Flowpath).

ACC#	197	101	207	207	120	120	67	99	95
SAMPLE	416-30-42	317-11-14	416-32-311	416-32-311	317-11-34	317-11-34	316-6-13	317-10-44	317-10-42
	OB1	OB1	M1	M2	M1	M2	M1	M1	M2
LITHOLOGY	al	al	ssbc	coal	ssbc	coal	ssac	ss,shbc	coal
SOURCE	SALT RIVER PROJECT & NMBM&MR								
	CONSTITUENT (MG/L)								
CA	21.1	6.3	3.8	6.2	3.8	8.2	163.5	8.1	9.2
MG	9.4	0.6	1.9	4.2	5.8	1.3	27.3	2.1	2.2
NA	141.6	142.2	152.4	175.0	201.6	203.8	136.5	232.8	214.0
K	3.0	2.3	1.4	8.7	1.4	1.9	3.8	5.2	3.1
FE	0.2	0.4	0.6	1.5	0.3	0.4	0.6	0.3	1.3
HCO3	479.0	327.7	376.3	375.5	280.3	449.8	374.8	455.3	409.5
CO3	0.0	0.0	0.0	29.0	0.0	0.0	0.0	0.0	24.0
SO4	5.7	20.8	12.3	41.2	100.1	92.9	518.9	141.9	106.8
HS	0.00	0.00	0.04	0.15	0.07	0.13	0.00	0.00	0.07
NO3	9.8	7.0	3.5	4.1	4.3	3.5	6.3	2.4	3.9
CL	11.6	6.2	8.5	13.3	19.8	19.9	10.2	28.7	18.3
F	1.0	1.9	1.2	2.3	3.2	1.5	0.6	1.8	2.4
Si	15.4	6.4	7.0	4.8	7.2	8.2	11.0	7.4	7.2
TDS	495.0	425.0	438.0	515.0	589.0	618.0	1098.0	732.0	663.0
EC(us/cm)	772.0	675.0	690.0	818.0	906.0	960.0	1451.0	1150.0	1037.0
PH	7.7	8.2	8.0	8.6	8.3	8.3	7.0	8.2	7.9
TEMP (C)	13.5	14.8	16.0	16.0	14.5	15.0	14.4	16.0	15.0
HYDROCHEM FACIES	Na HCO3	Na HCO3	Na HCO3	Na HCO3	Na HCO3	Na HCO3	Ca-Na SO4	Na HCO3	Na-HCO3
DAF (km)	12.1	9.5	12.9	12.9	7.7	7.7	1.6	9.3	9.7

Table 14. Water quality data from the Salt River Project and NMBM&MR, (DAF = Distance Along Flowpath).

Three samples were taken from each well and filtered through a standard Geopump filter into a 500 ml polyethylene sample container. The Geopump works through the action of peristalsis; therefore, oxidation of the sample is minimized. One set of the sample containers was pretreated with zinc acetate (4 drops in each 500 ml bottle) for preservation of hydrogen sulfide. Another set of bottles was pretreated with hydrochloric acid for preservation of metals and nitrate ion. The third set of bottles was left untreated for analysis of the major cations and anions and total dissolved solids (TDS). Ph, conductivity, temperature, and alkalinity were determined in the field.

Table 15 lists all the analyses performed and the methods used to arrive at the concentration of each dissolved constituent. Exact procedures for each analysis were those in Kand (1975). Sulfide content was determined as described in Golterman (1969). Analyses were performed in the following order to minimize the effects of alteration during storage of the sample; Fe^{2+}-Fe^{3+}, HS^- - SO^{42-}, TDS, Na^+, Mg^{2+}, Ca^{2+}, SiO_2, K^+, Cl^-, Total Fe, NO_3^-, F^- (Lynn Branvold, personal communication, 1986).

Detectable levels of Fe^{2+} were not found in any of the samples. It seems likely that Fe^{2+} was present in these samples, but was oxidized during sampling. This ion is extremely reactive and converts rapidly to Fe^{3+} in the presence of oxygen. Therefore, Eh approximations were based

METHODS OF ANALYSIS FOR WATER QUALITY DATA

CONSITUENT	ANALYTICAL METHOD
Ca	TITRATION
Mg	ATOMIC ABSORPTION
Na	ATOMIC ABSORPTION
K	ATOMIC ABSORPTION
TOTAL Fe	ATOMIC ABSOPRTION
HCO3	HACK FIELD TEST
CO3	HACK FIELD TEST
SO4	GRAVIMETRIC
HS	TITRATION
NO3	COLORIMETRIC
CL	TITRATION
F	SPECIFIC ION ELECTRODE
SiO2	COLORIMETRIC
TDS	GRAVIMETRIC
EC	YSI MODEL 33 S-C-T METER
PH	ORION METER

Table 15. Analytical methods used for water quality analysis.

solely on the redox pair, HS^-/SO_4^{2-}. Sulfide was found at detectable levels in a few samples, and Eh was calculated using these data. The redox state of groundwater was not used in geochemical modeling (to be discussed in Chapter 5) due to the absence of sufficient data (Appendix 2, a discussion pE and Eh with respect to problems associated with its use).

Graphical Methods Used for Analysis of Water Quality Data

Alexander Zaporovec (1972) presents a very useful compilation of the various graphical methods which can be employed to interpret and evaluate water quality data (also see Freeze and Cherry 1975). Because of its simplicity and wide use, the Piper Diagram (Piper, 1944) was chosen for the purposes of hydrochemical classification of the various samples chosen for this study. (The reader is referred to two papers, Back, 1966 and Krothe and Bergenson, 1981, for examples of the use of hydrochemical facies in groundwater studies.) A graphical technique not described in Zaporovec's paper was devised to aid in the interpretation of the hydrogeochemistry of in the Moreno Hill Formation. This method will be addressed in detail following a short discussion on Piper Diagrams.

Piper Diagrams

Figure 17 is a Piper Diagram (Piper, 1944) of all data

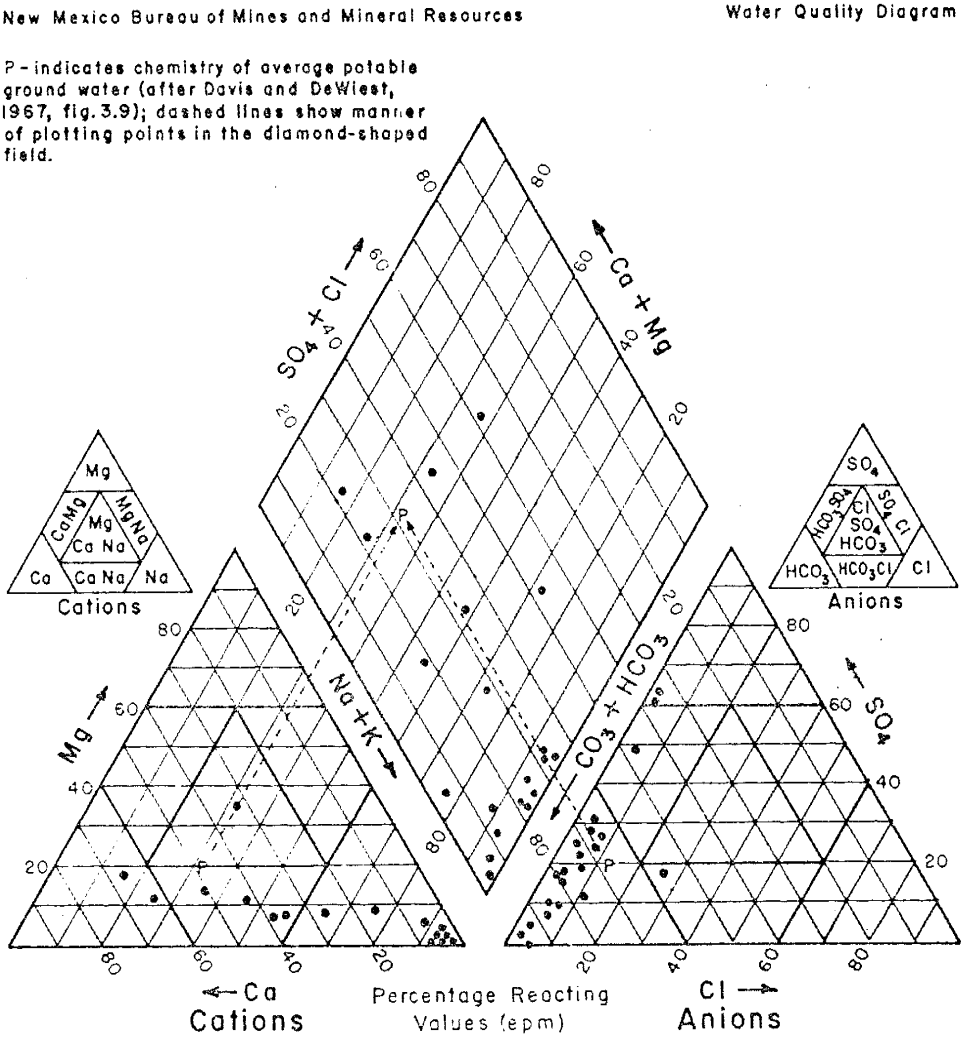

Figure 17. Piper Diagram of water-quality analyses.

considered in this study. A great majority of the data points fall towards the bottom corner of the diamond where primary alkalinity (carbonate alkali) exceeds 50%. These waters are considered to be extremely soft (ie. contain a great deal more Na^{+} than Ca^{2+}) in proportion to their total dissolved solids content. Some of the data occur in the center portion of the diamond where no one cation-anion pair exceeds 50%. Three of these data points fall in the upper half of the diamond, a subfield characterized by secondary alkalinity (or carbonate hardness) exceeding 50%. Here, the chemical properties of the water are dominated by alkaline earths and weak acids. Finally, there is one data point in the left side of the diamond where primary salinity (or non-carbonate alkali) exceeds 50%. The chemical properties of these waters are dominated by the alkalies and strong acids.

Mixing of hydrochemical facies can be examined through the use of Piper Diagrams. Water-quality data from two distinct facies would tend to plot along a straight line in each of the three fields previously described. The endpoints of these lines would represent the chemical character of the two separate waters. Most of the data in Figure 17 do appear to fall on a straight line, particularly in the two lower subfields. However, as Piper (1944) explained, these graphic criteria alone cannot justify the probability of mixing; therefore, he devised an algebraic

method to lend support to graphical observations.

This method was applied to various sample combinations which could possibly fit a mixing trend as described above. Samples 232 and 67, which consistantly plot off-trend from the other data, due to higher concentrations of calcium and sulfate, were employed as one end member, while sample 86, which has the greatest value for distance along a flowpath, was chosen as the other. If these samples, 67 and 232 represented water of a different geochemical facies, then Piper's mixing method should reveal this condition. The results of this evaluation were not at all convincing, indicating that the simple mixing of two types of waters is not a controlling process.

Groundwater Chemistry as a Function of Flowpath Length

An interesting graphical method, which may be used to interpret the distribution of dissolved ions in groundwater, is to plot ion concentration as a function of distance along a flowpath (DAF). This method has the benefit of showing directly how water chemistry evolves as it moves in response to the local hydraulic gradient.

Ideally, in order to have much faith in the conclusions reached as result of this excercise, four criteria must be met in the study area; 1) an understanding of the hydrogeology; 2) groundwater samples from wells screened only in the formation or formations of interest; 3) data

from wells located along a flowpath extending from a recharge area to a discharge area; and, 4) a homogeneous aquifer with details of its mineralogy understood. The first three of these criteria are are adequately met at the site; however, the fourth one poses some difficulties which will be brought to light in the following discussion.

The Moreno Hill Formation is very heterogeneous with discontinuous lenses of sandstones and coals, localized sandstone cementation, and layers of mudstones, siltstones, silty mudstones, muddy siltstones, etc.. These variations in lithology throughout the formation impose complications on an already complex system. However, despite all the variability and uncertainty with respect to mineralogy and well construction, some distinct relationships between groundwater chemistry and DAF are apparent.

Determination of the DAF value for each sample location shown in Figure 2 was an interpretive process. Groundwater flow from points of recharge to points of discharge is controlled by the elevation and shape of the water table which is in turn controlled by topography in this area (McGurk and Stone, 1986). Though actual flow paths in the Moreno Hill Formation are much more complex due to the heterogeneity previously described, a simplified model can be invoked to facilitate an understanding of groundwater chemistry. Though discontinuous sandstone lenses do provide for localized areas of recharge and discharge along a

flowpath, a regional perspective of groundwater flow assumes that recharge occurs in the higher elevations and upper reaches of the major draws, with discharge occuring in the lower reaches of the Nation's Draw and Largo Creek valleys.

Using this simplified model of groundwater flow in the Moreno Hill Formation, DAF's were measured from U.S.G.S. 7 1/2 minute quadrangle maps with the aid of a K&R Instruments, Inc. Map Measurer. Prior to the measurement of flowpath lengths for each sample location, the accuracy of this instrument was tested using the scales provided on the quadrangle map. It was found that this instrument was accurate to 0.1 mi. Measurement of DAF began at each sample location and continued back along major drainages to the areas of recharge, namely the higher elevations and the upper reaches of major draws. This process provides an estimation of the distance of each sample location from a designated recharge area. A scaling factor was introduced into the plotting program (Appendix 3) so that the size of the data point, shown in the following illustrations, is a direct reflection of the magnitude of DAF (refer to Tables 12 through 14).

Chemical Trends

As discussed above, the only sample analyses which were considered in this study had ion-balance errors of 5% or less. A graphical method for checking for the accuracy of

water quality data is to plot electrical conductivity against total dissolved solids (TDS). TDS (mg/l) is related to specific conductance (umhos/cm) by a factor which varies from 0.55 to 0. 75 for waters with a maximum TDS value of up to a few thousand milligrams per liter (Hem, 1985). Therefore, an x:y plot of these two variables should yield a straight line. Groundwater with dominant anions being bicarbonate and chloride will have a factor near the lower end of this range, while groundwater with sulfate as the dominant anion will have a factor near the upper end of this range.

Figure 18 illustrates the relationship between TDS and Specific Conductance. A linear regression analysis was used to draw the best fit line which has an R^2 value of 0.95. This indicates an excellent straight-line fit for the data. Some of the scatter in these data is attributable to differences in the major anions (SO^{42-} vs HCO_3^-, Cl^-) between the various samples.

Total dissolved solids plotted against DAF is illustrated in Figure 19. An R^2 value of 0.37 indicates quite a bit of scatter in these data, though clearly there exists a positive correlation between the magnitude of DAF (which corresponds to the size of the symbol) and the value for TDS. Samples 67 and 232 were not used in the regression analysis (as illustrated by the crosses on the diagram). For reasons which will be brought to light in

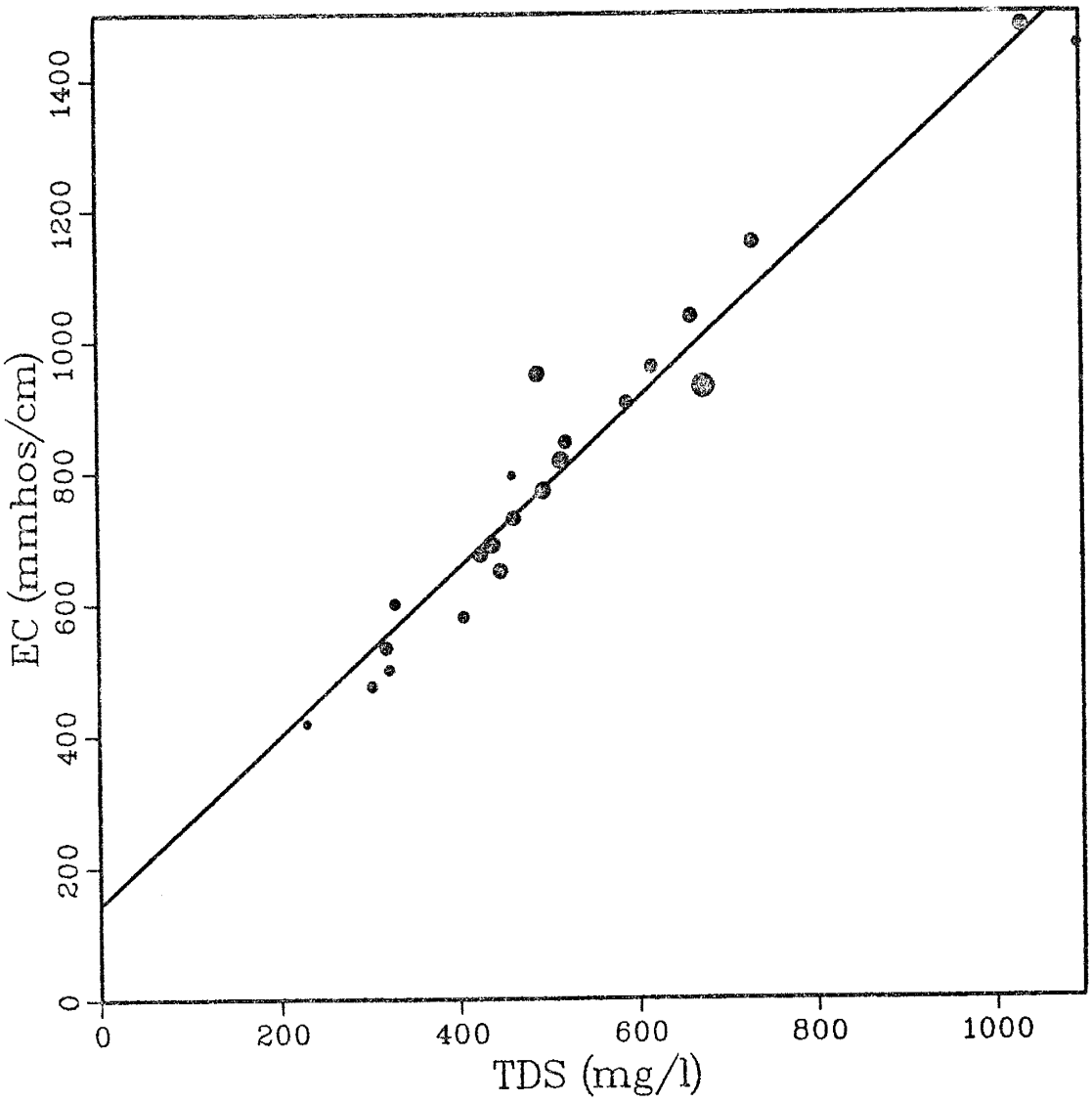

Figure 18. Total dissolved solids vs specific conductance.

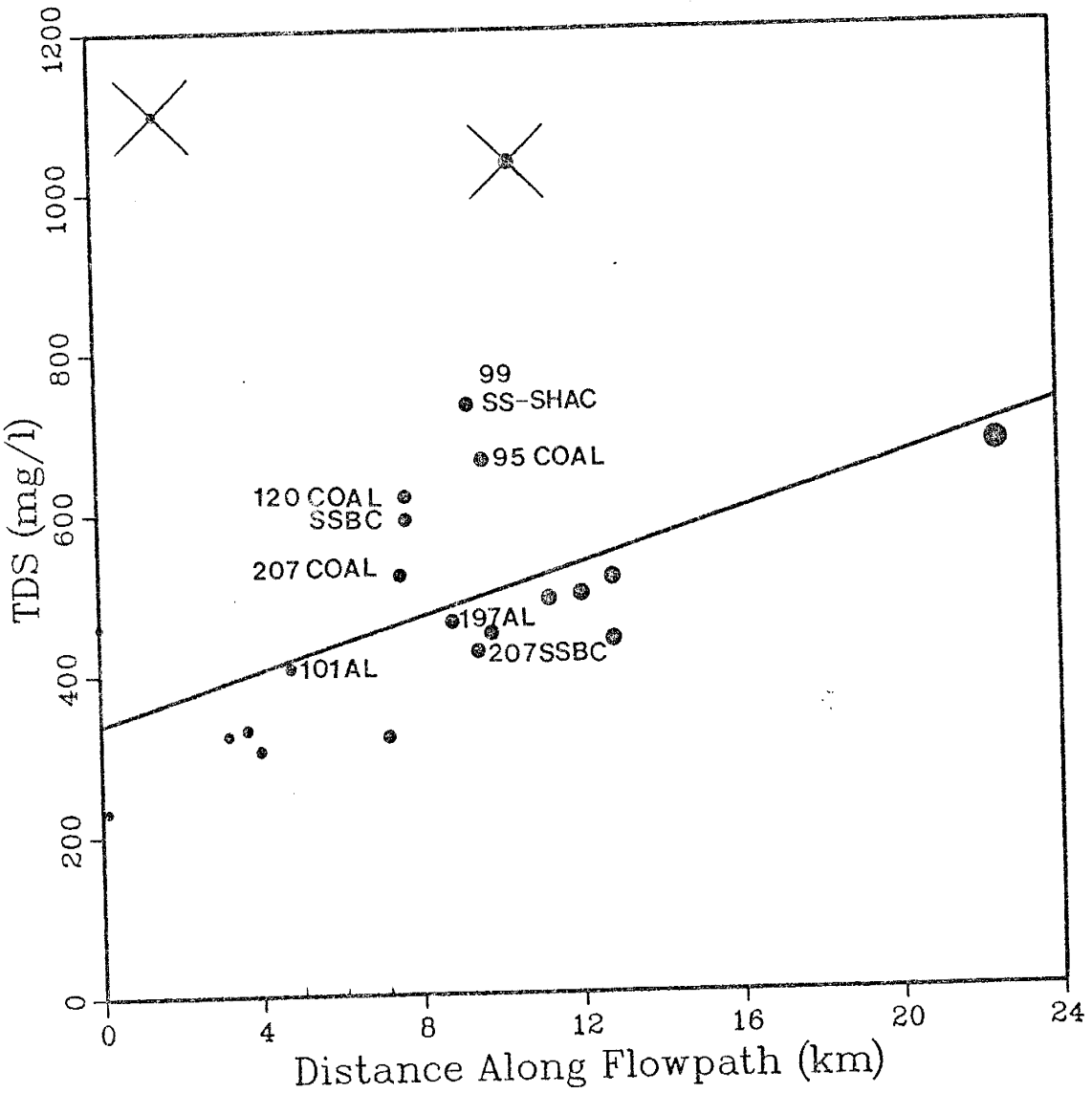

Figure 19. Total dissolved solids vs distance along a flowpath.

upcoming chapters, it is believed that these samples reflect localized conditions in aquifer and are not representaive of the system as a whole. Relative to the other samples, 67 and 232 have very high calcium and sulfate concentrations.

A myriad of explanations is available to explain the scatter in these data. Most importantly, when considering the heterogeneity of the Moreno Hill Formation, it would be surprising if there were not some scatter in the data. Therefore, the positive correlation which does exist between DAF and TDS suggests that interpreted values for DAF are relevant to the study, and can be used with some degree of certainty for comparison of data. Data from the SRP monitor wells exhibit a great deal of scatter. As discussed earlier, these wells are screened in different lithologies which are indicated in Figure 19. Heterogeneity is responsible for some of the scatter in these data as illustrated by the data from these nine wells. Many of the other wells from which data has been obtained for this study are probably screened in different sandstone lenses throughout the formation, and many are used as water supply wells for cattle. Data from wells screened in similar lithologies may conform more closely to a given trend.

Figure 20 illustrates the relationship between sodium (Na^+) and DAF. Once again a positive correlation exists in these data, but the R^2 value was low at 0.45. Significant to this study is the fact that sodium increases dramatically

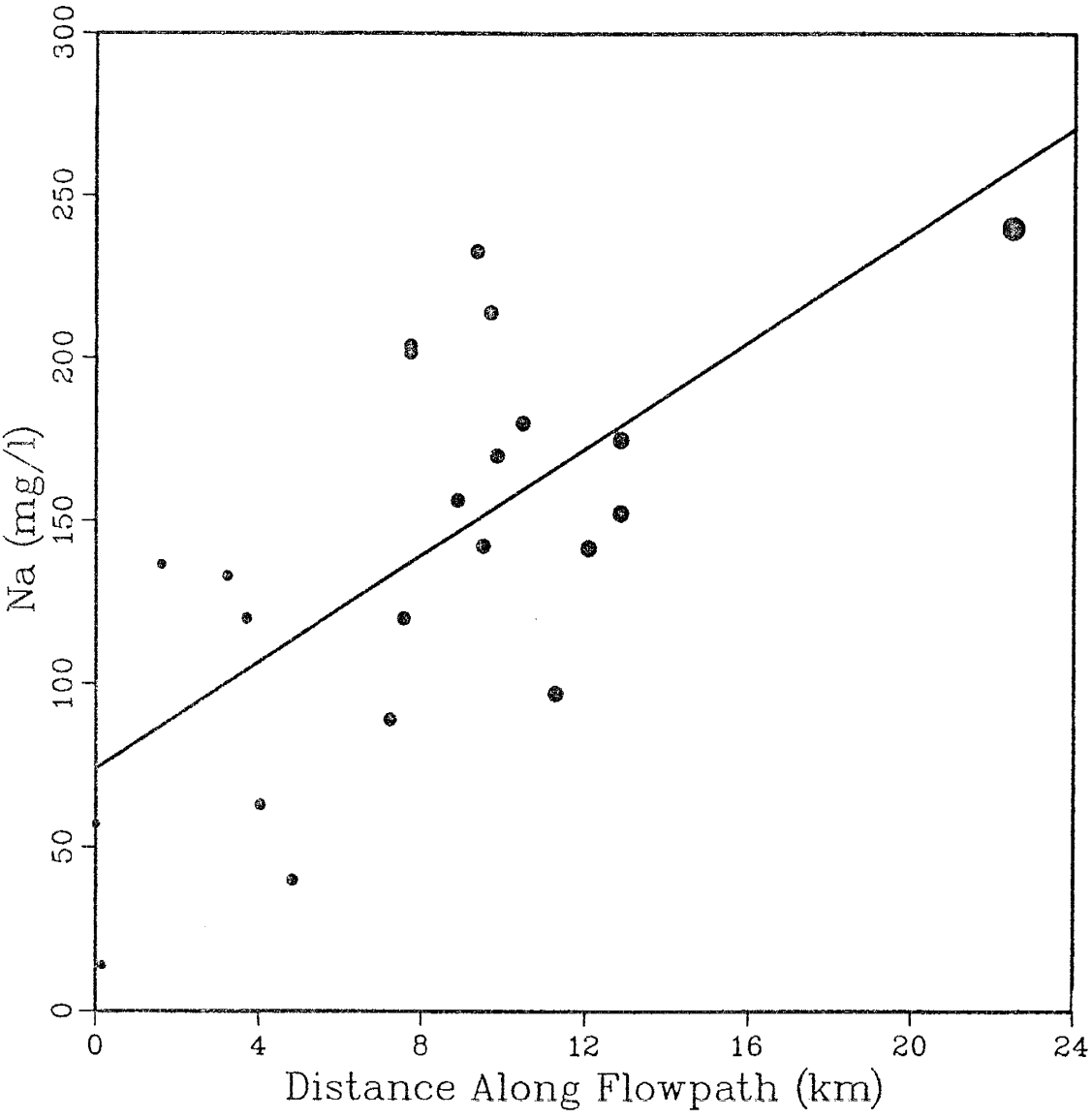

Figure 20. Sodium concentration as a function of distance along a flowpath.

with DAF (from a low of 14 mg/l to a high of 240 mg/l).

When Na^+ has been brought into solution by the alteration of minerals, it tends to remain in that state because there are no important precipitation reactions which can maintain a low Na^+ concentration (Hem, 1985). One way that Na^+ can be attenuated is by the process of adsorption on mineral surfaces, particularly the clay minerals, which have a high cation exchange capacity (CEC). However, adsorption of monovalent cations is much weaker than divalent cations; therefore, if the latter are available, they will generally be preferentially exchanged for the monovalent cations. In most groundwater systems, Na^+ increases with distance along a flowpath. How rapidly this change occurs over distance is dependent on the number of geochemical processes involved which act as sources for this constituent.

The sodium content of dilute waters (<1000ppm) is nearly all in the form of Na^+ ion. Sources for this constituent in sedimentary rocks include alteration of feldspar, particularly albite, and clay minerals with exchangeable Na. When sandstone units and clay-rich units are interbedded, as in the case of the Moreno Hill Formation, water and Na^+ can be retained in the less permeable, clay-rich strata. If wells penetrate these alternating units, and are pumped consistently for long periods of time, saline solutions present in the less

permeable strata can be induced to move into the more permeable zones. An increase in Na^+ concentration over time in a heavily pumped well has been attributed to this mechanism (Hem, 1985) though this theory was not tested. Since the wells used for this study are multipurpose (some are pumped constantly by windmills for cattle while others are pumped sporadically for monitoring water quality), this process could be invoked to explain some of the scatter in these data.

Alkalinity vs DAF is illustrated in Figure 21. A positive correlation exists between these data ($R^2 = 0.51$). There is a slightly better fit between these data than those for sodium vs DAF, but scatter is still a problem. Bicarbonate ion, HCO_3^-, is by far the dominant contributor to the total alkalinity for these samples, most of which did not have detectable levels of carbonate, CO_3^{2-}.

Bicarbonate is formed from the reaction of carbon dioxide, CO_2, and water. Sources of CO_2 include; 1) soil gas, 2) biologically mediated sulfate reduction, and 3) the dynamochemical breakdown of organic material (Chapter 6). The HCO_3^- concentration of natural water is held within a moderate range due to the effects of low carbonate mineral solubilities. Concentrations can reach as high as 1000 mg/l in waters that are low in calcium and magnesium, and where processes which release CO_2 are ocurring (Hem, 1985). Commonly, surface waters contain concentrations around 200

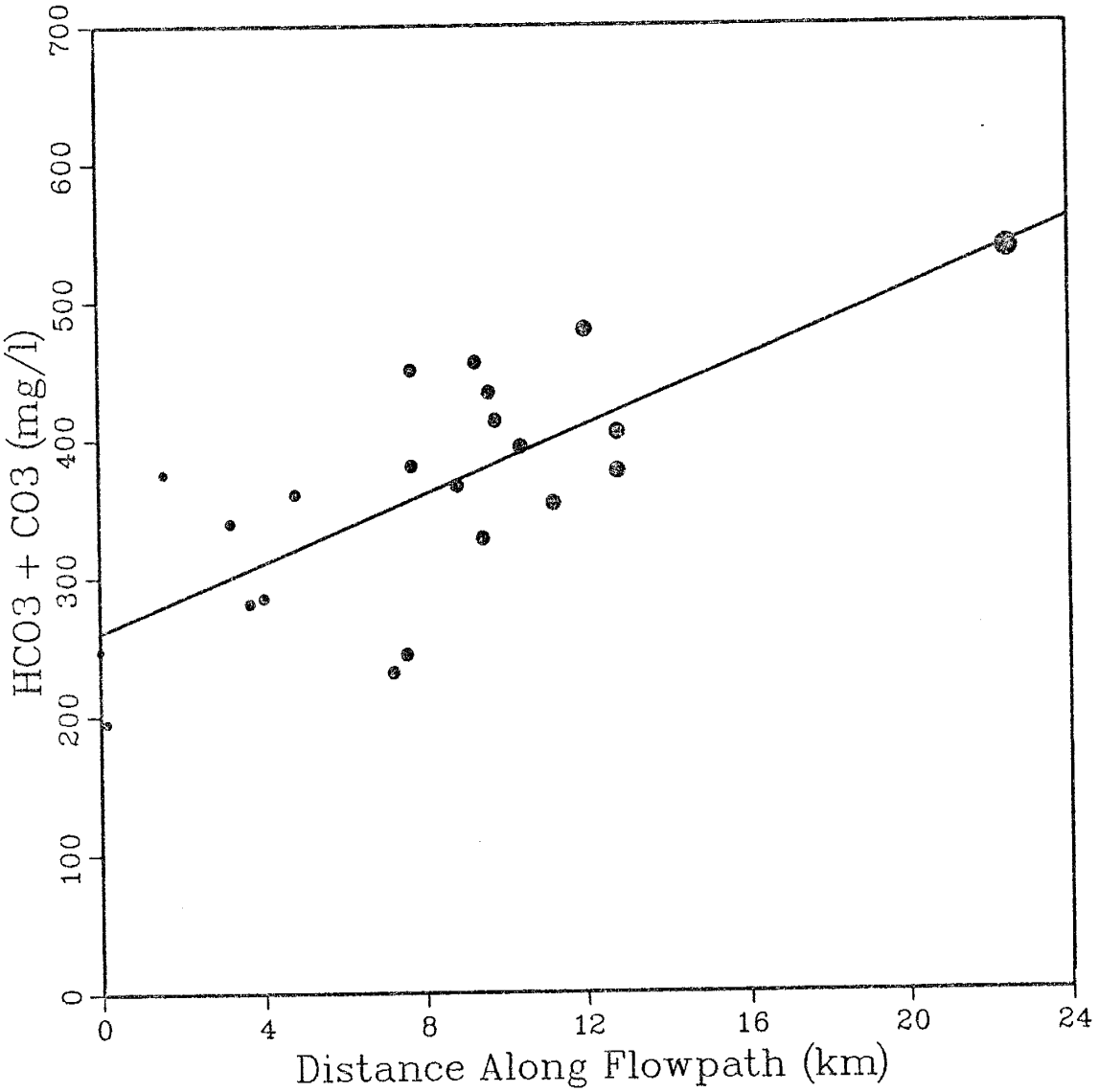

Figure 21. Total alkalinity as a function of distance along a flowpath.

mg/l, while groundwater can have somewhat higher concentrations. Most of the samples considered in this study had HCO_3^- concentrations in excess of 300 mg/l. A maximum of 536 mg/l was found in sample 86. This suggests that there are processes at work to produce CO_2 in this system (most samples have relatively low concentrations of calcium and magnesium).

Figure 22 is a graph of calcium (Ca^{2+}) as its concentration varies with flowpath length. Data from samples 67 and 232 were ignored in the regression analysis. Though correlation is poor ($R^2 = 0.37$), the trend exhibits a decrease with flow path length.

Sources of Ca^{2+} in natural waters include plagioclase, calcite ($CaCO_3$), dolomite ($CaMg(CO_3)_2$), and gypsum ($CaSO_4$). Ca^{2+} can form a complex with organic ions, and this process may be responsible for removing some of the Ca^{2+} from the system; however, it was not explored by this study, and this process is considered insignificant by Hem (1985). Precipitation of carbonate minerals as well as the cation exchange process controls the solubility of calcium in most natural waters. Cation exchange is the dominant process which reduces the concentration of Ca^{2+} along a flowpath in this system.

The trend of magnesium (Mg^{2+}) as it varies with DAF is similar to the calcium trend, however scatter in these data is even more pronounced (Figure 23). Though a decrease in

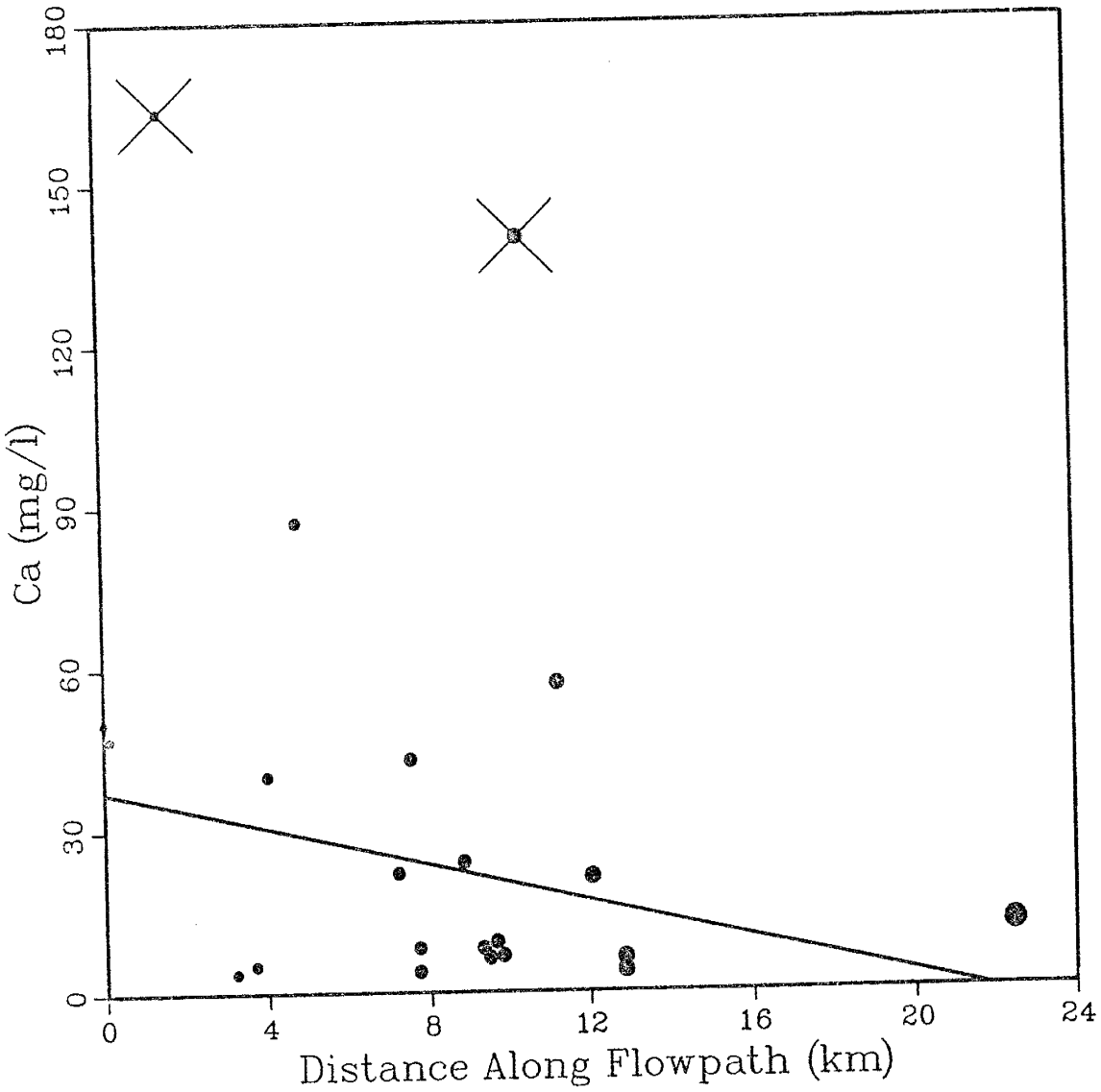

Figure 22. Calcium concentration as a function of distance along a flowpath.

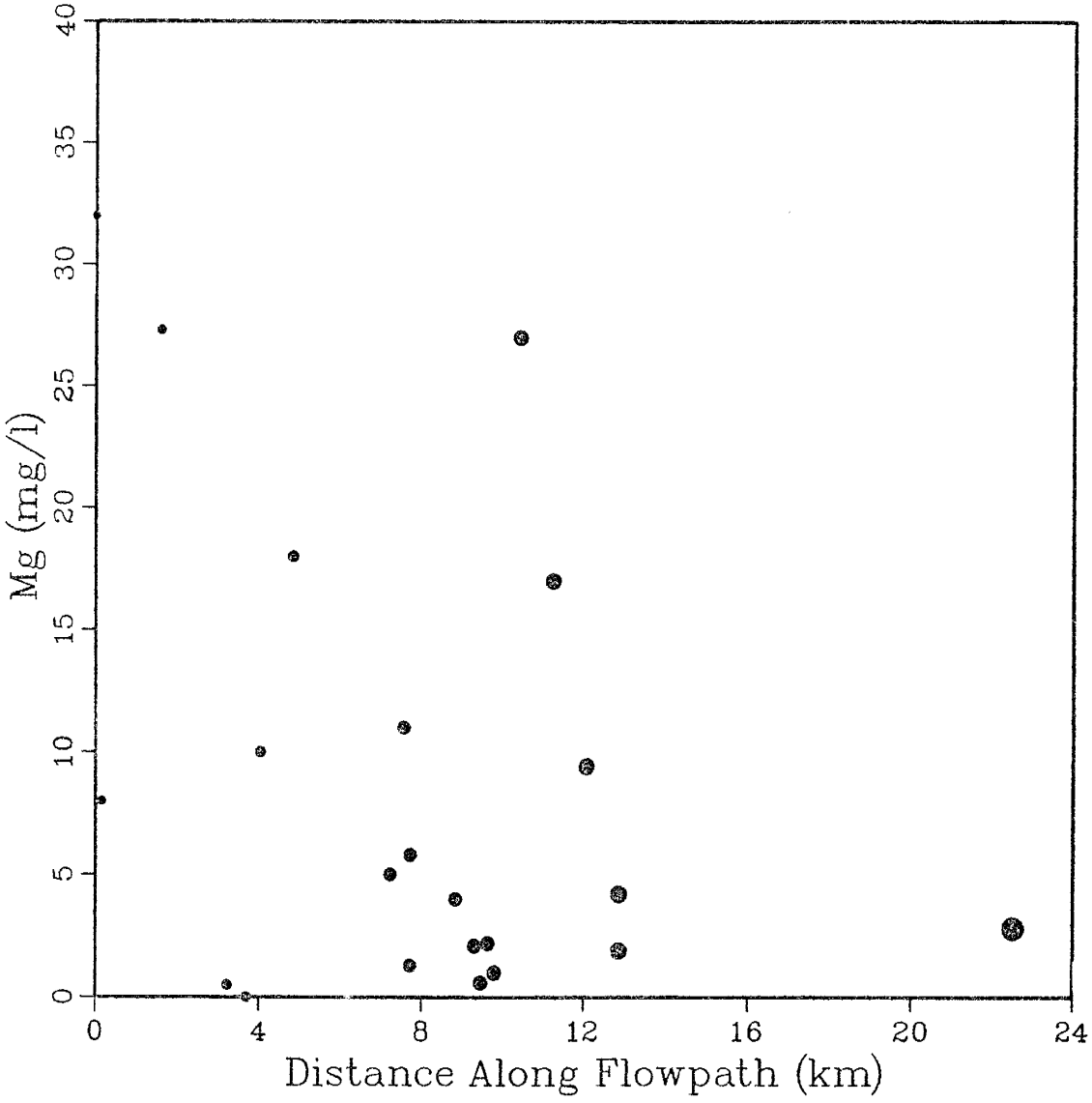

Figure 23. Magnesium concentration as a function of distance along a flowpath.

concentration can be inferred, a regression line was not calculated as the fit between data, even ignoring samples 67 and 232, is so poor.

Contrary to what may seem intuitive, the geochemical behavior of Mg^{2+} is much different than Ca^{2+}. This is due mainly to the fact that Mg^{2+}, holds a strong hydration shell, similar to the behavior of aluminum (Hem, 1985). For this reason, crystalline magnesium compounds, such as dolomite, contain water molecules in their structure. One similarity that both these ions do share is the fact that they both contribute equally to water quality in the form of hardness.

Sources of Mg^{2+} in sedimentary rocks include dolomite (which contains an equal proportion of Ca^{2+}) biotite, and chlorite (a very minor constituent of the sandstones within the Moreno Hill Formation). The Mg^{2+} ion is the form in which magnesium is present in most natural waters where $^{S}_{u}$lfate and HCO_3^- are present in amounts <1000 mg/l. A considerable amount of supersaturation is necessary for any magnesium-carbonate species to precipitate from solution. This process is rarely significant in limiting the Mg^{2+} concentration of natural waters. The cation-exchange behavior of Mg^{2+} is similar to that of Ca^{2+}: both are adsorbed strongly by clay minerals. As cation exchange is a dominant geochemical control in clay-rich sedimentary rocks, it is not surprising that both Ca^{2+} and Mg^{2+} decrease

in concentration with increasing DAF.

Sulfate (SO_4^{2+}) exhibits a general increase with DAF, although R^2 for these data is low, 0.30 (Figure 24). The regression line can therefore only portray a trend, and cannot be used for predicting concentration at various points along a flowpath. Both SO_4^{2+} and Ca^{2+} are seen to have comparatively high concentrations in samples 67 and 232.

The element sulfur occurs in oxidation states ranging from S^{2-} to S^{6+}; therefore, the redox state of groundwater strongly affects its oxidation state. The oxidized form of sulfur, SO^{42-}, has a stable four-coordinated structure with oxygen. Because iron is a common element and widely distributed, iron sulfides, such as pyrite, have a significant influence on sulfur geochemistry depending upothe redox state of the groundwater.

Redox propeties of groundwater are difficult to quantify. Recently, it has been shown that Eh meters do not adequately measure this property (Appendix 2). If the concentrations of several redox couples (such as HS^-/SO_4^{2+}, Fe^{2+}/Fe^{3+}, or NH_4^+/NO_3^-) are known, a closer approximation of the redox state for the system can be obtained. The HS/SO_4^{2-} pair was used to attempt to establish the redox state of groundwater samples from the SRP monitor wells. Due to insufficient data, oxidation-reduction phenomenon were not considered in this study. Sulfur, in its reduced

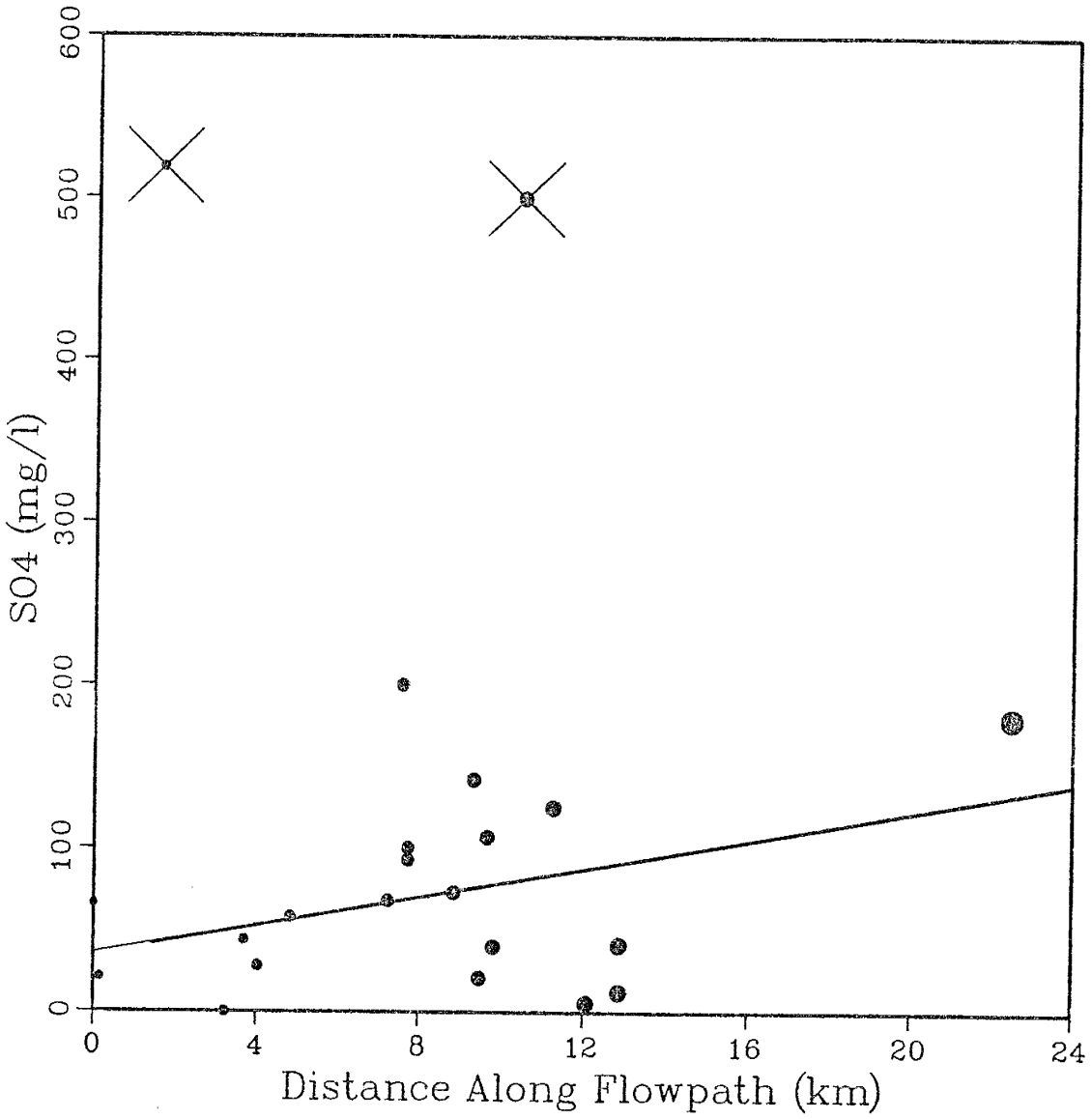

Figure 24. Sulfate concentration as a function of distance along a flowpath.

form, is a common consituent of sedimentary rocks as metallic sulfide, FeS_2, or pyrite. When these sulfide minerals undergo weathering due to contact with oxygen, SO_4^{2-} is liberated along with hydrogen.

Chloride (Cl^-) is seen to increase slightly with DAF, though the overall variation in concentration between data points is not great enough to establish any definite trends (Figure 25). Sample 260 had an anomalously high concentration of Cl^- (63 mg/l) which can not be explained by the data available for this study.

Chloride can occur in various oxidation states, from Cl^- to Cl^{7+}; however Cl^- is the most common form in natural waters exposed to the atmosphere (Hem, 1985). Chloride forms ion pairs or complex ions with some cations. These complexes are not considered stable enough to be of importance.

Sources of Cl^- are few as minerals which contain chloride as an essential component are rare (though atmospheric Cl^- is a source not considered in this study). In marine sedimentary environments Cl^- can be introduced as a soluble salt. Fine-grained marine shale might retain some of this Cl^- for long periods of time. Prolonged pumping of wells in interstratified formations may effect increased concentrations of chloride with time.

Chloride's contribution to geochemical processes is insignificant in most natural waters other than brines. For

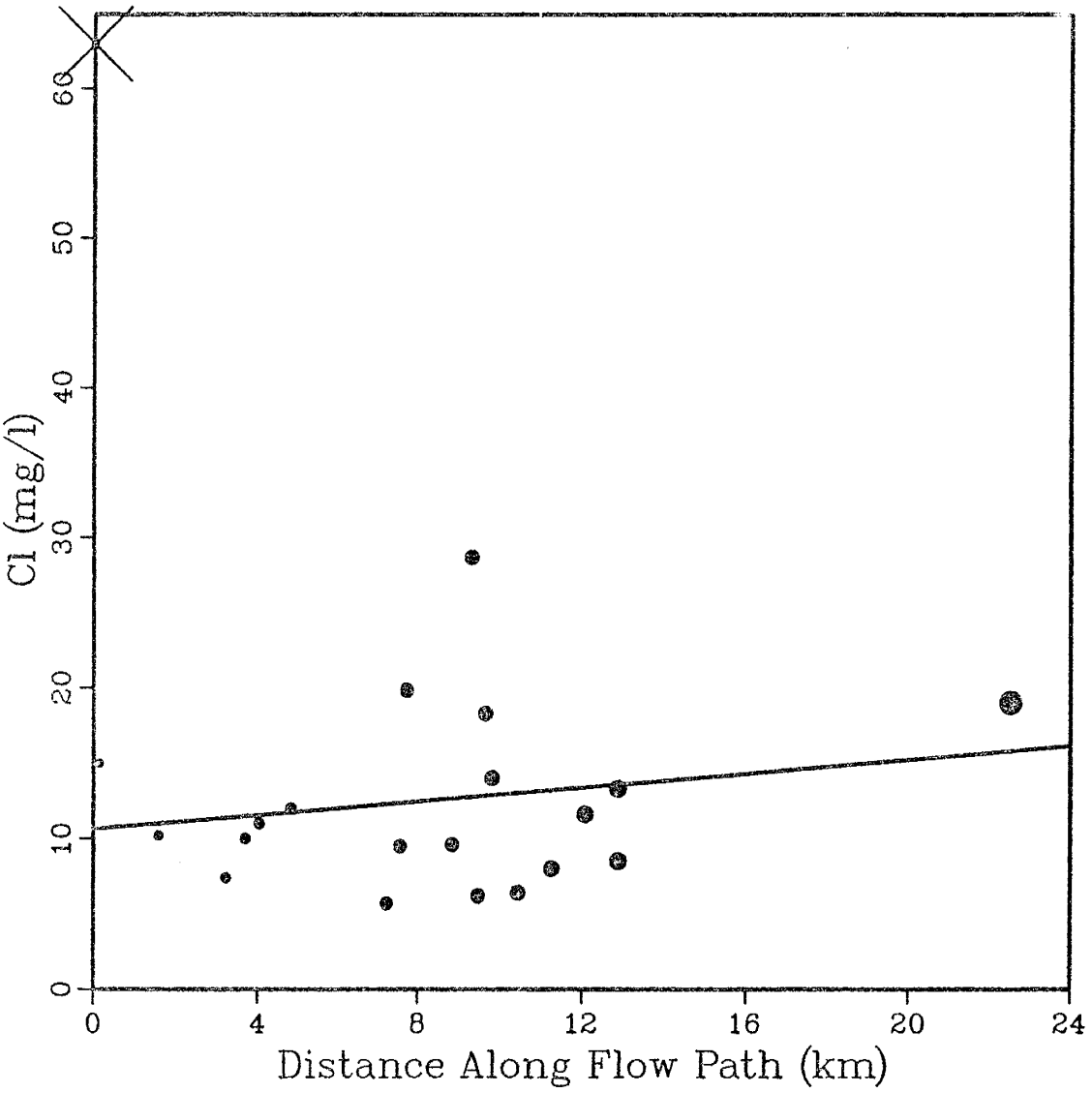

Figure 25. Chloride concentration as a function of distance along a flowpath.

this reason, it can be referred to as a conservative ion which enters into few chemical processes other than dissolution when present as a soluble salt or metal complex. This conservative behavior is disrupted when movement of groundwater is through a compacted clay or shale. Chloride ions are very large and are retained by the tight formations. Due to the heterogeneity of the Moreno Hill Formation, this phenomenon could account for some of the scatter in these data. In many groundwater studies Cl^- is used as an indicator ion for length of flowpath due to its conservative behavior. However, concentrations are so low, with variation in the data so minimal, that the true behavior of the chloride ion is not apparent in Figure 25.

There does not appear to be any significant trend (therfore a regression line was not calculated) in potassium (K^+) concentration as it varies with DAF (Figure 26), and there are several possible explanations for this. During the weathering of silicate minerals, particularly feldspars, K^+ is liberated with much greater difficulty than Na^+. Once introduced into solution, K^+ has a strong tendency to be incorporated into solid weathering products such as clay minerals. Therefore, due to more complicated geochemical processes, the concentration of K^+ in most natural waters is much less than that of Na^+, even though both constituents are present in great abundance in alkali feldspars. Also, K^+ is one of the more difficult constituents to analyze;

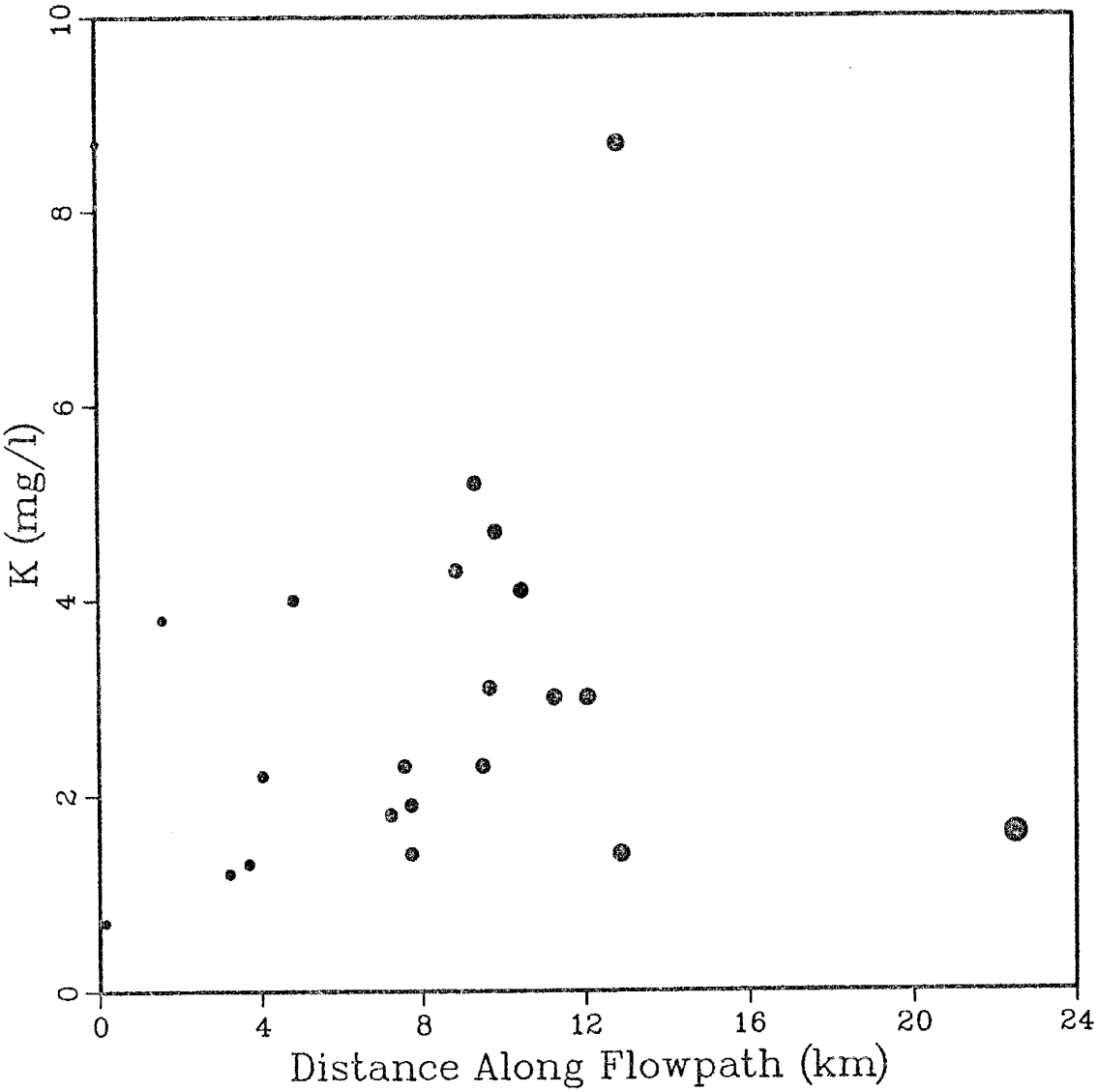

Figure 26. Potassium concentration as a function of distance along a flowpath.

therefore, analytical errors are a likely cause of some of the scatter in these data.

The principle sources of K^+ in sedimentary rocks are orthoclase and microcline (Hem, 1985); they occur in sandstones as unaltered feldspar grains. The large potassium ion, when present in some clay minerals such as illite, is held in spaces between crystal lattices and is not removed by ion exchange processes.

Figure 27 illustrates the relationship between silica (SiO_2) and DAF. The scatter in these data is so great that a regression line was not calculated, though general decrease in silica concentration is seen when comparing samples with small DAF values to samples with large DAF values; the relationship is by no means clear. As was discussed with regard to potassium, it is believed that the scatter in these data can be explained by geochemical processes, such as the formation of secondary minerals. Analytical error may also play a role. Garrells and MacKenzie (1967), state that the total dissolved silica content of groundwater is obtained in the first few feet of travel by the breakdown of silicate minerals, particularly the plagioclase feldspars. This theory appears to apply to these data (observe symbol size variation in Figure 27). Some precipitation event must be at work to remove silica from the system as DAF increases.

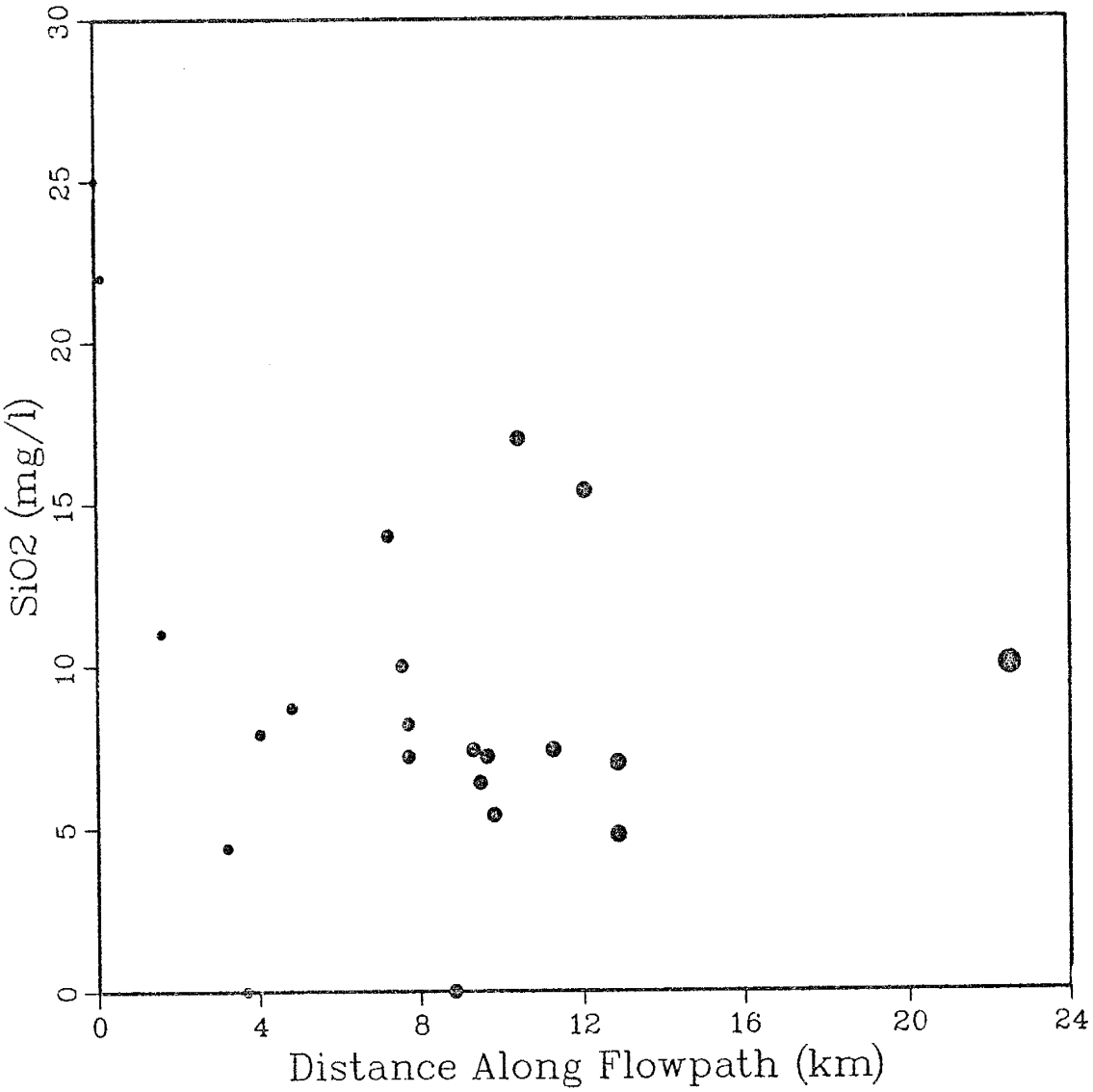

Figure 27. Silica concentration as a function of distance along a flowpath.

Molar Ratios of Dissolved Constituents

A plot of Na^+ versus HCO_3^- is illustrated in Figure 28. An R^2 value of 0.63 for the regression line indicates a relatively strong positive correlation for these data. The weathering of feldspars is believed to be a dominant geochemical process in this system, and is responsible for this positive correlation. This will be discussed further in Chapter 6.

The regression line for Figure 29 of Ca^{2+} vs SO_4^{2-} has an R^2 value of 0.67. This depends on the values for 67 and 232 without which the correlation would be poor. Locally, dissolution of gypsum involves the simultaneous release of Ca^{2+} and SO_4^{2-} ions into solution. The distribution of dot sizes suggests that this process is not related to DAF.

In Figure 30, HCO_3^- was added to the SO_4^{2-} values to consider the possibility of more than one source for Ca^{2+} The effect of this was to lower the R^2 value for the regression line to 0.41. The addition of Mg^{2+} to the plot lowered the R^2 value to 0.38 (see Figure 31). These results point to the complicated geochemical processes at work in this system.

To look for the possibility of a dominant cation exchange process at work in this system, Figure 32 was generated. The results indicate that cation exchange is not the only process which contributes Na^+ to the system. When cation exchange processes are largely exhausted, Na^+ is

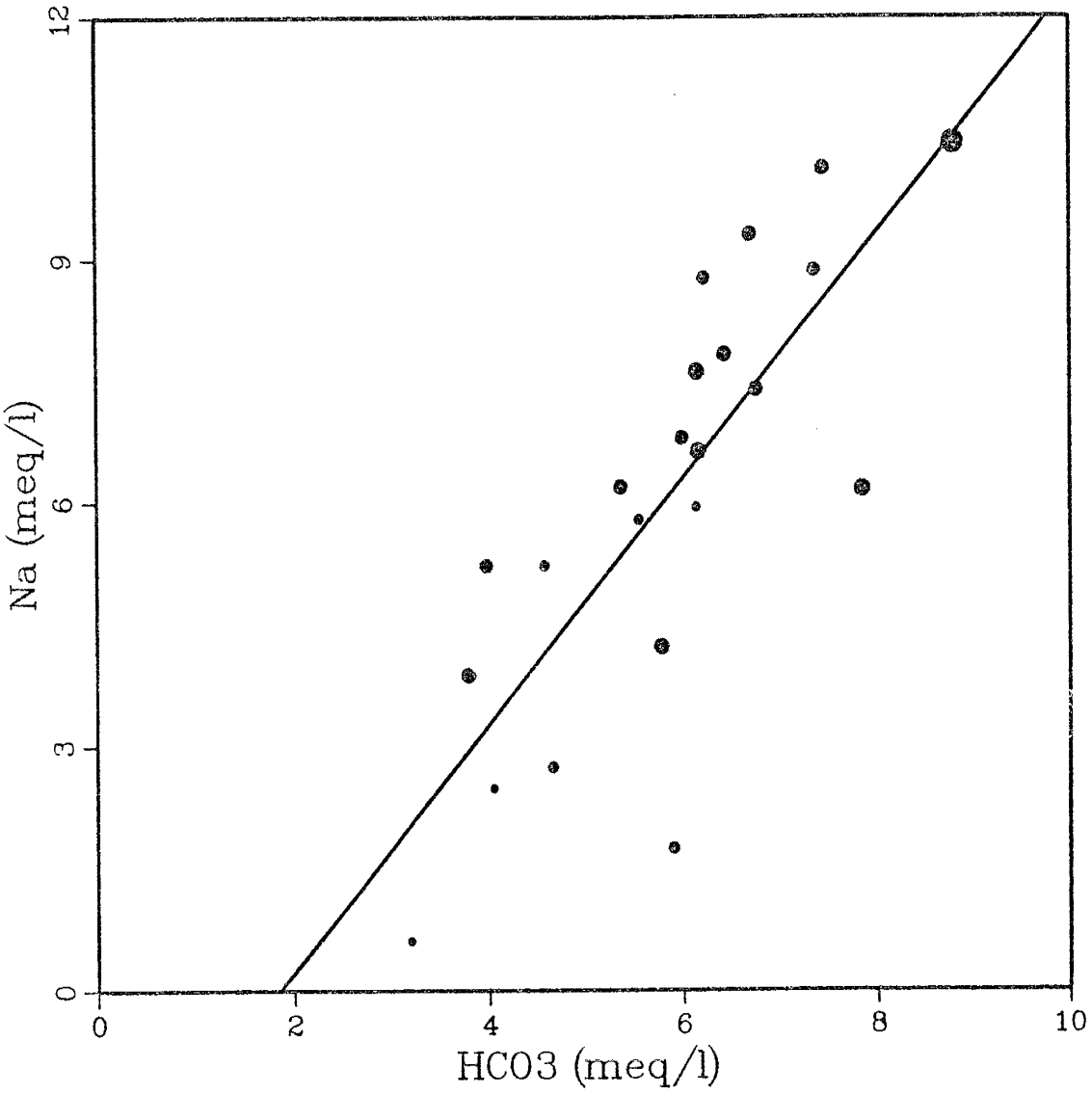

Figure 28. Sodium vs bicarbonate, size of dot is directly proportional to flowpath length.

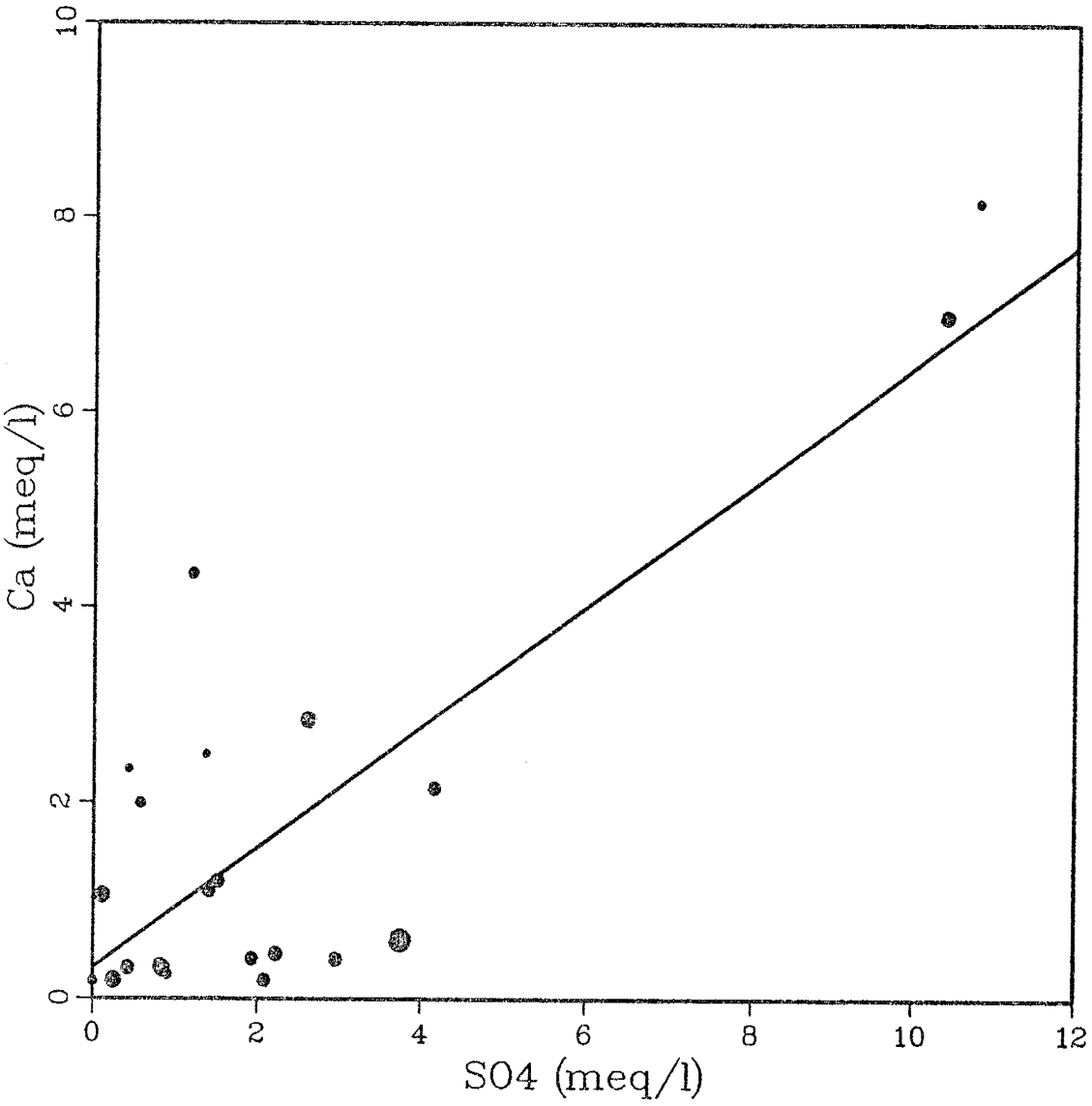

Figure 29. Calcium vs sulfate, size of dot is directly proportional to flowpath length.

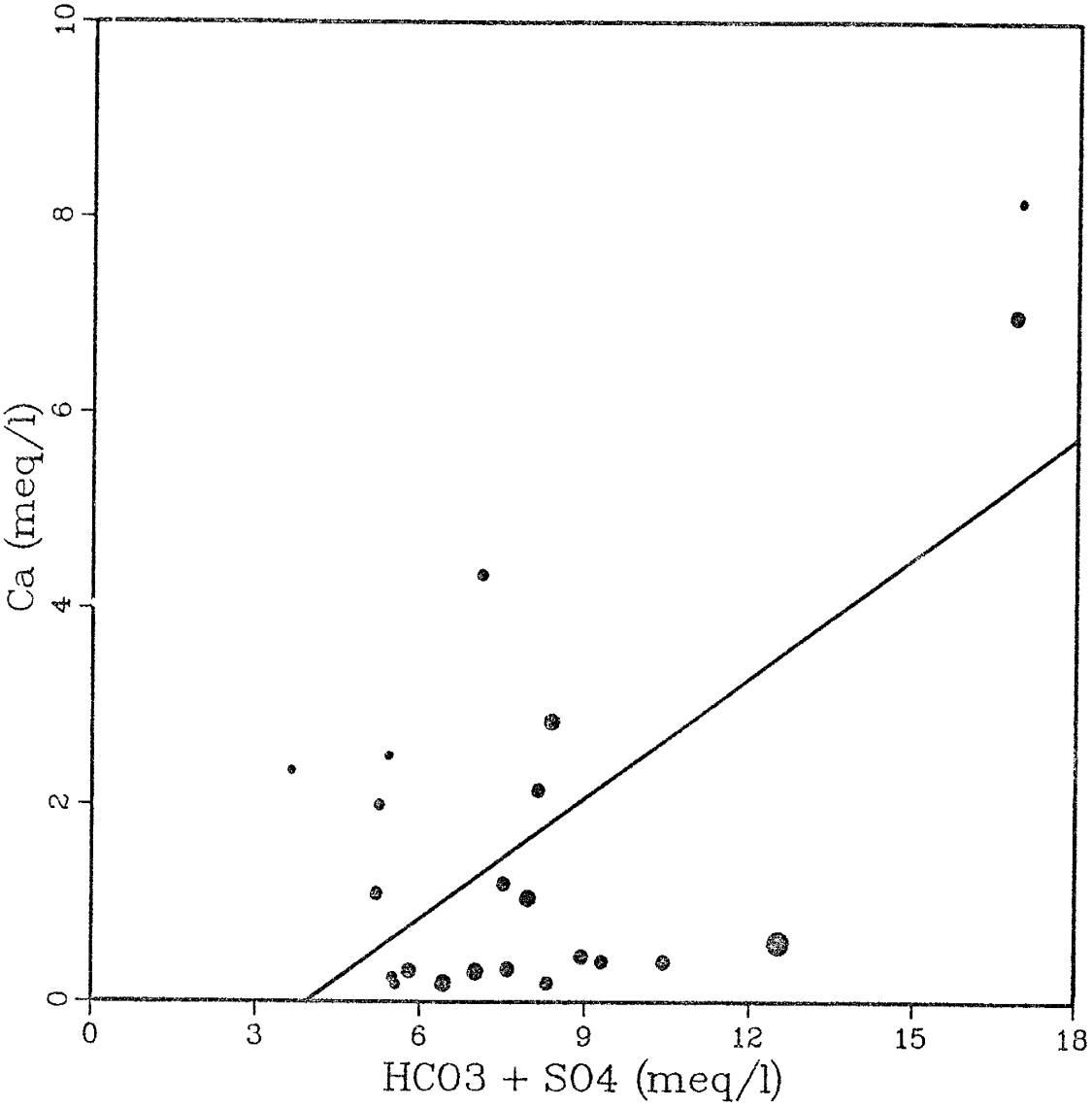

Figure 30. Calcium vs sulfate plus bicarbonate, size of dot is directly proportional to flowpath length.

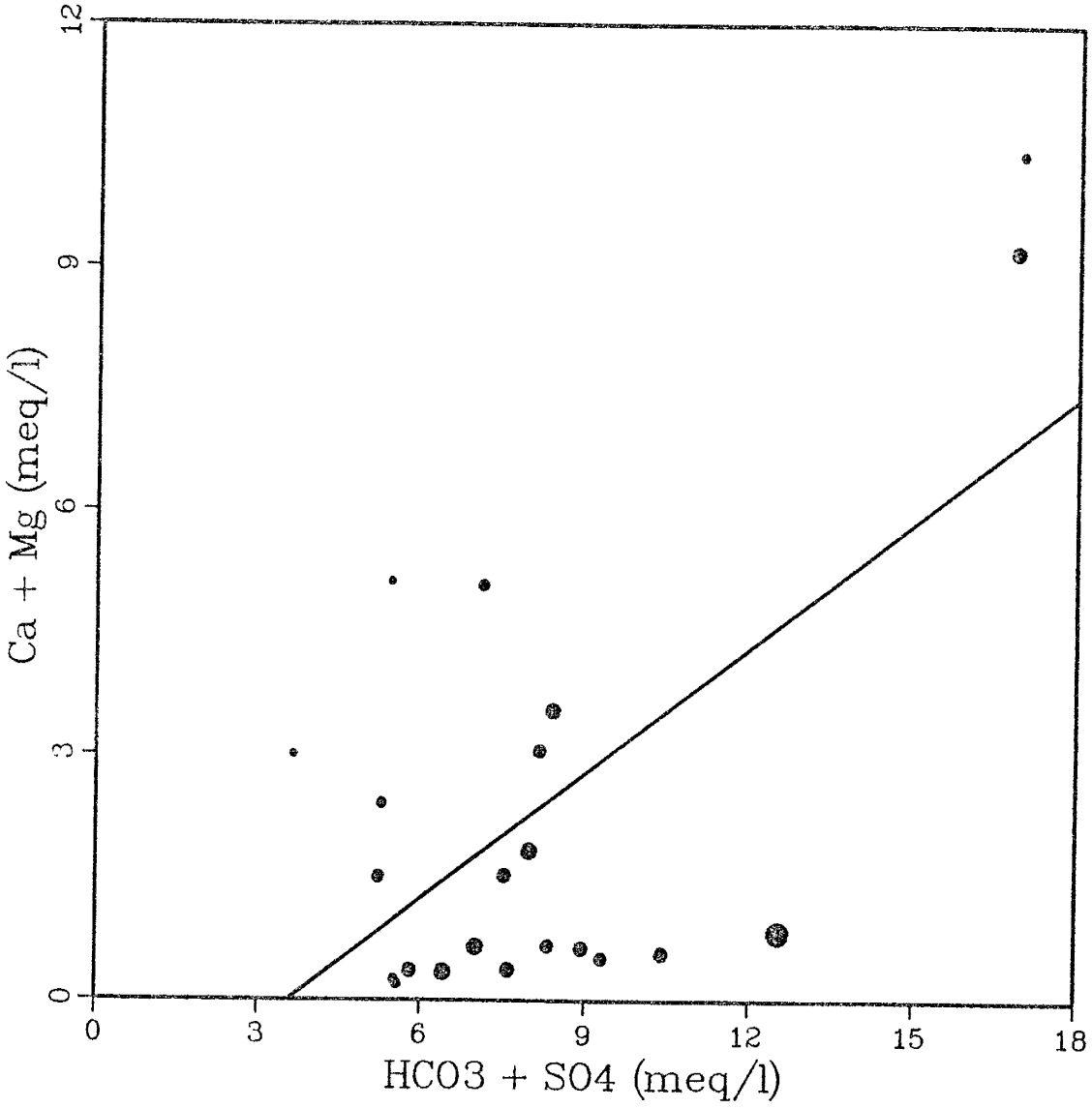

Figure 31. Magnesium plus calcium vs sulfate plus bicarbonate, size of dot is directly proportional to flowpath length.

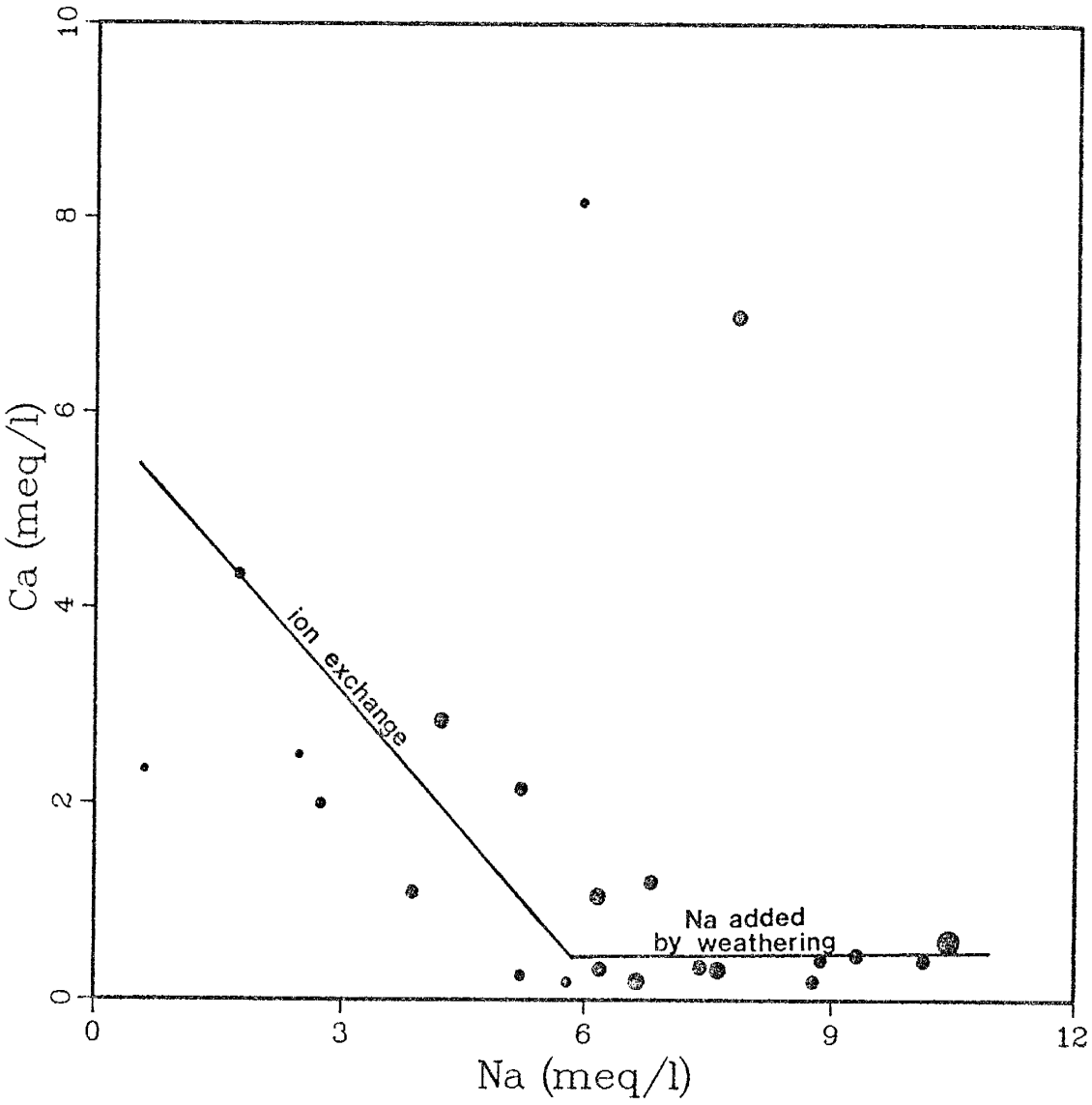

Figure 32. Sodium vs calcium, cation exchange and albite weathering processes, size of dot is directly proportional to flowpath length.

added to the system by the weathering of albite. Lastly, Figures 33 and 34 illustrate the relationship between Na^+, K^+, and SiO_2; there are no obvious trends. Though the weathering of feldspars introduces cations to the system, other processes are at work to remove silica from the system, such as precipitation of kaolinite or aluminum oxide. Therefore, direct correlation between these constituents is obscured.

In summary, the above discussion brought to light some relationships that occur between major cations, anions, and distance along a probable flowpath. The relationship between Na^+ and HCO_3^- is worth noting because of the positive correlation with DAF values and each other. A great deal of scatter in some of these data, particularly concentrations of Ca^{2+} and Mg^{2+}, is explained by complicated geochemical processes, aquifer heterogeneity, localized deviations from regional flow directions, and limited data. At best only generalized hydrochemical trends can be drawn from data analysis.

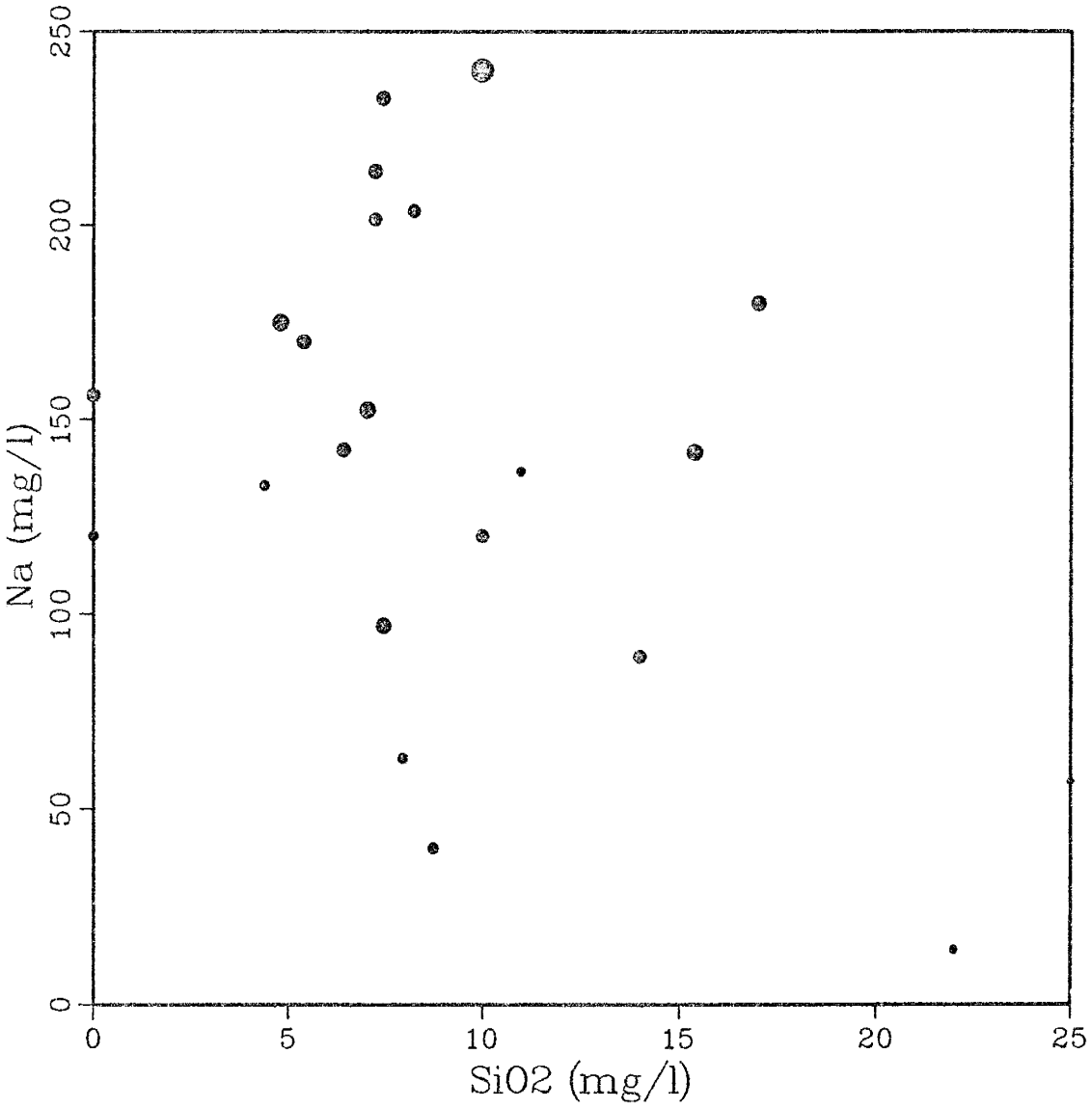

Figure 33. Sodium vs silica, size of symbol is directly proportional to flowpath length.

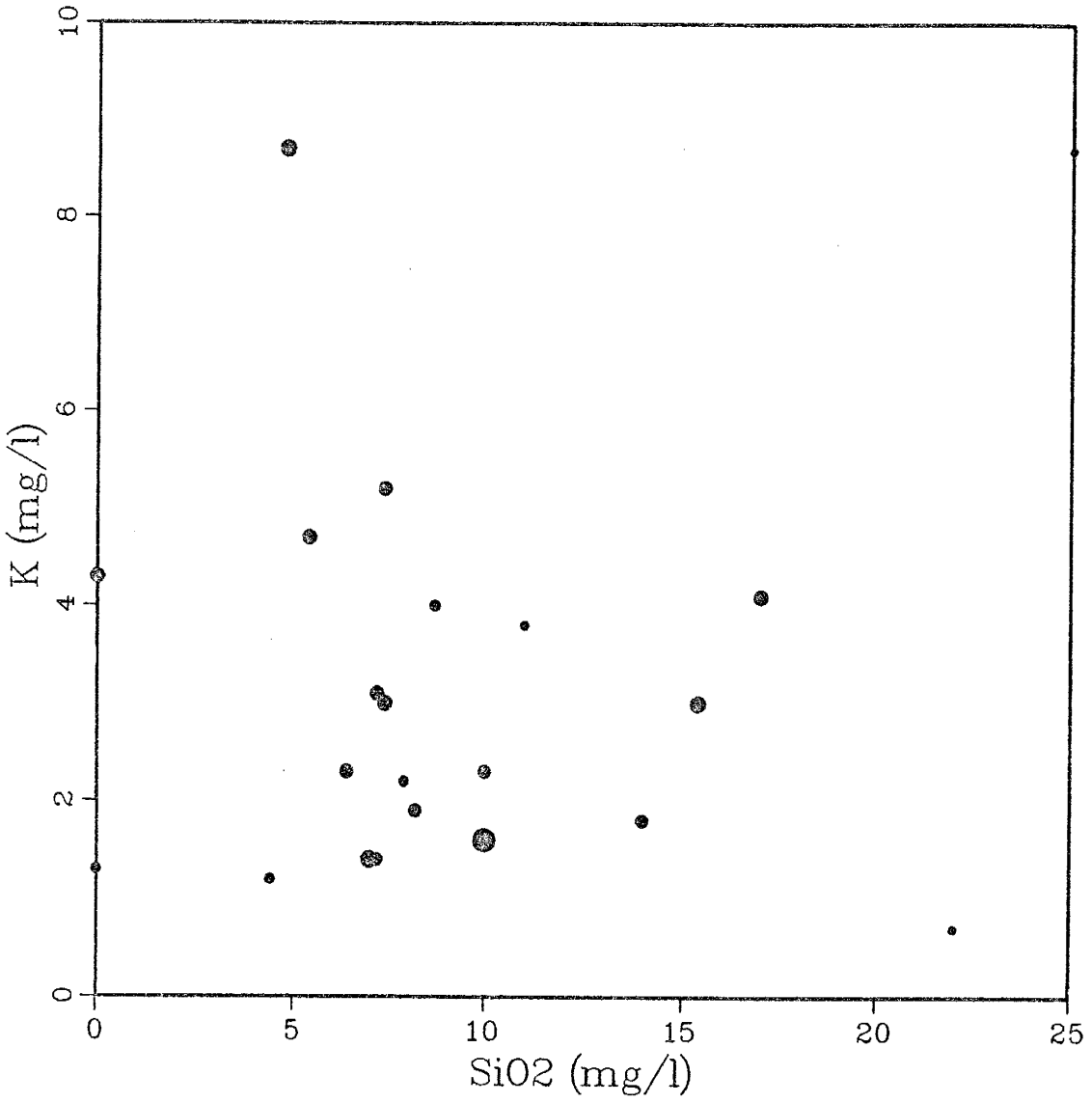

Figure 34. Potassium vs silica, size of symbol is directly proportional to flowpath length.

GEOCHEMICAL REACTION MODELING

In this section a geochemical reaction model is developed from available data to explain the most likely chemical reactions which have occurred between the solid phases, present as aquifer material, and the liquid phase, groundwater. A mass balance approach was adopted to analyze the available water-chemistry data (Plummer et al.; 1983, Plummer and Back, 1980; Plummer, 1977). This method employs the use of equilibrium speciation and mass transfer calculations to test the feasibility of the proposed reaction model.

Speciation calculations determine the saturation state of the groundwater with respect to various minerals and gases based on a thermodynamic model and observed water-quality data. A computer program called WATEQF (Plummer et al., 1984) was employed to perform these calculations. Mass transfer calculations determine the amounts of mineral and/or gas reactants and products that must dissolve or precipitate between two points along a flow path in order to explain the observed changes in amounts of dissolved consituents. For these calculations the computer program BALANCE (Parkhurst et al., 1982) was used.

Following is a description of the mass balance approach, a discussion of its limitations, and the results

of this method as applied to available mineralogical and hydrochemical data from the Moreno Hill Formation.

THE MASS BALANCE APPROACH

Groundwater chemistry can be related to specific mineral weathering reactions with the mass balance approach. An assumption is made that observed changes in chemistry between chosen initial and final points along a flowpath are solely the result of these reactions. Net chemical reactions responsible for these changes can be quantified by means of mass transfer calculations (Plummer and Back, 1983). Further, it is assumed that waters originate in recharge areas, as defined above, and evolve by interaction with the more reactive minerals of the Moreno Hill Formation, in response to the imposed hydraulic gradient, until the point of discharge.

Mass Transfer Calulations

With the combined knowledge of chemical composition of initial and final groundwater, and a defined set of hypothetical reactants and products, mass transfer calculations are performed on chosen constituents along an interpreted reaction path according to the following equation:

$$\sum_{p=1}^{P} \alpha_p b_{p,k} = m_{T,k}(F) - m_{T,k}(I) = \Delta h_{T,k}$$

for each element

where P is the number of total reactant and product phases in the net reaction, α_p is the calculated mass transfer of the p^{th} phase, $b_{p,k}$ is the stoichiometric coefficient of the k^{th} element in the p^{th} phase, $m_{T,k}$ is the total molality of the k^{th} element in solution and J is the number of elements included in the calculations. In problems with only element mass balance equations (no redox or mixing), P must equal J, one equation for each constituent (in mass balance calculations $\Delta m_{T,k}$ is an independent variable used to derive α_p, while in mass transfer calculations, $\Delta m_{T,k}$ becomes the dependent variable (Plummer, 1977).

Mass transfer calculations for chosen reacting phases are obtained by simultaneous solution of P equations. This otherwise tedious operation is circumvented by use of the computer code BALANCE. This program produces a set of numbers which indicates the millimoles of each phase (per kilogram of water) which must react with initial waters in order to produce the final groundwater composition observed.

Speciation Calculations

Speciation calculations are critical to the validation of any mass balance approach since mass transfer calculations are not constrained by thermodynamic data, and can imply reactions that are thermodynamically impossible. The results of speciation calculations are based on a

chemical equilibrium model of an aqueous solution and thermodynamic data for the relevant mineral-water reactions. These calculations reveal whether a given phase would tend to dissolve or precipitate in the system. They rely heavily on the accuracy of thermodynamic and analytical data.

Input data for speciation calculations are a chemical analysis of the groundwater (including pH, Eh, and temperature), and thermodynamic data for all reactions considered. Activities, mineral solubilities, and mineral-species distribution are calculated by the aqueous model (in this case WATEQF) using mass action and mass balance equations. The basic assumption in this model is that there are complexes whose formation can be described by mass action expressions of the form:

$$K = \frac{aD^d * aE^e}{aB^b * aC^c}$$

where

$$bB + cC = dD + eE$$

and a is the activity of the element. Activity coefficients of simple ions and complexes are assumed to be described by equations which depend only on the temperature and ionic strength of the solution. From this basis a series of simultaneous equations is generated; the equations are solved iteratively by a computer.

The activity of a substance can be thought of as its

ideal concentration (Drever, 1982). The activity coefficient is the ratio of the activity of a species to its concentration. For uncharged species, the following approximation applies:

$$\gamma = 10^{0.1I} = a_i/M$$

where is the activity coefficient, I is the ionic strength of the solution, a is the activity of the constituent, and m is the molality of that constituent in the solution. For ionic species, the activity coefficient is much more difficult to define, but is approximated by the Debye Huckel Theory (Drever, 1982). This theory provides the basis for computing activity coefficients in constituents of dilute solutions and is employed by the WATEQF model (for more concentrated solutions would use the Davies equation is required and is also available in this code). The basic equation for calculating activity coefficients is as follows:

$$\log \gamma = -Az^2_i * I^{1/2}$$

where is the activity coefficient, A is a constant dependent on pressure and temperature, z is the charge on the ith ion, and I is the ionic strength of the solution.

Equilibrium partial pressures of gases as well as the

saturation state of the solution with respect to plausible mineral phases are obtained from the aqueous model (WATEQF). The saturation state of a mineral is defined as follows:

$$SI = \log \frac{IAP}{K}$$

where SI is equal to the saturation index, IAP is equal to the ion activity product for the mineral-water reaction, and K is the equilibrium constant (the value of IAP observed at equilibrium). If SI is zero, the mineral is in equilibrium with the aqueous solution, if SI is less than zero, the solution is undersaturated with respect to that mineral, and if SI is greater than zero, the solution is supersaturated. Therefore, the value of SI indicates whether a mineral would tend to dissolve or precipitate in an aqueous environment.

SI values can be used to determine the thermodynamic feasibility of mass transfer calculations. For example, if mass transfer calculations indicate that a particular phase would tend to dissolve (or have a positive value), then the SI for that phase in the initial solution should indicate that the solution is undersaturated with respect to the phase (or have a negative value).

Other useful information which is arrived at through speciation calculations is the mass of elements which were not directly analyzed. For example, values for total inorganic carbon, used in the mass transfer calculations, are calculated by the aqueous model from the field pH and

alkalinity.

As many as 50 speciation models were known to exist, as of Plummer's report in 1984 on geochemical modeling, yet no single code is capable of encompassing all environmental problems which can make use of equilibrium calculations. As gathered by various researchers through experience with the different codes available, most aqueous models, such as WATEQF, do well with the major inorganic element chemistry in dilute solutions that are characteristic of most groundwater systems (ionic strength <0.1); however, published thermodynamic equilibrium constants for many minerals vary widely, particularly for the aluminosilicates.

Limitations to Geochemical Reaction Modeling and the Mass Balance Approach

"If reaction rates are fast and groundwater flow is slow, then local equilibrium assumptions are applicable; however, if reaction rates are slow and flow is fast, then reaction kinetics will control chemistry, and one cannot assume local equilibrium" (Jenne, 1979, p. 3). This assumption of local equilibrium is fundamental to the mass balance approach. "Natural waters are open, dynamic systems with continually variable inputs and outputs of mass and energy in which true equilibrium is never attained" (Morgan, 1967, p.1). Both of these statements point to characteristics of natural systems which will create

problems when attempting to translate the results of geochemical reaction modeling to the field environment. In the Moreno Hill Formation, flow rates are slow and reaction rates are assumed to be fast; therefore the assumption of local equilibrium is applicable.

As Plummer (1984, p. 151) stated, "there are probably no groundwater systems that are in overall equlibrium with their host mineralogy". Even if reactions rates are fast, then there can be shifts in temperature and pressure which affect the equilibrium concentration of the system. Therefore, even in a system which may be at equlibrium, there is the factor of reaction progress as a function of temperature and pressure changes which serves only to complicate the problem further.

Plummer defined a state of "partial equilibrium", applicable to many groundwater systems, where mineral-water equilibrium shift nearly reversibly in response to an irreversible process such as changes in temperature and pressure. In a system where partial equilibrium exists, minerals which may appear to be in equilibrium are actually linked to some irreversible reaction(s). The common ion effect or changes in the value of activity coefficients are examples of potential irreversible reactions.

If the SI of a mineral-water reaction is near zero, then a state of apparent equilibrium may exist (Plummer, 1984). An example of apparent equilibrium is a mineral

continually reacting near equilibrium in response to some irreversible reaction. One way to distinguish between equilibrium and apparent equilibrium is by mass transfer calculations. If a mineral is reacting at apparent equilibrium, its mass transfer along a flow path will not be zero.

A mineral is considered to be at equilibrium with a solution if it is both saturated and has zero mass transfer. Apparent equilibrium exists if the mineral appears to be saturated yet has nonzero mass transfer along a flowpath. In this case, the mineral is reacting in a partial equilibrium system. If a mineral has nonzero mass transfer along a flowpath, but is not saturated in the system, it is reacting irreversibly. Lastly, minerals that are not saturated in the system and have zero mass transfer are either not present or not reacting in the system.

In order to apply these definitions of equilbrium to a field problem, the choice of mineral phases for the reaction model must be correct. The more one understands about the mineralogy of an aquifer, the more confident one can be about the validity of the geochemical reaction model. Petrologic, SEM, and X-ray diffractometry data have added much to the overall understanding of the hydrogeochemistry of this system. Without this information geochemical reaction modeling is reduced to mere speculation.

Along these same lines, understanding the hydrogeology

of an area is critical to any geochemical reaction modeling effort. To try and relate the geochemistry of groundwater from wells that are not located along the same flowpath is meaningless. Though ideally a researcher would wish to have a large, regionally confined flow system to model, geochemical modeling techniques can be applied to other systems given sufficient hydrogeochemical data.

Limitations to the mass balance approach include problems with the defined mineralogy of a system. The maximum number of minerals that can be considered in mass transfer or mass balance calculations is equal to the number of equations necessary to describe the system. In other words, only a few idealized mineral compositions can be input to the model, when in reality, a particular mineral may vary in composition throughout the system (Plummer and Back, 1981). The mass transfer calculations do not reflect the fact that many other minerals of slightly different compositions may be involved in the system.

The validity of the reaction coefficients derived from the mass transfer calculations depend on the accuracy of analytical data, which always contains some element of mechanical and human error. Errors accrued in water quality analyses will translate directly to uncertainties in calculations of the reaction coefficient.

Plummer (1984) described another geochemical modeling problem which he called "saturation-insufficient" data.

As in any sedimentary enviroment, many different minerals of varying compositions are available to react with groundwater, which they all do to some degree. The complexity of the mineralogy, in most cases, renders a unique reaction model unattainable. However, effects on the overall chemistry of groundwater by slow-reacting minerals, such as quartz, are much less than the fast-reacting minerals, such as some feldspars and the carbonates. This effect becomes even more important when fast-reacting minerals are in greater abundance than slow-reacting minerals (Chapelle, 1983).

Based on the knowledge of mineral abundance in the Moreno Hill Formation, and that all of the chosen phases are fast-reacting in this system, it is assumed that these six phases exert dominant control over the evolution of the groundwater chemistry. Accordingly, a reaction model is developed which, though not unique, is both useful and applicable to this system.

The following equations describe the rock-water interactions to be explored in this modeling effort:

Formation of Carbonic Acid

$$CO_2 + H_2O = H^+ + HCO_3^- = H_2CO_3 \qquad 1)$$

Calcite Solution/Precipitation

$$CaCO_3 + H_2CO_3 = Ca^{2+} + 2HCO_3^- \qquad 2)$$

Dolomite Solution/Precipitation

$$CaMg(CO_3)_2 = Ca^{2+} + Mg^{2+} + 2CO_3^{2-} \quad 3)$$

Gypsum Solution/Precipitation

$$CaSO_4 \cdot H_2O = Ca^{2+} + SO_4^{2-} + H_2O \quad 4)$$

Cation Exchange Reactions

$$Ca^{2+} + 2Na^{+}X = CaX_2 + 2Na^{+} \quad 5)$$

Albite Weathering to Kaolinite

$$2NaAlSi_3O_8 + 2H_2CO_3 + 9H_2O = Al_2Si_2O_5(OH)_4 + 4H_4SiO_4 + 2Na^{+} + 2HCO_3^{-} \quad 6)$$

Though these reactions are assumed to be the major geochemical processes affecting groundwater chemistry, other reactions and minerals are considered to play a role in the geochemical evolution of these waters. They are not considered in the reaction modeling various reasons.

CO_2 Production From Decay of Organic Material

$$CH_2O + O_2 = CO_2 + H_2O \quad 7)$$

This reaction is responsible for adding CO_2 to the system, but there are no data for total organic carbon.

Pyrite Oxidation

$$FeS_2 + 5O_2 + H_2O = Fe(OH)_3 + 2SO_4^{2-} + 2H^+ \quad 8)$$

This reaction is responsible for adding SO_4^{2-} to the system and lowering the pH, but data available for describing the redox properties of this system are inconclusive (Appendix 2); therefore, it is impossible to quantify the contributions of this process to total sulfate concentration. Pyrite is present in the system associated with discontinuous coal and lignite seams (Tables 10 and 11).

Sulfate Reduction

$$SO_4^{2-} + 9H^+ + 8e^- = HS^- + 4H_2O \quad 9)$$

Sulfate reduction occurs in this system (HS^- was found at detectable levels in some of the samples, see Table 12); however, this is considered an important process in the system as sulfate concentration increases flowpath length (see Figure 24).

Potassium Feldspar Weathering to Kaolinite

$$2KAlSi_3O_8 + 11H_2O = Al_2Si_2O_5(OH)_4 + 4H_4SiO_4 + 2K^+ + 2OH \quad 10)$$

For reasons described above, potassium feldspar weathering is considered to be of minor importance to this

system as the reaction rates for sodium feldspars are so much higher then potassium feldspars.

Results of Mass Transfer Calculations

The program BALANCE (Parkhurst et al., 1980) was used to calculate mass transfer (or amounts of phases entering or leaving the aqueous phase) necessary to account for the observed change in composition between two points along a flowpath. In order to use this program, the total concentrations for each element under consideration must be known for two sample localities (an initial and a final water).

Various combinations of data were used to explore the mass transfer of phases in this system. In all cases, sample 86 was the input final water, while the input initial water was varied. Samples 232 and 67 were chosen as initial input water because of their high concentrations of calcium and sulfate. The intent was to see how the reaction model responded to waters uncharacteristic of this area. Samples 260 and 263 were chosen as input initial water because they are considered to be from a recharge area. Sample 155 was randomly chosen as another sample location which was close to a recharge area on the eastern border of the study area.

The input data and results of these mass transfer calculations are listed in Tables 16 and 17. Total inorganic carbon (C) was calculated by WATEQF from field pH

MASS TRANSFER FOR INITIAL (I) AND FINAL (F) WATERS

	mm/kg-H2O					
I-F	Na	Ca	Mg	S	C	Si
260-86	2.5-10.4	1.3-0.3	1.3-0.1	0.7-1.9	4.1-13.0	0.4-0.2
263-86	0.3-10.4	1.2-0.3	0.4-0.1	0.2-1.9	3.3-13.0	0.4-0.2
232-86	7.8-10.4	3.5-0.3	1.1-0.1	5.2-1.9	6.5-13.0	0.3-0.2
67-86	5.9-10.4	4.1-0.3	1.1-0.1	5.4-1.9	7.2-13.0	0.2-0.2
155-86	1.7-10.4	2.2-0.3	0.7-0.1	0.6-1.9	7.0-13.0	0.1-0.2

Table 16. Input concentrations for mass transfer calculations.

MASS TRANSFER FOR INITIAL (I) AND FINAL (F) WATERS

	DELTA PHASE (mm/kg-H2O)					
I-F	CALCITE	DOLOMITE	GYPSUM	ION EX	CO2	ALBITE
260-86	-0.9350	2.8207	1.1870	4.0217	4.2247	-0.0833
263-86	-2.3150	4.8748	1.6550	5.0888	2.2633	-0.0667
232-86	1.1330	0.3285	-3.3310	1.3245	4.7970	-0.0390
67-86	0.7560	1.2458	-3.5280	2.2538	2.2663	-0.0057
155-86	-2.5160	3.7205	1.2700	4.3465	1.0810	0.0070

Table 17. Amounts (in mm/kg-H2O) of reacting phases dissolving or precipitating (-) between initial and final waters

and alkalinity. There are no data for dissolved aluminum, and it is assumed that its mass transfer is zero in this system. The mass balance equations for the six chosen phases are as follows:

m_T, Na = 2 ION EX + 1 ALBITE

m_T, Ca = 1 CALCITE + 1 DOLOMITE + 1 GYPSUM - 1 IONEX

m_T, Mg = 1 DOLOMITE + -1 ION EX

m_T, S = 1 GYPSUM

mT, C = 1 CALCITE + 2 DOLOMITE + 1 CO2

m_T, SI = 3 ALBITE

Results of the mass transfer calculations for samples 260 and 263 (initial waters) and 86 (final waters) as shown in Table 17 indicate that 0.9350 or 2.3150 mm/kg respectively of calcite precipitates and 2.8207 or 4.8748 mm/kg respectively of dolomite dissolves from the initial solutions to produce waters of the final composition. To check the thermodynamic feasibilty of these reactions, the calcite and dolomite saturation indices calculated by WATEQF were plotted versus DAF for all samples (Figures 35 and 36).

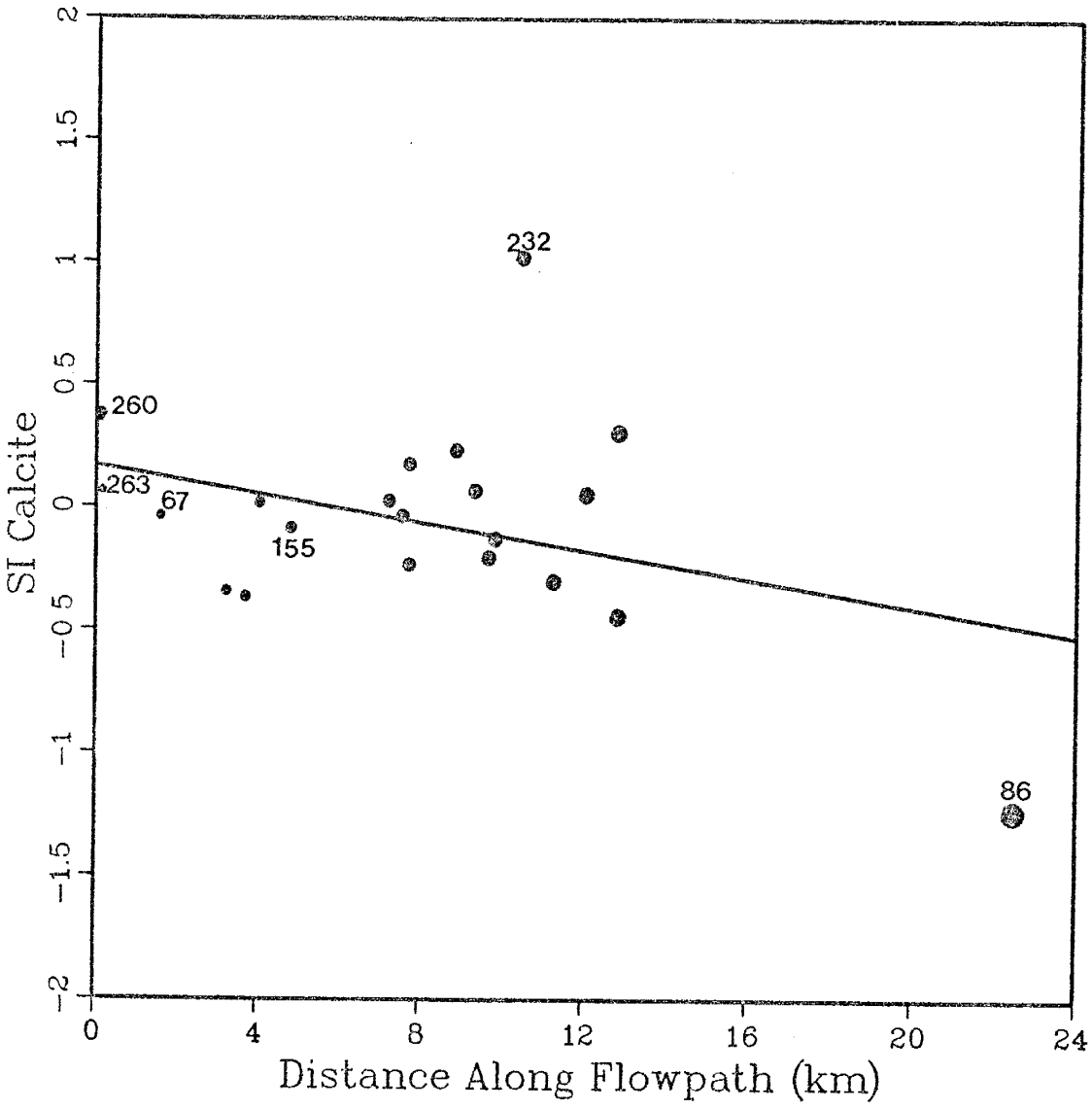

Figure 35. Saturation index for calcite as a function of distance along a flowpath.

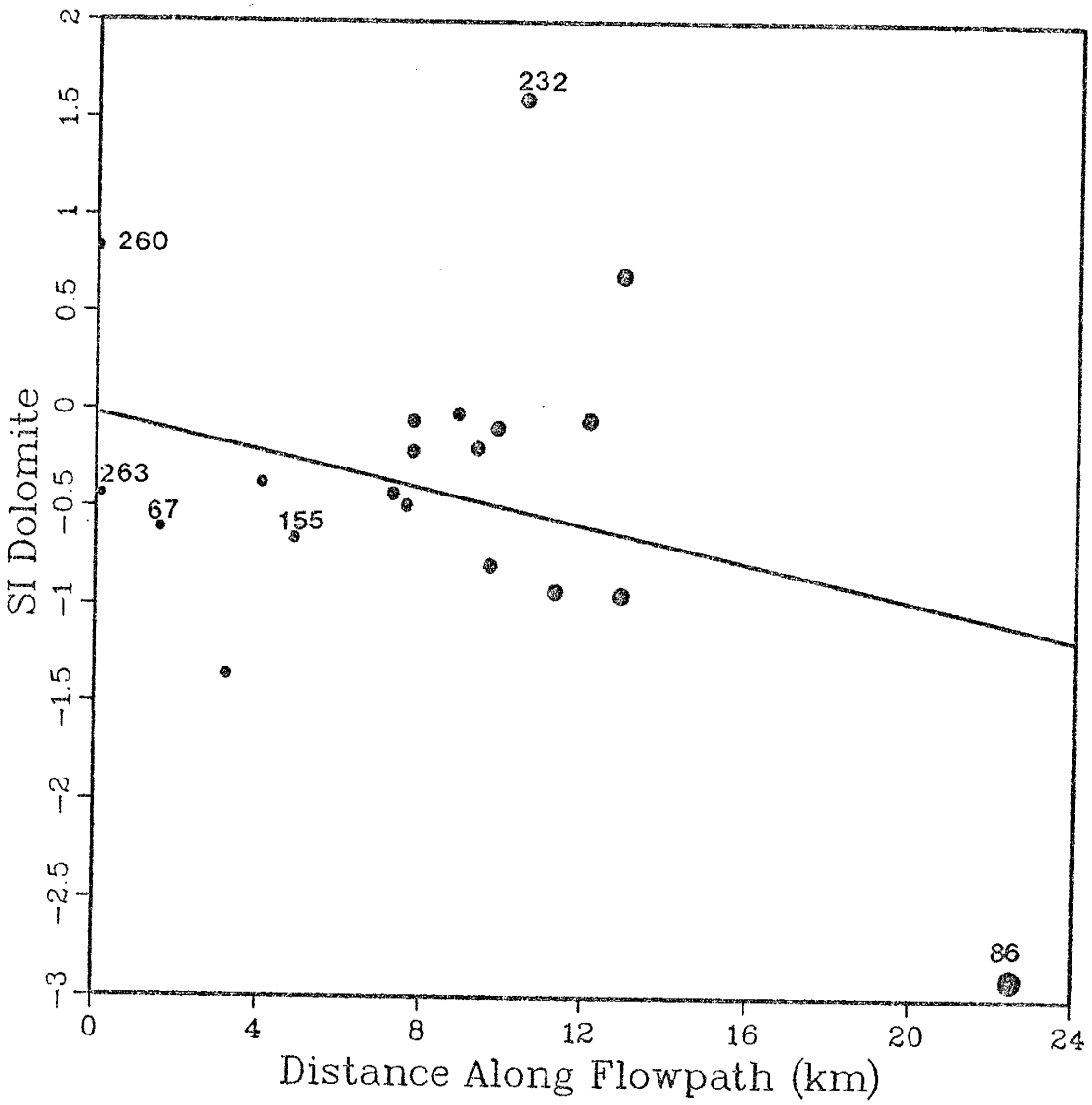

Figure 36. Saturation index for dolomite as a function of distance along a flowpath.

Samples 260 and 263 are both supersaturated with respect to calcite, while sample 86 is undersaturated. This agrees with the BALANCE calculations which call for precipitation of the calcite phase. An inconsistancy in these data is that sample 263 plots very close to equilibrium with calcite, yet the mass transfer indicates a relatively significant amount of precipitation for this phase, while sample 260 plots farther away from equilibrium, yet requires less precipitation.

Dolomite is dissolving in the system according to mass transfer calculations for both cases, yet sample 86 is relatively more undersaturated with respect to this phase than either sample 260 or 263. Therefore, the direction of the calculated mass transfers is thermodynamically impossible. Sample 260 has a positive SI for dolomite, yet direct precipitation of this mineral is rare in this setting. According to Hem (1984), dolomite is more often formed by replacement which is not incorporated in mass transfer calculations; therefore, these data are less meaningful with regard to this phase.

The majority of data points in Figures 35 and 36 hover near saturation or equilibrium with respect to calcite and dolomite in this system, yet neither of these phases has zero mass transfer. Therefore, according to Plummer's (1984) definitions of equilibrium presented above, these minerals could be continually reacting in a partial

quilibrium system in response to an irreversible reaction, n this case gypsum dissolution. Incongruent dissolution of olomite (dolomite dissolution and calcite precipitation) ccompanied by gypsum dissolution is one process which could xplain these data and is relevant to the system.

Figure 37 shows that the system is everywhere ndersaturated with respect to gypsum. Mass transfer alculations indicate a relatively minor amount of gypsum is issolving in the system. The relationship between samples 63 and 86 is supported by the mass transfer calculations, et this not the case for samples 260 and 86 which xperience little change in the saturation state of gypsum etween these data.

Ion exchange (ION EX) is a very important process in his system according to mass transfer calculations (see elative magnitudes of Delta Phases, Table 17). For these alculations to be valid, Ca^{2+} and Mg^{2+} must be taken out of he system while sodium is added. Figure 38 illustrates the elationship between the activities for Ca^{2+} and Na^{+} based n WATEQF calculations. These data support the idea of alcium being lost and sodium gained along the flowpath from amples 260 and 263 to 86. Figure 39 shows that the behavior f calcium and magnesium is similar in this system (R^2 is .78). Ion exchange is supported by mass transfer alculations as being a more important process than either reciptation of calcite or dissolution of dolomite in the

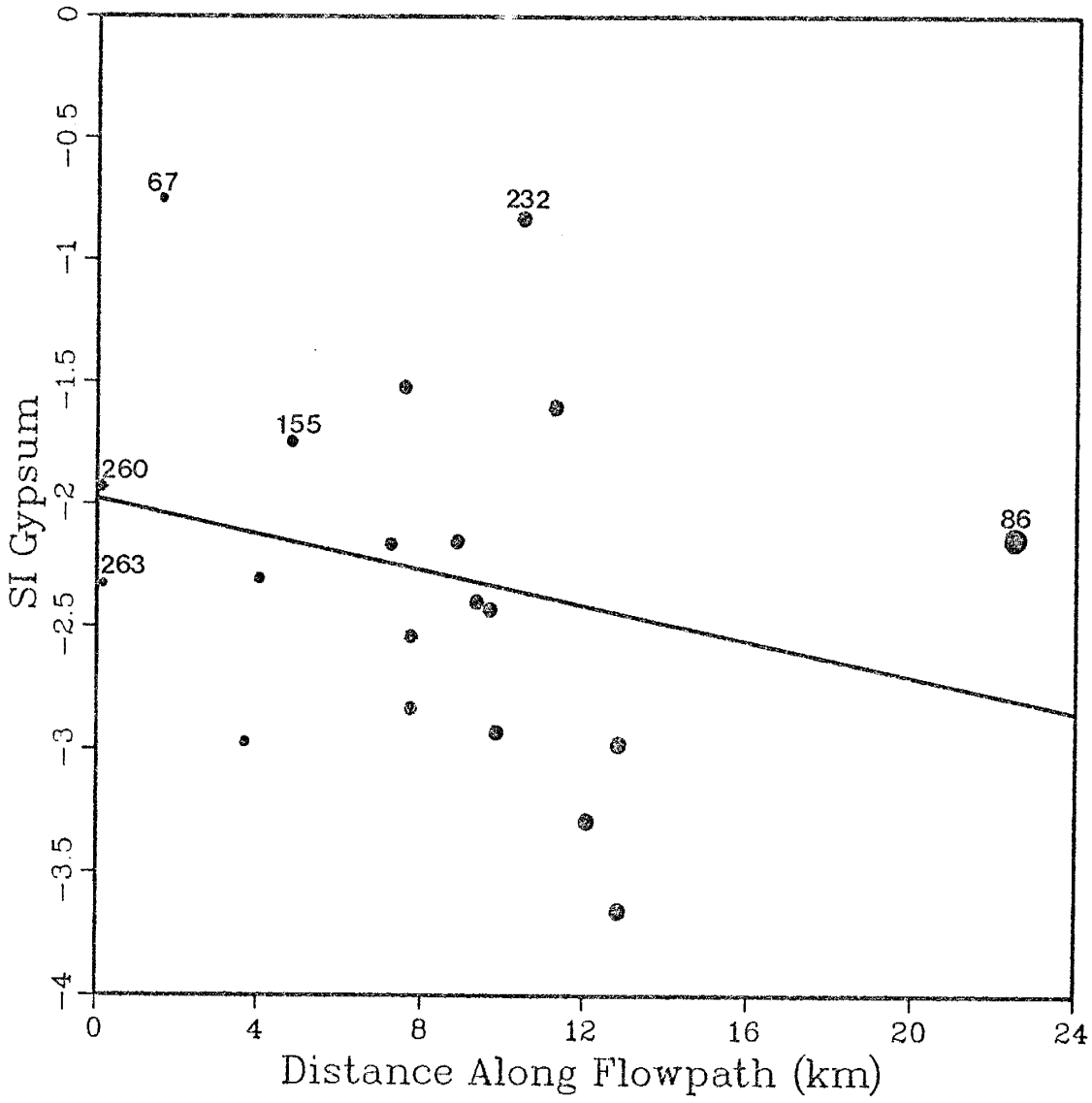

Figure 37. Saturation index for gypsum as a function of distance along a flowpath.

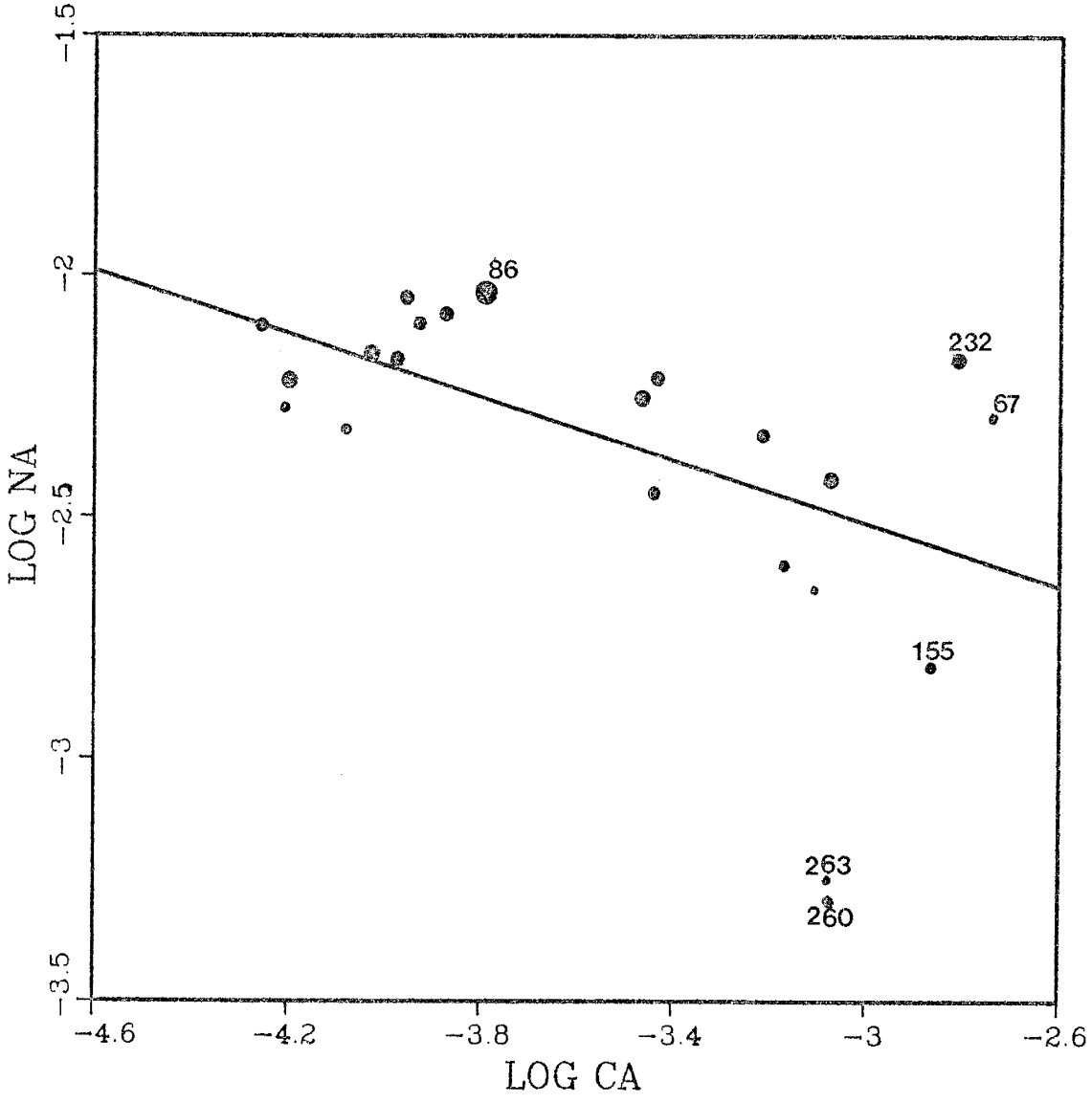

Figure 38. Calcium activity vs sodium activity, size of dot directly proportional to flowpath length.

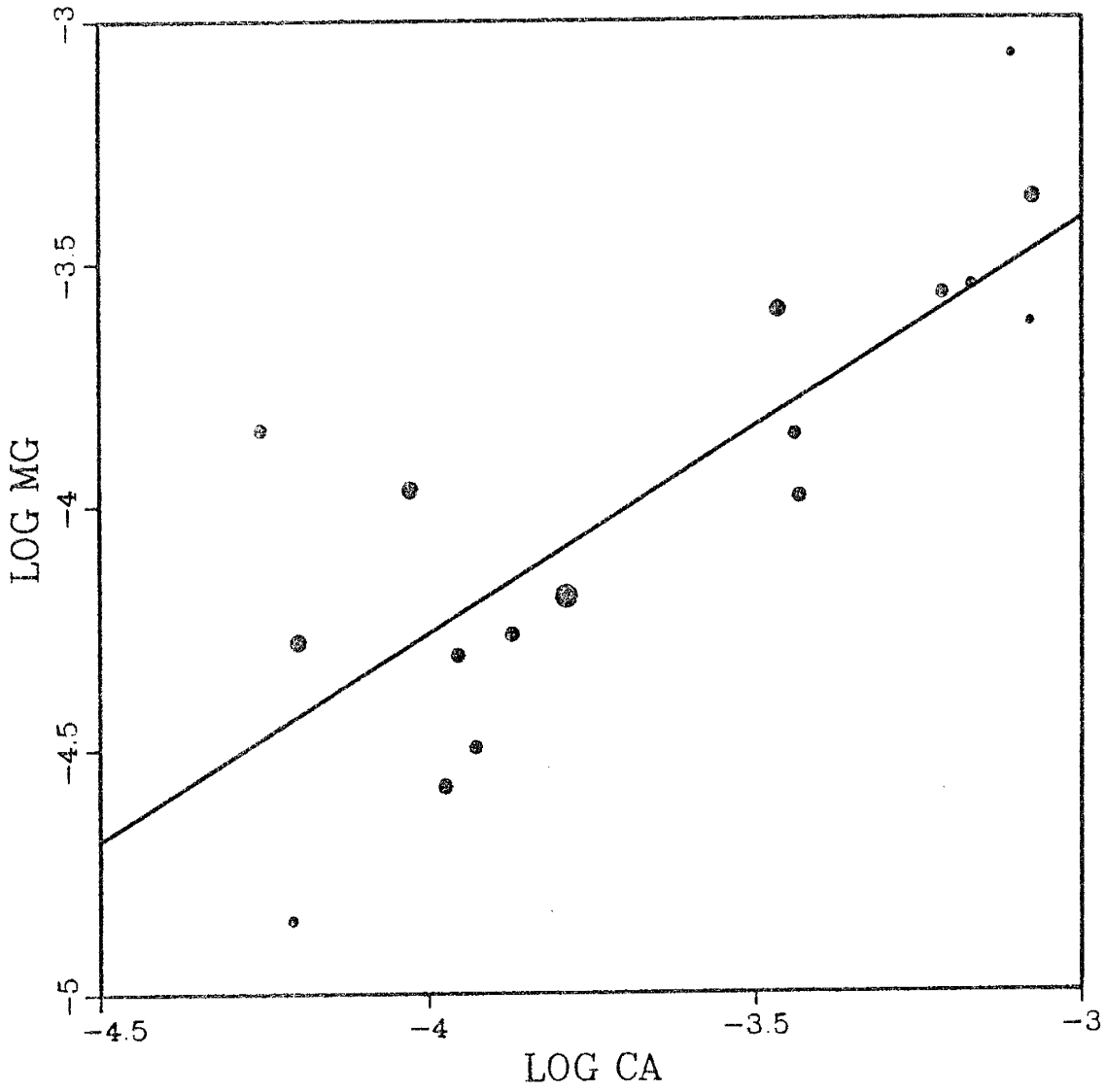

Figure 39. Calcium activity vs magnesium activity, size of dot directly propotional to flowpath length.

geochemical evolution of these waters.

Dissolution of carbon dioxide gas is required by mass transfer calculations. This is supported by WATEQF calcuations which show an increase in the partial pressure of this gas between 260,263 and 86 (Table 18). The reaction of CO_2 with water results in the formation of HCO_3^-. As illustrated in Figure 21, HCO_3^- is seen to increase with DAF in this system. Since P_{CO2} is calculated from field pH and alkalinity by WATEQF, the effect of contributions from sources other than atmospheric and soil gas, such as the breakdown of organic matter, cannot be addressed in these calculations. The role of organic matter in the geochemical evolution of groundwater will be discussed in Chapter 6.

According to mass transfer calculations, albite is precipitating in this system, but is of relatively minor importance. The saturation index for albite was not calculated by WATEQF as there were no data for dissolved aluminum content. Therefore, the thermodynamic feasibilty of these calculations cannot be tested. In all of the samples analyzed for dissolved silica, values are very low.

Figure 33 illustrates the relationship between dissolved Na^+ and SiO_2. In this figure, Na^+ concentrations increase by an order of magnitude with DAF, yet silica concentrations remain quite low (this is partially a result of the contribution of sodium to solution by cation exchange processes). These data are not supported by the reaction

ACC#	CALCIUM	MAGNESIUM	SODIUM	H4SIO4	Pco2	SI CALCITE	SI DOLOMITE	SI GYPSUM
197 (al)	-3.46	-3.60	-2.25	-3.59	7.9E-04	0.05	-0.05	-3.29
207 (coal)	-4.03	-4.00	-2.16	-4.11	1.0E-04	0.31	0.69	2.98
207 (ssbc)	-4.20	-4.28	-2.22	-3.94	3.2E-03	-0.44	-0.95	-3.66
120 (ssbc)	-4.26	-3.83	-2.10	-3.93	1.6E-03	-0.23	-0.05	-2.53
120 (coal)	-3.87	-4.50	-2.10	-3.87	1.9E-03	0.18	-0.02	-2.83
67 (ssac)	-2.74	-3.27	-2.08	-3.73	3.0E-02	-0.04	-0.61	-0.74
99 (ss,shbc)	-3.95	-4.31	-2.05	-3.91	2.4E-03	0.07	-0.19	-2.40
95 (coal)	-3.87	-4.27	-2.08	-3.92	4.3E-03	-0.02	-0.79	-2.43
164	-3.44	-3.86	-2.45	-3.63	1.9E-03	0.03	-0.43	-2.16
165	-3.22	-3.57	-2.33	-3.63	3.9E-03	-0.03	-0.49	-1.52
222	-4.08	-----	-2.32	------	1.9E-03	-0.37	-----	-2.97
232	-2.81	-3.28	-2.17	-3.55	2.5E-03	1.02	1.60	-0.83
260	-3.11	-3.07	-2.65	-3.38	1.9E-03	0.40	0.81	-1.91
263	-3.08	-3.63	-3.25	-3.44	3.3E-03	0.06	-0.43	-2.33
86	-3.79	-4.19	-2.03	-3.78	8.7E-02	-1.23	-2.89	-2.14
123	-3.43	-3.99	-2.21	-----	3.0E-03	0.23	-0.02	-2.15
170	-3.07	-3.37	-2.42	-3.91	2.3E-02	-0.30	-0.93	-1.60
167	-4.21	-4.85	-2.27	-4.14	1.8E-03	-0.34	-1.34	-----
56	-3.97	-4.58	-2.17	-4.05	2.7E-03	-0.13	-0.89	2.93
155	-2.87	-3.33	-2.80	234.00	2.3E-02	-0.08	-0.66	-1.74
156	-3.17	-3.55	-2.60	-3.88	6.0E-03	0.02	-0.37	-2.30

Table 18. Activities and saturation indices calculated by WATEQF.

stoichiometry of albite weathering to kaolinite. The silica concentrations are kept low in this system by the precipitation of secondary minerals such as kaolinite, not the precipitation of albite. This theory could not be tested by mass transfer calculations. For reasons, which have been discussed in Chapter 3, and will be discussed further below, it is believed that feldspar weathering, particularly, albite weathering to kaolinite, is a process which is very important to the geochemical evolution of these waters but which cannot be tested adequately by the mass balance approach.

Mass transfer calculations for samples 155 and 86 indicate the same basic geochemical pathways are relevant, though the SI values for calcite and gypsum do not lend support to mass transfer calculations. The fact that this sample location is midway along a flowpath, or farther from the recharge area (Figure 2), may be one reason for this. Localized reactions may act to mask regional hydrochemical phenomenon.

Mass transfer calculations for samples 67 and 232 with sample 86 require the precipitation of gypsum and dissolution of both calcite and dolomite. This is thermodynamically impossible for sample 232 according to SI calculations. Also, in a system which is everywhere undersaturated with respect to gypsum, the precipitation of gypsum is impossible. Though sample 86 is much more

undersaturated with respect to gypsum than samples 67 or 232, precipitation of this mineral would require supersaturation. It is likely that processes not considered in this modeling effort are removing some SO_4^{2-} from the system before saturation is reached. One such process is sulfate reduction. The addition of sulfate reduction to the reaction model would have required some additional data for dissolved constituents and redox conditions (in order that N = P, see discussion above) which was not possible. However, if removal of SO_4^{2-} was required via different pathways, the mass balance may not have required gypsum precipitation, and Ca^{2+} removal via cation exchange would again be dominant. This example points to a major drawback with this modeling approach; conclusions can be drawn which are thermodynamically impossible.

In summary, controlling reactions for this system according to mass transfer calculations include calcite precipitation, dolomite and gypsum dissolution, increase in dissolved CO_2 concentration, and cation exchange. Contributions to the system caused by the weathering of feldspars are not adequately addressed through this method of geochemical reaction modeling. Inconsistancies in the data suggest that there are problems with considering carbonate dissolution/precipitation as a dominant geochemical process in this system. Localized areas in the

system which exhibit increased concentrations of calcium due to dissolution of gypsum are not accurately modeled by the mass balance approach since data are incomplete. Without the benefit of knowledge of any or all of the following: CH_2O concentrations, adequate oxidation-reduction data for all sample locations, actual mineral stoichiometry, dissolved aluminum concentrations, or isotopic data, the geochemical reaction model contains inconsistancies and is nonunique.

MINERAL STABILITY DIAGRAMS

To further investigate the role of albite weathering as a contributor to the geochemical evolution of these waters, a mineral-stability diagram was generated using the program DIGRAM, which is available at NMIMT. Equilibrium relationships between the solid phases considered are those of Tardy (1971). In order to employ this program, dissolution equations with a common varible (in this case gibbsite) must be written for all the solid phases. Input data consist of equilibrium constants and stoichiometry for the various reactions. With these data, DIGRAM plots a mineral-stability diagram (Figure 40).

Data calculated by WATEQF are plotted on this diagram. All data fall within the kaolinite-stability field and in the Na-montmorillonite-stability field. In natural waters, kaolinite is formed until waters become so rich in cations

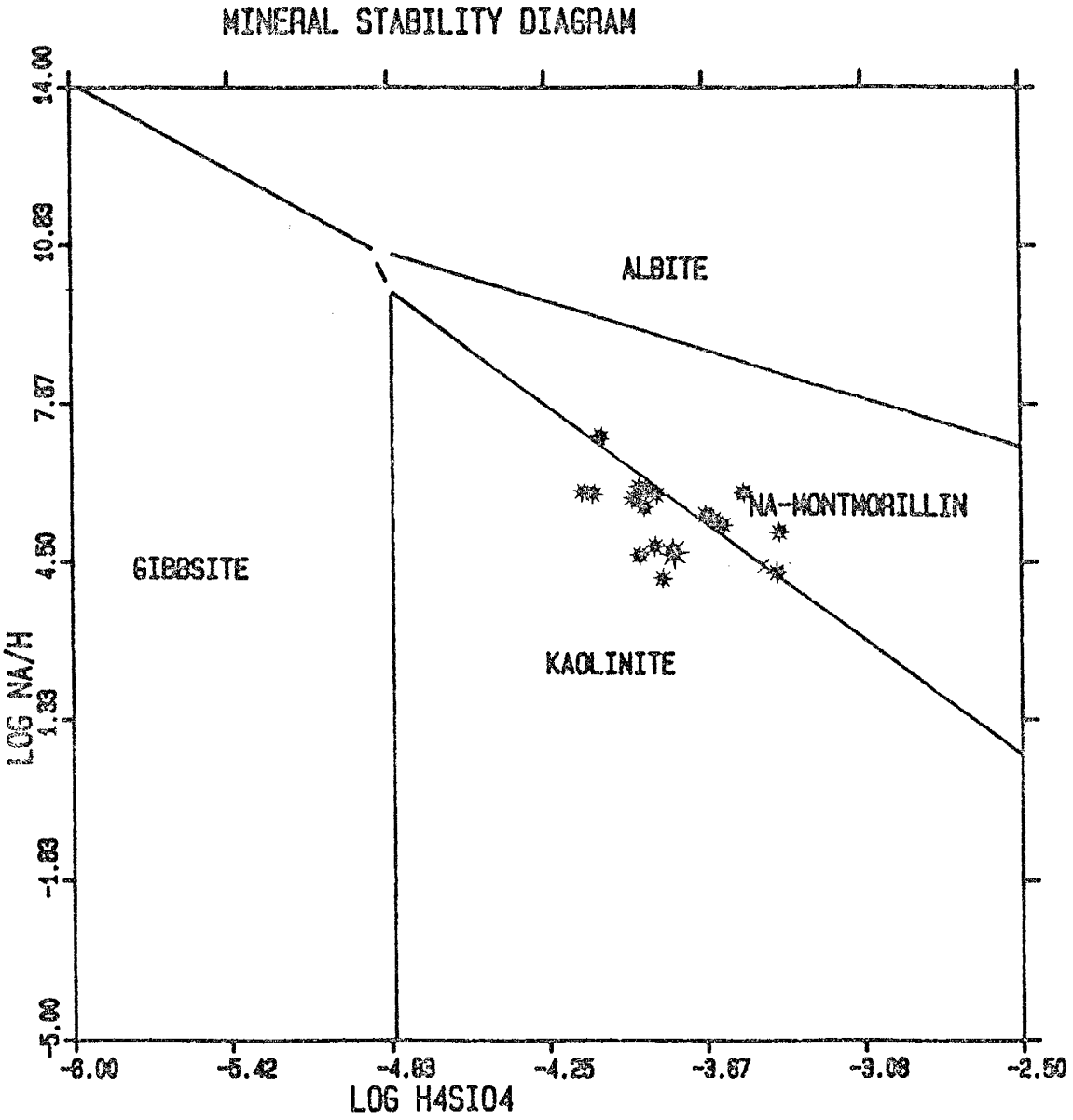

Figure 40. Mineral stability diagram for the system Na-Al-SiO_2.

ınd silica that Na-montmorillonite forms (Bricker and ;arrels, 1967). In no case are these waters seen to be in ;quilibrium with albite. This lends support to the idea ;hat feldspars are rapidly reactive, and thus, albite ;eathering must strongly influence the geochemical ;volution of these waters considering its widespread ;ccurrence in the system.

SUMMARY AND DISCUSSION

Many geochemical processes are at work to control the evolution of groundwater chemistry in the heterogeneous Moreno Hill Formation. The previous sections have attempted to highlight the most important of these processes as evidenced by mineralogical data, observable trends in groundwater chemistry as a function of distance along a flowpath, and computer modeling. In this section all of the supporting data are brought together for comparison and discussion. Each of the reactive mineral phases considered in this study will be discussed separately in terms of its contribution to groundwater chemistry evolution. The final conclusions of this study are highlighted in a summary diagram (Figure 41). This flow chart illustrates a conceptual geochemical model of groundwater evolution in the Moreno Hill Formation.

Feldspar Weathering

Several important studies have addressed groundwater quality in coal-bearing formations (Powell and Larson, 1985; Groenewald et al., 1981; Thorstenson and Fisher, 1979; Moran et al., 1978a; Moran et al., 1978). Although all of these studies discuss aquifers with mineralogies similar to that of the Moreno Hill Formation, none point to the weathering of feldspars as a significant buffering process

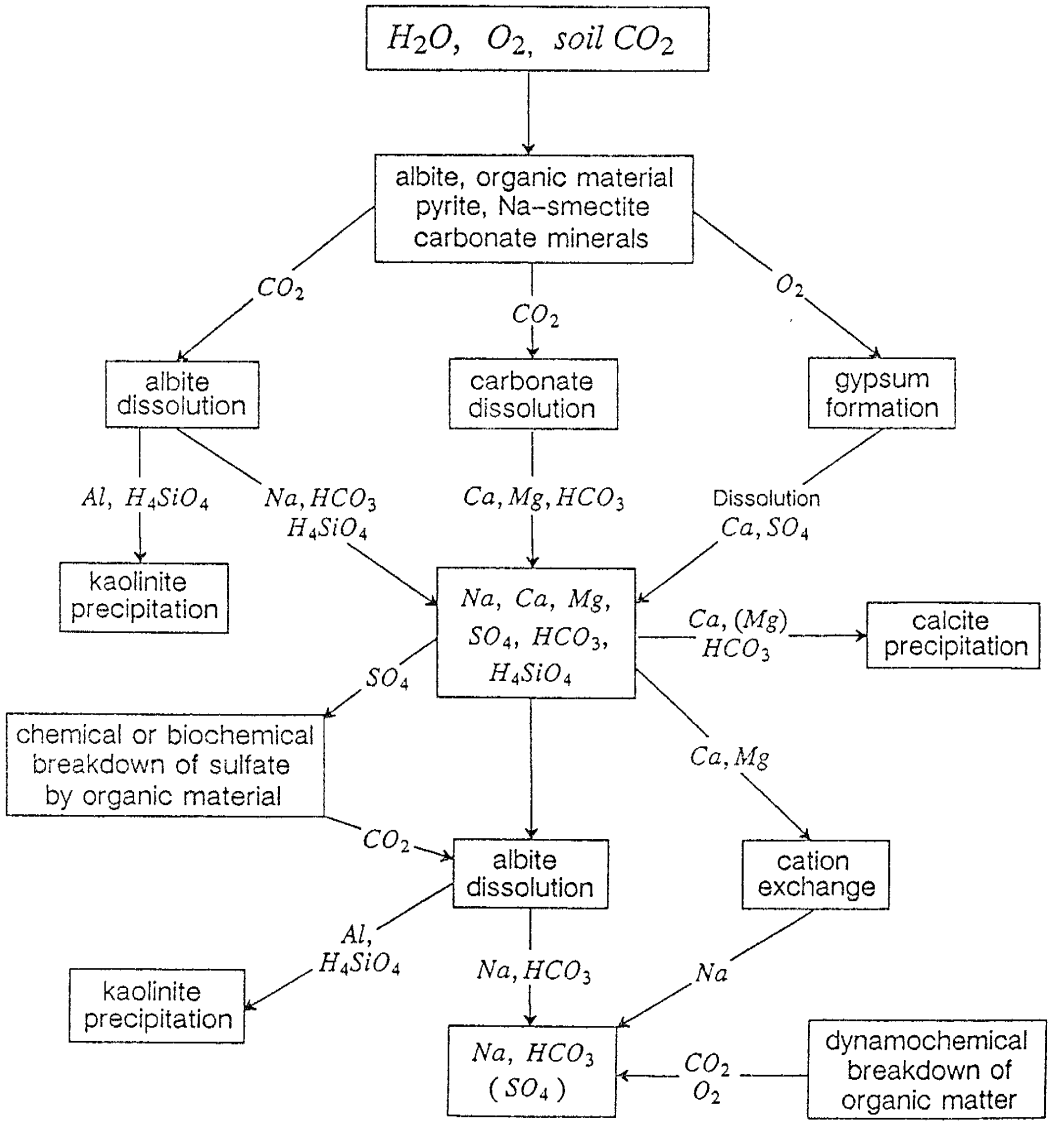

Figure 41. Conceptual geochemical model of groundwater evolution in the Moreno Hill Formation.

controlling the geochemical evolution of groundwater. Powell and Larson (1985) considered plagioclase as a contributing phase, but did not discuss its relative importance in the many proposed models. Thorstenson and Fisher (1979) concluded that the weathering of silicates is not an important buffering process. This conclusion was based on low dissolved silica concentrations in groundwater, and isotopic data which did not confirm silicate minerals as the source for $HCO3^-$.

Mineralogic and groundwater chemistry data discussed in this study support the conclusion that the weathering of albite is an important geochemical process which exerts control on the groundwater chemistry evolution of the Moreno Hill Formation. Geochemical reaction modeling was not supportive in considering this process for the conceptual geochemical model for the following reasons: 1) there are no data for the dissolved aluminum content of these waters, 2) thermodynamic data for the aluminosilicate minerals vary widely, and 3) the mechanism for weathering of feldspars is different from that of other reactive minerals which experience simple, linear stoichiometric dissolution, a process assumed by equilibrium models. In combination these factors render the method of reaction path modeling incapable of adequately addressing the influence of silicate minerals, particularly the feldspars, on groundwater quality. Following is a discussion in support of these

conclusions.

An interesting paper by Holdren and Berner (1979), described the method of feldspar weathering in some detail. With the aid of Scanning Electron Microscopy (SEM) and X-ray Photoelectron spectroscopy (XPS), they concluded that the mechanism for feldspar weathering is selective chemical reaction at the feldspar-solution interface. This idea is contrary to the widely-accepted theory that a chemically-altered, protective surface layer regulates the dissolution of these minerals (Palmer and Cherry, 1984/85), and that weathering continues by uniform diffusion through this layer, an extremely slow process.

Holdren and Berner (1979) were unable to find any evidence for this "protective" coating in their studies. Yet it remained for them to explain the significance of the nonlinear, parabolic dissolution rates, which were continually observed in their studies of feldspars. The experiments described in theis paper showed that particle size is the controlling factor for the dissolution of feldspar grains. Grains with the very smallest diameters (<1 micron) are highly unstable and dissolve at an accelerated rate. As these particles are consumed, subsequent dissolution occurs on grains at selective sites of high energy (such as structural deformations or the planar intersection of fluid inclusions). Therefore, depending on the structural integrity or developemental

history of a mineral grain, it could be highly reactive. Normally, this second process occurs at a slower rate, and is the primary mode by which plagiclase and K-felspars dissolve during weathering in nature.

SEM photographs of feldspars shown above illustrate pervasive dissolution textures of feldspar grains. These photographs are typical of what was observed in all samples analyzed. Berner and Holdren (1979) described the attack by dissolution of the feldspar grain as a nonuniform process which follows an etching sequence characterized by the developement and growth of distinctive etch pits (Figure 13). All plagioclase feldspars analyzed were albites (no calcium detected or no anorthite component), an atypical primary composition for detrital plagioclase. Albite can be a chemically stable diagenetic product inasmuch as it does occur as a cement (although it was not observed as such in this study). These observations indicate that plagioclase grains were diagenetically "albitized", a process which would release calcium to the pore fluids. The process of diagenesis causing the removal of calcium from the structure of these feldspars could act to create structural weaknesses, or sites of high energy, which would allow for enhanced dissolution during the weathering process.

Holdren and Burner (1979) have shown that feldspars dissolve stoichiometrically. Solution concentrations do not reflect this process as dissolved aluminum quickly forms a

precipitate. This precipitate may nucleate on feldspar grains, but does not act to inhibit dissolution. Also, the precipitation of aluminum and silica to form aluminosilicate minerals, such as kaolinite, acts to confuse the stoichiometric balance.

Results from the point-counting study show that surface sandstones have more porosity and total feldspar, while subsurface sandstones have more epimatrix (in approximately the same proportions). The following is a suggested explanation for these data which follows from the Holdren Burner (1979) study. Recharging waters in this system affect the initial phase of feldspar dissolution, where fine-grained particles are rapidly dissolved. In the subsurface, as additional silica and aluminum are added to the system as a result of the second phase of weathering of larger grains, solutions become supersaturated with respect to kaolinite which is subsequently precipitated as epimatrix. Groundwater remains low in dissolved silica and continued weathering of feldspars is experienced. Figure 27, shows that recharging groundwater is initially high in dissolved silica and the concentration drops off rapidly downgradient.

Bricker and Garrels (1967) considered the importance of silicate phases in controlling the chemical equilibrium of natural waters. In their discussion of this process, they assumed that silicates, considered as bulk phases, are

rapidly reactive, and that many constituents of groundwater, namely CO_2, Na, SiO_2, and HCO_3, as well as pH , are controlled by equilibrium with one or more silicate phases. The fact that all sample points plotted in the equilibrium fields for kaolinite or Na-montmorillonite and not albite in Figure 40 supports the idea of rapid rates of reaction for the feldspar minerals. Though they admitted that more work was necessay to adopt these claims, they concluded that, if the minerals are considered to be rapidly reactive, then silicate equilibria as well as carbonate equilibria must be considered as part of the chief buffering systems (ie. loss of CO_2 and gain of HCO_3^-) of natural waters (Kramer, 1968; Bricker and Godfrey, 1968; Garrels, and MacKenzie, 1967).

More evidence for the control of silicate minerals, in this case albite, on geochemical evolution of groundwater are data that were presented in Chapter 4. If the concentration of Na^+ and HCO_3^- in solution were controlled solely by the weathering of albite, then one would expect the slope of the regression line to equal to one as dictated by the stoichiometry of the reaction. In this case the slope of the line is greater than 1, approximately 1.5, indicating that Na^+ is being contributed to solution faster than HCO_3^- (Figure 28). Therefore, an additional source of Na^+ is necessary to explain these data, namely cation-exchange. As illustrated in Figure 32, cation exchange processes are exhausted, while Na^+ continues to be added to

the system through the process of feldspar weathering. Initially (or locally), dissolution of carbonate minerals adds calcium to the system. As CO_2 is lost to the weathering of albite, calcite dissolution no longer occurs. If gypsum were considered the sole source for Ca^{2+} in this system, carbonate dissolution as a source for Ca^{2+} would not be required by the geochemical model.

Due to nonlinear dissolution and formation of secondary solids, such as aluminum oxide, kaolinite, or montmorillinite, incorporation of silicate mineral equilibria into geochemical reaction modeling for this study is not possible with the tools available. The reactivity of albite in this system, and its major contribution to the geochemical evolution of these waters is supported by all available data. More work is necessary to establish the distribution of carbonate minerals in this system, and, if they are abundant, to determine the relative contributions.

Pyrite-Gypsum Relationship

Though pyrite is a common consituent of coal-bearing deposits, the magnitude of its contribution to the evolution of groundwater chemistry is not adequately addressed in this study due to lack of data on redox relationships. However, as discussed in Chapter 3, pyrite was a major constituent of coal samples in the surface and in the subsurface. Most important to this study of groundwater chemistry is pyrite's

role in the precipitation of gypsum.

Though Moran (1978a) had shown that oxidation of pyrite by recharge waters does cannot account for high SO_4^{2-} concentrations in groundwater, they point to this process as the initial step in the ultimate formation of gypsum, which is highly soluble in natural waters. Nearly all waters that infiltrate below the ground surface in arid climates evaporate or are transpired before reaching groundwater. If this process is repeated, pore fluids will eventually be concentrated with ions and gypsum can precipitate. Due to gypsum's high solubility, considerable concentration would have to take place before gypsum would precipitate.

Another process is described by Moran (1978a) which could lead to the formation of gypsum. When sediments are eroded by running water, pyrite is exposed to the air, and HS^- is readily oxidized to SO_4^{2-}. Sulfide grains are carried as bed load and suspended load, and sulfate is moved as dissolved load. When sediments are ultimately deposited in local depression or valleys, sulfide grains are oxidized once more. Dissolved SO_4^{2-} is carried to groundwater or is left at or just below, the surface as a precipitate. When the valley becomes wet again, the sulfate is transported with recharge water to the water table, particularly when groundwater is shallow.

Either or both of these processes of gypsum formation can be invoked to explain the relatively high concentrations

of calcium and sulfate found in samples 67 and 232. The chemical character of these waters could be explained by localized recharge; however, because of the depth to groundwater (128 ft. at location 67), and the slow rates of recharge in this system, this process is not realistic. The same processes could occur if groundwater high in dissolved oxygen encountered pyrite-rich sediments or coal seams, and this seems more likely given the local hydrogeologic conditions.

In a system that is everywhere undersaturated with respect to gypsum (Figure 37), the presence of this mineral is very important to the geochemical evolution of groundwater. Dissolution of gypsum adds calcium to the system which initiates the process of cation exchange in clay-rich sediments. This process also affects carbonate equilibria through the common ion effect. The dissolution of calcite and dolomite can be driven irreversibly by the presence of gypsum in the system.

Carbonate Mineral Equilibria (Calcite and Dolomite)

The $CaCO_3$-H_2O-CO_2 system is usually held responsible for the pH-buffering capacity of groundwater systems. For reasons described above, the weathering of silicate minerals is seen to have an important role in the pH-buffering (or pH-controlling, as CO_2 is consumed and HCO_3^- is produced by albite weathering) process. However, dissolution of

carbonate minerals is a process that must be considered as these minerals are present in the system, are highly reactive, and are a source for Ca^{2+} and Mg^{2+}. They constitute an initial source of buffering capacity, although the pH-buffering in the system is ultimately controlled by silicate mineral equilibria.

Carbonate cement was found to be a dominant constituent of three sandstone samples. Samples 416-31-44 and 416-32-SS-5 are pervasively cemented by calcite, while sample 119-8-104 has patchy areas of cementation. These data point to the presence of carbonate minerals in the system but not to their widespread regional occurrence. However, the presence of carbonate minerals in the system, even in small amounts, is an important consideration due to their reactivity. (As Palmer and Cherry (1984/85) pointed out, only 0.13 wt.% gypsum is required to cause saturation of water, while 1.0 wt.% calcite at a constant P_{CO2} of 10^{-2} bar is needed for saturation. At such small concentrations, these minerals could go undetected in petrographic work).

Without knowledge of the exact composition of carbonate minerals present, geochemical modeling interpretations are limited. Since Mg^{2+} can substitute for Ca^{2+} in the calcite structure, many variations in composition can exist. The composition of the mineral will greatly affect its chemical properties. For example, the solubility of Mg-calcite is greater than pure calcite.

Dolomite, $CaMg(CO)_3$, has long puzzled earth scientists. As suggested by Bricker and Garrels (1967), "interpretation of chemical equilibrium in natural water systems is only meaningful if the detailed chemical and structural variability of the solid phases are considered". Perhaps this is an extreme viewpoint, but one that is worth noting for the purpose of perspective. Ideal concentrations for calcite and dolomite were assumed in the modeling effort described above

When pure water moves through the vadose zone, it can reach CO_2 partial pressures of $10^{-2.5}$ to 10^{-1}. These CO_2-charged waters would dissolve calcite (and weather feldspars) until equlibrium is reached in an open system where partial pressures of CO_2 are maintained (equilibrium pH values are between 6.7 and 7.7 in open system). If Ca^{2+} is taken out of the system, as through the process of ion exchange, the pH and HCO_3^- concentrations of the system will continue to rise as calcite continues to dissolve and equilibrium is maintained. If Ca^{2+} is added to the system, as through the process of gypsum dissolution, then solutions become supersaturated with respect to calcite and the mineral precipitates.

Buffering caused by the weathering of silicate minerals works in much the same way as the process just described for the carbonate-mineral system. Carbon-dioxide gas is consumed while bicarbonate concentration and pH rise.

However, this process is not fueled by cation-exchange phenomenon, but by the addition of CO_2.

In a study Foster (1950), which concerns an area with a similar geologic history to the Moreno Hill Formation, the concept of calcite dissolution working in concert with cation exchange processes and the weathering of organic material is explored. Foster (1950) showed experimentally that the interaction of lignite, calcite, and a base-exchange mineral, such as smectite, will produce high pH-high alkalinity waters. Calculated pH values for various combinations of this ideal system were in the range of those measured in samples from the Moreno Hill Formation. However, HCO_3 concentrations were approximately double (1014 mg/l) that of sample 86 which had the highest HCO_3 concentratrions (536 mg/l).

Several hypotheses are offered to explain the discrepancies in bicarbonate concentrations. If pH-buffering is dominantly controlled by the weathering of albite, less HCO_3^- is produced as a result of this reaction (dissolution of 1 mole of calcite will produce 2 moles of HCO_3^- while weathering 1 mole of albite only produces 1 mole of HCO_3^-). Gypsum dissolution is a source for Ca^{2+} and therefore, carbonate mineral dissolution is not a requirement of the geochemical model. If carbonate minerals are present in the system in significant amounts, and reacting in the system, then the weathering of feldspars

could be a dominant buffering process, and may actually act to inhibit calcite dissolution by robbing the system of CO_2. Finally, calcite dissolution may be the initial stage of buffering, followed by the weathering of albite.

Na-smectite and Cation Exchange

As discussed in Chapter 3, semi-quantitative clay analysis revealed only Na-smectite, no Ca-montmorillonites were detected. This observation is inconsistent with what is expected for a continental-sedimentary environment. The Moreno Hill Formation consists of continental sediments, whereas the Na-rich composition of these clay rocks would be more characteristic of a marine environment.

As pointed out by Moran (1978a), fresh continental waters have selectivity coefficients (K^*) for the Na-Ca exchange reaction that are characteristically less than one, where:

$$K^* = \frac{Ca\ (Ca)\ N2\ Na}{Na^2\ (Na)^2\ N\ Ca}$$

and Ca^{2+} and Na^+ represent the activity coefficient of calcium and sodium respectively, the quantities in parentheses are the concentrations in molality or molarity, and N denotes the mole fraction of the absorbed cation.

Also, the Na/Ca molar ratio is characteristically not very large. Clays deposited in most fluvial or deltaic environments will have nearly all the cation exchange sites filled by Ca^{2+}. Since Ca^{2+} is preferentially adsorbed, in order for a clay to become Na-rich, it must at some point become submerged in Na-rich waters.

One could postulate many reasons for how the exchange sites on these clays became filled with Na^{+}, but without an in-depth study of geologic evidence to support a hypothesis, it is not useful to discuss this problem. Suffice it to say that, at some time in the geologic history of the Moreno Hill Formation, the sediments were invaded by Na-rich waters (such as a marine invasion or upward flow of brackish water). The groundwater flow system is presently at work to replace Na^{+} with Ca^{2+} ions, however flow is so slow in this area that Na^{+} is still the dominant cation.

With all the available exchangeable Na^{+}, and the presence of clays with high CEC values, the cation exchange process has a strong effect on the evolution of groundwater chemistry in this area as was supported by the geochemical modeling effort. However, as is illustrated by Figure 32, it is not the only process which significantly contributes to the sodium content of these waters.

Organic Material

Organic material is present as discontinuous coal and

lignite beds in alternating sequences with shales and sandstones as well as detrital particles within these units. The presence of organic material in this system is extremely important to the geochemical evolution of groundwater as it is a source (other than soil gas) for CO_2.

The CO_2 content of soil-air is much greater than atmospheric air ($10^{-2.5}$ to 10^{-1} and $10^{-3.5}$ respectively, Hem, 1985). Meteoric waters moving through the vadose zone dissolve CO_2 and become enriched. The biochemical decomposition of soil organic material, combined with the respiration process occuring on plants, will liberate large amounts of CO_2 to the soil atmosphere.

Another source for CO_2 is the chemical or biochemical breakdown of sulfate by carbonaceous material or by the dynamochemical breakdown of the material itself (Foster, 1950). The dynamochemical process is the progressive elimination of volatile matter from organic sediments by the readjustment of the internal molecular structure of the material. This causes the detachment of simple volatile substances from large unstable molecules. Carbon dioxide gas is a primary constituent of these gases.

The result of this weathering process is the increased enrichment of waters with CO_2. These aggressive waters are able to pervasively alter feldspars and dissolve carbonate minerals. In Table 15 values for pCO_2, calculated by WATEQF from total alkalinity and pH, show that many samples

had relatively high values for this consituent. This points to the fact that this groundwater system is not closed with respect to CO_2 (sample 86, which should be relatively more depleted in CO_2 from the action of albite weathering imposed at all points along a flowpath, had one of the highest values, 8.7E10-2). Organic material is seen to play a major role in the extremely weathered condition of albite in these samples.

Conclusions

Figure 41 illustrates a synthesis of information presented in this study. This geochemical model depicts the various pathways available to the major cations and anions considered. A few important observations can be drawn in review of this figure. The hydrogeochemical system is complex, and a uniquely-defined geochemical model is impossible without additional data for mineralogy and groundwater chemistry. Albite dissolution (or the weathering of albite and the formation of kaolinite) is the dominant process controlling the pH of this system. The chemical and dynamochemical breakdown of organic matter acting as a constant source provides the fuel (or CO_2) for this process. Cation exchange is an important contributer to the system due to the presence of Na-smectite, the source for exchangeable sodium. These three geochemical processes are assumed to be regional geochemical controls governing the evolution of groundwater chemistry towards a Na-HCO_3 hydrochemical facies. Locally, gypsum dissolution and carbonate mineral precipitation or dissolution cause variable inputs of calcium, magnesium, and bicarbonate. These variables are acted on by the regional controls and Na-HCO_3 waters are produced.

REFERENCES

Al-Ruwaih Fawzia (1984) Ground-water chemistry of Dibdiba formation, North Kuwait. Ground Water 22, 413-417.

Austin G. (1985) Personal communication.

Ball J. W., Jenne E. A., and Nordstrom D. K. (1979) Wateq2-a computerized chemical model for trace and major element speciation and mineral equilibria of natural water. In Chemical Modeling in Aqueous Systems (ed. E. A. Jenne) , Am. Chem. Soc. Symp. Series 93, pp. 815-835.

Back W. and Freeze R. A. (1983) Chemical Hydrogeology, Benchmark Papers in Geology **73** (eds. William Back and R. Allen Freeze) 416p., Hutchinson Ross Publishing Company.

Back W. (1966) Hydrochemical facies and groundwater flow patterns in the northern part of the Atlantic Coastal Plain. U. S. Geol. Survey Prof. Paper 498-A, 42p.

Barnes I. and Hem J. D. (1973) Chemistry of subsurface waters. Annu. Rev. Earth Planet. Sci. 1, 157-301.

Bates R. L. and Jackson J. A. (1980) Glossary of Geology, 751p. American Geological Insititute, Falls Church, Virginia.

Berner R. A. (1981) A new geochemical classification of sedimentary environments. J. of Sed. Pet. 51, 359-365.

Berner R. A. and Holdren Jr. G. A. (1979) Mechanism of feldspar weathering - II. Observations of feldspars from soils. Geochim. Cosmochim. Acta 43, 1173-1186.

Berner R. A. (1978) Rate control of mineral dissolution under earth surface conditions. Amer. J. of Sci. 278, 1235-1252.

Berner R. A. (1975) Diagenetic models of dissolved species in the interstitial waters of compacting sediments. Amer. J. of Sci. 275, 88-96.

Berner R. A. (1971) Principles of Chemical Sedimentology 240p. McGraw-Hill, New York.

Blatt H., Middleton G. and Murray R. (1980) Origin of Sedimentary Rocks 782p. Prentice Hall Inc., Englewood Cliffs, New Jersey.

Bowers T. S., Jackson K. J. and Helgeson H. C. (1984) Equilibrium Activity Diagrams for Coexisting Minerals and Aqueous Solutions at Pressures and Temperatures to 5kb and 600º, 400p. Springer-Verlag, Berlin, Heidelberg, New York, Tokyo.

Bricker O. P., Godfrey A. E. and Cleaves E. T. (1968) Mineral-water interaction during the chemical weathering of silicates. Trace Inorganics in Water. Advan. Chem. Ser. 73, 128-142.

Bricker O. P. and Garrels R. M. (1967) Mineralogic factors in natural water equilibria. In Principles and Applications of Water Chemistry, (eds. S. D. Faust and J. V. Hunter) pp. 449-468. John Wiley and Sons, New York.

Brindley G. W. and Brown G. (1980) Crystal structure of clay minerals and their X-ray identification. Mineralogical Society Monograph no. 5, 495p.

Berry Frederick A. F. (1959) Hydrodynamics and geochemistry of the Jurassic and Cretaceous systems in the San Juan Basin, northwestern New Mexico and southwestern Colorado. Ph.D. thesis, Stanford University.

Brownlow A. M. (1979) Geochemistry, 498p. Prentice-Hall Inc., Englewood Cliffs, New Jersey.

Campbell F. and Roybal G. H. (1984) Geology and coal resources of the Fence Lake 1:50,000 quadrangle Catron and Cibola Counties, New Mexico. New Mexico Bureau of Mines and Mineral Resources Open File Report 207, 34p.

Campbell F. (1981). Geology and coal resources of Cerro Prieto and the Dyke quadrangles. New Mexico Bureau of Mines and Mineral Resources Open File Report 144, 44p.

Cather S. M. and Johnson B. D. (1984) Eocene tectonics and depositional setting of west-central New Mexico and eastern Arizona. New Mexico Bureau of Mines and Mineral Resources, Circular 192, 33p.

Cederstrom D. J. (1946) Genesis of ground water in the coastel plain of Virginia. Econ. Geol. **41**, 218-245.

Chapelle F. H. and Knobel L. L. (1983) Aqueous geochemistry and the exchangeable cation composition of Glauconite in the Aquia Aquifer, Maryland. Water Resources Research **21**, 343-352.

Chapelle F. H. (1983) Groundwater geochemistry and calcite cementation of the Aquia Aquifer in southern Maryland. Water

Resources Research 19, 545-558.

Chebatorev I. I. (1955) Metamorphism of natural waters in the crust of weathering. Geochim. Cosmochim. Acta 8, 22-48, 137-170, 198-212.

Cleaves E. T, Godfrey A. E. and Bricker O. P. (1970) Geochemical balance of a small water-shed and its geomorphic implications. Geo. Soc. Am. Bull. 81, 3015-31032.

Degens E. T. (1965) Geochemistry of Sediments, 342p. Prentice-Hall Inc., Englewood Cliffs, New Jersey.

Dickinson W. R. (1970) Interpreting detrital modes of graywacke and arkose. J. of Sed. Pet. 40, 695-707.

Drever J. I. (1982) The Geochemistry of Natural Waters, 388p. Prentice Hall Inc., Englewood Cliffs, New Jersey.

Drever J. I. (1971) Early diagenesis of clay minerals, Rio Ameca, Mexico. J. of Sed. Pet. 41, 982-994.

Eugster H. P. and Jones B. F. (1979) Behavior of major solutes during closed-basin brine evolution. Amer. J. of Sci. 279, 609-631.

Forcella L. S. (1982) Geochemistry of thermal and mineral watrs in the Cascade Mountains of western North America. Ground Water 20, 39-47.

Freeze. R. A. and Cherry J. A. (1975) Groundwater 604p. Prentice-Hall Inc., Englewood Cliffs, New Jersey.

Foster M. D. (1950) The origin of high sodium bicarbonate water in the Atlantic and Gulf Coastal Plains. Geochim. Cosmochim. Acta 1, 33-48.

Fritz B. (1985) Multicomponent solid solution for clay minerals and computer modeing of the weathering process. In The Chemistry of Weatering, (ed. J. I. Drever), pp. 19-34. D. Reidel Publishing Co. Boston, Massachusets.

Garrels R. M. and MacKenzie F. J. (1967) Origin of chemical composition of some springs and lakes. Equilibrium Concepts in Natural Water Systems. Advan. Chem. Ser. 67, 222-242.

Garrels R. M and Christ C. L. (1965) Solutions, Minerals and Equlibria, 450p. W. H. Freeman and Co., San Francisco, California.

Garrels R. M. and Howard P. (1957) Reactions of feldspars and mica with water at low temperatures and pressures. Clays

and Clay Miner. 2, 68-88.

Golterman H. L. (1969) Methods for the Chemical Analysis of Fresh Waters. International Biological Programme Handbook No. 8 (ed. H. L. Golterman), 172p. Blackwell Scientific Publications, San Francisico, California.

Grim R. E. (1968) Clay Mineralogy, 596p. McGraw-Hill Book Company, New York.

Groenewold G. H., Rehm B. W. and Cherry J. A. (1981) Depositional setting and groundwater quality in coal-bearing sediments and spoils in western North Dakota. Soc. Econ. Petr. and Miner. Spec. Pub. no. 31, 157-167.

Harris W. H. and Matthews R. K. (1968) Science **168**, pp. 77-79.

Helgeson H. C. (1970) Description and interpretation of phase relationships in geochemical processes. Am. J. Sci. **268**, 415-438.

Hem J. D. (1985) Study and interpretation of the chemical characteristics of natural water. U.S. Geol. Survey Water Supply Paper 2254, 263p.

Hess P. C. (1966) Phase equilibria of some minerals in the K_2O-Na_2-O-Al_2O_2-SiO_2-H_2O system at 25°C and 1 atm. Amer. J. of Sci. **264**, 289-309.

Holdren G. R. and Berner R. A. (1979) Mechanism of feldspar weathering. Geochem. Cosmochem. Acta 43, 1161-1171.

Hostettler J. D. (1984) Electrode electrons, aqueous electrons, and redox potentials in natural waters. Amer. J. of Sci. **284**, 734-759.

Hower J. and Mowatt T C. (1966) The mineralogy of illites and mixed-layer illite/montmorillonites. Amer. Mineralogist 51, 825-854.

Jackson D. and Lloyd J. W. (1984) An integrated hydrochemical approach to deduce the response of an aquifer system during its history of abstraction. Ground Water 22, 735-745.

Jenne E. A. (1979) Chemical modeling-goals, problems, approaches, and priorities. In Chemical Modeling in Aqueous Systems, (ed. E. A. Jenne), pp. 3-21. Am. Chem. Soc. Symposium Ser. 93.

Jones B. F., Eugster H. P. and Rettig S. L. (1977)

Hydrogeochemistry of the Lake Magadi Basin, Kenya. Geochim. Cosmochim. Acta 41, 53-72.

Kand M. C., Greenburg A. E. and Taras M. J. (1975) Standard Methods for the Examination of Water and Wastewater, 14th Edition, American Public Health Association, Washington, D. C., 1193p.

Kenoyer G. J. (1982) Groundwater chemistry evolution in a silicate aquifer. Geol. Soc. of Amer. Abs. with Programs 14, 529.

Kramer J. R. (1968) Mineral-water equilibria in silicate weathering. 22nd Int. Geol. Congr. 6, 149-160.

Krauskopf A. M. (1967) Introduction to Geochemistry, 721p. McGraw-Hill Book Company, New York.

Krauskopff K. B. (1959) The geochemistry of silica in sedimentary environments. Soc.of Econ. Petr. and Miner. Spec. Pub. no. 7, 4-19.

Krothe N. C. and Bergenson M. P. (1981) Hydrochemical facies ina Tertiary basin in the Milligan Canyon area, southwetern Montana. Ground Water 19, 392-399.

Langmuir D. (1971) The geochemistry of some carbonate waters in central Pennsylvanian. Geochim. Cosmochem. Acta. 35, 1023-1045.

Laughlin A. W., Brookins D. G., Damon P. E. and Shafiqullah M. (1979) Late Cenozoic volcanics of the Central Jemez Zone, Arizona, New Mexico. Isochron West no. 25, 5-8.

Lindberg R. D. and Runnels D. D. (1984) Ground water redox reactions: Redox state applied to Eh measurements and geochemical modeling. Science 225, 925-927.

Lloyd J. W. and Heathcote J. A. (1985) Natural Inorganic Hydrochemistry in Relation to Groundwater, an Introduction, 296p. Clarendon Press, Oxford, England.

Mack G. H. and Grisby J. D. (1985) Mechanical and chemical diagenesis of the Hayner Ranch and Rincon Valley Formations (Sante Fe Group, Miocene), San Diego Moutain, New Mexico. New Mexico Geology 7 (no. 3), August.

McGurk B. E. and Stone W. J. (1986) Conceptual hydrogeologic model of the Nations Draw Area, Catron and Cibola Counties, New Mexico. Report to Fuels Department, Salt River Project, Phoenix, Arizona, 121p.

Merino E. (1979) Internal consistency of a water analysis and uncertainty of the calculated distribution of aqueous species at 25 C. Geochim. Cosmochim. Acta 43, 1533-1542.
Moran S. R., Cherry J. A., Fritz P., Peterson W. M., Somerville M., Stancel S. A. and Ulmer J. H. (1978) Geology, groundwater hydrology, hydrogeochemistry of a proposed surface mine and lignite gasification plant site near Dunn Center, North Dakota. Report of Investigation 61, 263p. North Dakota Geol. Survey.

Moran, S. R., Groenewold G. H. and Cherry J. A. (1978a) Geologic, hydrologic, and geochemical concepts and techniques in the overburden characteristics for a mined-land reclamation. Report of Investigation no. 63, 152p. North Dakota Geol. Survey.

Morgan J. J. (1967) Applications and limitations of chemical thermodynamics in natural water systems. Advan. in Chem. Ser. 67.

Morel F. and Morgan J. J. (1972) A numerical method for computing equilibria in aqueous chemical systems. Environ. Sci. and Tech. 6, 58-67.

Ollier C. D. (1969) Weathering, (eds. Olivier and Boyd), 340p. Edingurgh, England.

Ohse W., Matthess G. M. and Pekdeger A P. (1985) Equilibrium and disequilibrium between pore waters and minerals in the weathering environment. In The Chemistry of Weathering, (ed. J. I. Drever), 324p. D. Reidel Publishing Co., Boston, Massachusets.

Paces T. (1972) Chemical characteristics and equilibration in natural water-felsic rock-CO_2 system. Geochem. Cosmochim. Acta 36, 217-240.

Palmer C. D. and Cherry J. A. (1984/1985). Geochemical evolution of groundwater in sequences of sedimentary rocks. J. of Hydrol. 75, 27-65.

Parkhurst D. L., Plummer L. N. and Thorstenson D C. (1982) BALANCE- A computer program for calculating mass transfer for geochemical reactions in ground water. U.S. Geol. Survey Water-Resouces Investigations 82-14.

Piper A. M. (1944) A graphic procedure in geochemical interpretation of water-analyses. Trans. Amer. Geophys. Union 25, 914-928.

Plummer L. N., Jones B. F. and Truesdell A H. (1984) WATEQF: A Fortran IV version of WATEQ, a computer program for

calculating chemical equilibria of natural waters. U.S. Geol. Survey Water Resources Investigation Report 76-13.

Plummer L. N. (1984) Geochemical modeling: a comparison of forward and inverse methods. In Proceedings of the First Canadian/American Conference on Hydrogeology, (eds. B. Hithcon and E. I. Wallick), pp. 149-170. National Water Well Association, Worthington, Ohio.

Plummer L. N., Parkhurst D. L. and Thorstenson D C. (1983) Developement of reaction models for groundwater systems. Geochim. Cosmochim. Acta 47, 665-686.

Plummer L. N. and Back W. (1980) The mass balance approach: application to interpreting the chemical evolution of hydrologic systems. Amer. J. of Sci. 280, 130-142.

Plummer L. N. (1977) Defining reactions and mass transfer in part of the Florida aquifer. Water Resources Research 13, 801-812.

Powell J. D. and Larson J. D. (1985) Relation between ground-water quality and mineralogy in the coal-producing Norton formation of Buchanan County Virginia. U.S. Geol.Survey Water-Supply Paper 2274.

Rach H. W. and White W. B. (1977). Dissolution kinetics of carbonate rocks 1. Effects on lithology of dissolution rate. Water Resources Research 13, 381-394.

Reynolds R. C. and Hower J. (1970) The nature of interlayering in mixed-layer illite/montmorillonites. Clays Clay Miner. 18, 537-544.

Roybal G. H. and Campbell F. (1981) Stratigraphic sequence in drilling data, Fence Lake Area. New Mexico Bureau of Mines and Mineral Resources Open File Report 145, 28p.

Runnels D. D. (1969) Diagenesis, chemical sediments, and the mixing of natural waters. J. of Sed. Petr. 39, 1188-1201.

Salt River Project (1982) Coal and groundwater resources of Fence Lake Coal lease area, Catron County, New Mexico. Groundwater Planning Division, Salt River Project, Phoenix, Arizona, 25p.

Seifurt G. G. and Greenburg M A. (1985) Fence Lake Coal Project, groundwater monitering. In Groundwater Contamination and Reclamation. Proceedings, (ed. K. D. Schmidt), pp. 19-25. American Water Resources Association.

Senkayi A. L., Dixon J. B., Hossner L. R. and B. E. Viani

(1983) Mineralogic transitions during weathering of lignite overburden in east Texas. Clays and Clay Miner. 31, 49-56.

Stumm W. and Morgan J. J. (1981) Aquatic Chemistry 2nd Ed., 780p. Wiley-Interscience, New York.

Stone W. J. (1984) Recharge in the Salt Lake Coal Fields based on chloride in the unsaturated zone. New Mexico Bureau of Mines and Mineral Resources Open File Report 214, 56p.

Tardy Y. (1971) Characterization of the principle weathering types by the geochemistry of waters from some European and African crystalline massifs. Chemical Geology 7, 253-271.

Thorstenson D. C. (1984) The concept of electron activity and its relation to redox potentials in aqueous geochemical systems. U.S. Geol. Survey Open-File Report 84-072.

Thorstenson D. C., Fisher D. W. and Croft M. G. (1979) The geochemistry of the Fox Hills - Basal Hell Creek aquifer in southwestern North Dakota and northwestern South Dakota, Water Resources Research 15, 1479-1498.

Truesdall A. and Jones B. F. (1974) Wateq, a computer program for calculating chemical equilibria of natural waters. U.S. Geol. Survey J. of Research 2, 233-248.

van der Plas L. and Tobi A. C. (1965) A chart for judging the reliability of pointing counting results. Amer. J. of Sci. 263, 87-90.

Velbel M. A. (1985) Hydrochemical constraints on mass balances in forested watersheds of the southern Appalachians. In The Chemistry of Weathering (ed. J. I. Drever), 324p. D. Reidel Publishing Company, Boston, Massachusatts.

White D. E. (1965) Fluids in subsurface environments- a symposium. Amer. Ass. of Petr. Geol. Memoir 4, 130-142.

Wilson M. J. and Nadeau P. H. (1985) Interstratified clay minerals and weathering processes. In The Chemistry of Weathering, (ed. J. I.Drever), 324p. D. Reidel Publishing Co., Boston, Massachusets.

Zaporozec, A. 1972. Graphical interpretation of water-quality data. Ground Water 10, 32-43.

Appendix 1

Hand Sample and Petrographic Descriptions of Surface and Subsurface Sandstones

SURFACE SANDSTONES

SAMPLE #	HAND SAMPLE DESCRIPTION	PETROGRAPHIC OBSERVATIONS
417-3-SS-B	Lt. brown with some iron staining, lower-fine, subangular to subrounded, poorly-sorted, moderately-friable with lots of altered feldspar.	0.3mm, moldic porosity, quartz overgrowths, abundant iron cement (?)
417-3-SS-9	Buff, upper-v. fine, poorly-sorted subangular to subrounded, moderately-friable.	0.2mm, abundant iron-stained epimatrix, a few large micas.
416-17-SS-2	Buff to light-brown, iron staining, lower-coarse, moderately-sorted	1.0mm, moldic porosity, hematite cement, plagiclase with magnetite inclusions (?).
416-17-SS-3	Mottled buff-brown, upper-medium, well-sorted, subangular to subrounded, friable, abundant clay matrix.	0.8mm, abundant altered plagioclase, more characteristic of subsurface sample.
416-32-SS-4	Mottled buff-brown, lower-medium, well-sorted, subangular, friable, abundant clay matrix.	0.7mm, some of lithic fragments may actually be extremely altered feldpar, some volcanic rock fragments.
416-32-SS-5	Light-brown to dark-brown, upper-fine, moderately-sorted, subangular, well-indurated, abundant heavy minerals.	0.3mm, pervasive carbonate cement, quartz overgrowths, moldic porosity.
417-24-SS-6	Light-brown, lower-medium, poorly-sorted, subangular to subrounded, moderately friable, altered feldspars.	0.6mm, antiperthites, organic material.
416-31-SS-F	Buff, upper-fine, poorly-sorted, well-indurated, clay matrix.	0.1mm, sparse carbonate cement.

SURFACE SANDSTONES

SAMPLE #	HAND SAMPLE DESCRIPTION	PETROGRAPHIC OBSERVATIONS
416-31-SS-I	Buff to light-brown with some iron staining, lower-fine, poorly-sorted, well-indurated.	0.2mm, dissolution textures in many plagioclase feldspars.
417-25-SS-1	Light-brown with iron staining, lower-medium to very-coarse, poorly-sorted, angular to subrounded, friable, bands of coarser grains.	1.0mm, K-feldspar with silica overgrowths, abundant hematite cement, plagioclase altered to sericite.
418-7-SS-F1	Light-brown, lower-medium, poorly to moderately-sorted, subangular to subrounded, friable.	0.4mm, abundant porosity, mica psuedomatrix, hematite cement.
418-7-SS-F2	Buff to light-brown, lower-medium, moderately well-sorted, subrounded, friable.	0.5mm, zircon or apatite grains, antiperthites.
418-7-SS-F3	Buff to light-brown, upper-fine, moderately well-sorted, subrounded, friable.	0.3mm, plagioclase altering to sericite, dissolution textures, antiperthites.
219-26-SS-B	Greenish light-brown, upper-very fine, well-sorted, subangular.	0.1mm, a few large mica grains, abundant hematite cement.
219-26-SS-D	Greenish-brown, upper-very fine, well-sorted, subangular.	0.1mm, some biotite and chlorite grains, altered hard to identify.
219-26-SS-F	Light-brown, lower-fine, well-sorted, subangular.	0.2mm, hard to identify grains.
119-17-SS-1	Light-brown with iron staining, lower-moderate, moderately-sorted.	0.4mm, plagioclase not as altered relative to other samples.

SUBSURFACE SANDSTONES

SAMPLE #	HAND SAMPLE DESCRIPTION	PETROGRAPHIC DESCRIPTION
416-31-65	Light-brown, upper-fine, moderately-sorted, subrounded to rounded, clasts of organic material.	0.1mm, zircon and hornblende grains, pervasively altered plagiclase.
416-31-70	Light-brown, upper-fine, moderately-sorted, subrounded to rounded, organic material.	0.3mm, plagioclase almost altered to epimatrix, some minor carbonate cement, moldic porosity.
518-17-221	Buff, upper-very fine to lower-fine, poorly to moderately-sorted, extremely friable, no coal or mudstone in core.	0.1mm, laminations, epimatrix slightly yellow in color, K-feldspar dissolution, hornblende and zircon grains, organic matter.
518-17-226	Buff, upper-medium, moderately-sorted, subrounded, friable.	0.1mm, pseudomatrix abundant, dissolution rims on quartz, hard to identify grains.
519-20-285	Buff, upper-medium, moderately-sorted, subrounded, some organic fragments, no coal in core.	0.7mm, pervasively altered plagioclase, quartz dissolution.
519-20-275	Buff, upper-fine, moderately-sorted, subangular, no coal in box.	0.3mm, plagiclase altered to epimatrix, moldic porosity.
519-20-281	Buff, lower-medium, moderately-sorted, subangular to subrounded.	0.4mm, laminations, sedimentary lithic fragments, hematite cement (organic cement ?).
119-8-104	Whitish-gray, upper-fine, moderately-sorted, subangular, in contact with coal.	0.3mm, sample extremely altered, can not trust point count data.

SUBSURFACE SANDSTONES

SAMPLE #	HAND SAMPLE DESCRIPTION	PETROGRAPHIC DESCRIPTION
417-3-34	Buff with iron staining, upper-medium, well-sorted, subangular to subrounded, friable.	1.0mm, plagioclase altering to epimatrix, hematite cement.
417-3-36	Buff with iron-staining, lower-coarse, moderately to poorly-sorted, subangular to subrounded.	1.0mm, orthomatrix abundant, hornblende grain, organic material, quartz overgrowths.
417-3-37	Buff with minor iron staining, lower-very coarse, moderately to poorly-sorted, subrounded, clay coatings on grains, above coal.	2.0mm, orthomatrix, metamorphic, quartz, laminations.
416-32-40	Buff to light brown, lower-medium, poorly to moderately-sorted, subrounded, altered feldspars.	0.4mm, altered volcanic fragments, hematite cement.
416-32-42	Buff to light brown, lower-medium, poorly to moderately-sorted, subrounded, altered feldspars.	0.4mm, abundant hematite cement, small black inclusions, large sedimentary lithics, organic matter.
416-32-44	Buff to light-brown, lower-fine, moderately-sorted, subrounded.	0.2mm, extremely hard to identify lithic grains, plagiclase extremely altered, black inclusions in epimatrix.
416-31-44	Buff, upper-fine to lower-medium, poorly-sorted, subangular to subrounded, 4 ft. above coal zone.	0.3mm, hematite cement, lots of black inclusions (organic ?), plagioclase pervasively altered, silica replacing K-feldspar (?).
416-31-48	White to buff, lower-fine to upper-fine, moderately-sorted, subrounded, directly above coal bed.	0.2mm, plagioclase grains extremely altered with black inclusions.

Appendix 2

Problems Associated with the Parameter Eh and Its Use in Groundwater Quality Investigations

Thorstenson (1984) examined the concept of pE as $-\log_{10}$ (electron activity). He found that the analogy of pE and pH as master variables in a groundwater system was not founded. He also discovered that determination of a thermodynamically meaningful value of redox was not possible in disequilibrium systems. Additionally, it was determined that redox couples do not exist in disequilibrium systems, and can not be measured in natural waters.

Thorstenson (1984) showed that redox characteristics are only useful given data for multiple redox couples (such as Fe^{3+}/Fe^{2+}, HS^-/SO_4^{2-}, NO_2^-/NO_3^-, $NH_4/NO3^-$, and CH_4/HCO_3). Site-specific data is also extremely critical to a study. Redox processes can not be meaningfully considered when only electrode measurements and thermodynamic stability calculations are available.

A major problem with the concept of electron activity is the fact that concentrations of aqueous electrons can never achieve physically meaningful values. Difficulties encountered in the study of redox potential are attributed to reaction kinetics, when in fact, the problems are thermodynamic in nature. Thorstenson (1984) described the details of the calculations which led him to this conclusion in his paper.

In equilibrium systems, reaction kinetics are not involved. Natural groundwater systems are non-equilibrium systems. In a total disequilibrium system, the redox

potential of an aqueous phase is inherently undefinable and unmeasurable due to the absence of $e^-_{(aq)}$. In partial equilibrium systems, some reactions occur fast enough that equilibrium is achieved, while the kinetics of other reactions are slow and not achieved. Most groundwater systems are partial equilibrium systems, and these variations in the kinetics of reactions are the source of greatest confusion in dealing with redox reactions.

An Eh meter can only measure electron potential in a metal electrode (relative to the S.H.E. or standard hydrogen electrode) produced by electron-transfer reactions involving M, M^+, N, and N^+ at the electrode surface. The result of this measurement is a mixed potential resulting from disequilibrium reactions or dominant eletroactive couples. Thorstenson (1984) explained how, if multiple redox couples exist in a groundwater system, the Eh measurement is non-unique relative to the system.

If the species concentration of the dominant electroactive couple are known, and a known amount of contaminant is introduced to the system which reacts rapidly with the dominant couple, the final redox state of both species can be calculated. If the reaction of either or both couples with a platinum electrode is rapid, the final state may be obtained from an Eh measurement.

However, even if these criteria are satisfied, an electrode is still only useful as an analytical tool describing the

speciation of a particular redox couple, and not the system as a whole. If even one other redox couple in small amounts is present at disequilibrium in the system, a thermodynamic redox potential for the aqueous phase can not be defined (for more on the subject of problems inherent in the measurement and use of the parameter Eh, see Lindberg and Runnels, 1984, and Hostettler, 1984).

Bacterial sulfate reduction by organic matter described by the following reaction:

$$15CH_2O + 2Fe_2O_{3(s)} + 8SO_4^{2-}(aq) + H_2CO_3 =$$
$$4FeS_{2(s)} + 16HCO_3^-(aq) + 8H_2O$$

followed by disproportionation of organic matter:

$$2CH_2O = CH_{4(aq)} + CO_{2(aq)}$$

is assumed to be a viable process in the Moreno Hill groundwater system based on all information gathered and described in this study. Therefore, minerals not obviously present in the groundwater samples, but known to exist in the system (namely Fe_2O3, FeS_2, and lignitic carbon) may be acting to control the redox chemistry via bacterially-mediated, irreversible reactions. It is likely that redox geochemistry is controlled in situ by minerals and gases not represented in the groundwater samples. Sulfide and

sulfate concentrations were measured for each of the groundwater samples obtained from nine of SRP's monitor wells. Six out of the nine samples contained measurable quantites of HS-, and Eh values were calculated. The values ranged from -0.24 to -0.36. (The method of analysis for HS^- is a tedious and difficult titration (Golterman, 1969) which must include some amount of analytical error.)

After careful review of the papers referred to earlier, and consideration of the paucity of data available for characterization of this system, it was obvious that the redox potential of this system could not be considered in the geochemical evolution of groundwater in the Moreno Hill Formation. However, it should be noted that this parameter could be very useful in the interpretation of groundwater chemistry evolution, particularly with respect to understanding the relationship between pyrite and gypsum.

A complete geochemical study must include total analyses for all redox couples in the system, kinetic studies of the reactions not at equilibrium, and consideration of minerals, gases, and bacteria present where the groundwater sample is obtained, but not considered by water quality analyses. Further study is warranted in this area.

Appendix 3

Plotting Program

```
      PROGRAM PLTSYM
C-----------------------------------------------------------------------
C       GRAB X VERSUS Y DATA FROM COMBIN.OUT FILE

        CHARACTER     NAM(0:14)*8
        REAL          V(0:14),    X(50),Y(50)

C       V(0) = ACCESSION NUMBERS, K=1,26
C       V(1) = INTEGER.MANTISSA   INTEGER=SECTOR,MANTISSA=FRACTIONAL DIST
C       V(2) = Calcium
C       V(3) = Magnesium   etc. etc.


        WRITE(*,*)'(1) - EQUIVALENTS'
        WRITE(*,*)'(2) - CONCENTRATIONS'
        WRITE(*,*)'(3) - ACTIVITIES'
        READ(*,*) L
        IF(L.EQ.1) NC = 12
        IF(L.EQ.2) NC = 14
        IF(L.EQ.3) NC = 13
        IF(L.EQ.1) OPEN(UNIT=2,NAME='COMBIN_MEQ.NEW',STATUS='OLD',READONLY)
        IF(L.EQ.2) OPEN(UNIT=2,NAME='COMBIN_CON.NEW',STATUS='OLD',READONLY)
        IF(L.EQ.3) OPEN(UNIT=2,NAME='COMBIN_ACT.NEW',STATUS='OLD',READONLY)
        IF(L.NE.3) READ(2,10) (NAM(I),I=0,NC)
        IF(L.EQ.3) READ(2,11) (NAM(I),I=0,NC)
10      FORMAT(6X,15A8)
11      FORMAT(1X,15A9)
        READ(2,*)

        OPEN(UNIT=1,STATUS='NEW',CARRIAGECONTROL='LIST')

        SFAC =  1.609    ! KM/MILE CONVERSION
        XMAX = -1.E+15
        YMAX = -1.E+15
        XMIN = +1.E+15
        YMIN = +1.E+15

        IF(L.NE.3) THEN
          WRITE(*,*)'(0) - TWO NUMBERS ONLY'
          WRITE(*,*)'(1) - FOUR NUMBERS (ADD)'
          READ(*,*) ITOSS
          IF(ITOSS.EQ.1) CALL FOUR(X,Y,V,NC,L,SFAC)
        END IF

        WRITE(*,*)'ENTER TWO COLUMN NUMBERS  (X VS Y)'
        READ(*,*) L1,L2
        WRITE(*,15) NAM(L1),NAM(L2)
15      FORMAT(' ***** ',2A8)

        DO I=1,999
          READ(2,*,END=99) (V(J),J=0,NC)
          IACN = V(0)
C         IF(V(L1).GE.0 .AND. V(L2).GE.0) THEN
            N = INT(V(1))
            D = (V(1)-N)
            E = D * 14.0
            IF(L1.EQ.1) V(L1) = E * SFAC
C           A KLUGE TO IGNORE ACTIVITY QUOTIENTS EQUAL TO ZERO ...
C           ... WHICH GETS KLUGIER TO KEEP OTHER STUFF WORKING ...
C           IF(L.EQ.3 .AND. L2.EQ.5  .AND.  V(L2).EQ.0.)  GO TO 1000
            IF(L.EQ.3 .AND. (V(L1).EQ.0 .OR. V(L2).EQ.0)) GO TO 1000
            IF(L.NE.3 .AND. (V(L1).LT.0 .OR. V(L2).LT.0)) GO TO 1000
            XMIN = AMIN1(XMIN,V(L1))
            YMIN = AMIN1(YMIN,V(L2))
            XMAX = AMAX1(XMAX,V(L1))
            YMAX = AMAX1(YMAX,V(L2))
            WRITE(1,20) V(L1),V(L2),N,IACN,D
1000        CONTINUE
C         END IF
        END DO
20      FORMAT(2F10.3,2I5,F10.2)

99      CLOSE(UNIT=1)
        CALL PXVY(XMIN,XMAX,YMIN,YMAX,L)

        END
```

```
      SUBROUTINE FOUR(X,Y,V,NC,L,SFAC)
C-----------------------------------------------------------------
C       COMBINE DATA FROM MORE THAN ONE COLUMN

        REAL          V(0:14),    X(*),Y(*)


        XMAX = 0.
        YMAX = 0.

        WRITE(*,*)'ENTER FOUR COLUMN NUMBERS (C1+C2, C3+C4)'
        WRITE(*,*)'REPEAT COL NO IF YOU WANT JUST ONE, IE.'
        WRITE(*,*)'FOR (C1 VS C3+C4) ENTER C1,C1, C3,C4'
        READ(*,*) L1,L2,L3,L4

        DO WHILE(.TRUE.)
          READ(2,*,END=99) (V(J),J=0,NC)
          IACN = V(0)
          IF(V(L1).GE.0.AND.V(L2).GE.0.AND.V(L3).GE.0.AND.V(L4).GE.0) THEN
            N = INT(V(1))
            D = (V(1)-N)
            E = D * 14.0
            IF(L1.EQ.1) V(L1) = E * SFAC
            X1 = V(L1)
            Y1 = V(L3)
            IF(L1.NE.L2) X1 = V(L1) + V(L2)
            IF(L3.NE.L4) Y1 = V(L3) + V(L4)
            XMAX = AMAX1(XMAX,X1)
            YMAX = AMAX1(YMAX,Y1)
            WRITE(1,20) X1,Y1,N,IACN,D
          END IF
        END DO
20      FORMAT(2F10.3,2I5,F10.2)

99      CLOSE(UNIT=1)
        CALL PXVY(XMIN,XMAX,YMIN,YMAX,L)

        STOP
        END


        SUBROUTINE PXVY(XXMIN,XXMAX,YYMIN,YYMAX,L)
C-----------------------------------------------------------------------
C       PLOT X VERSUS Y DATA (FOR CINDY AGAIN)    ! READ FROM FOR001.DAT

        CHARACTER     XT*40,YT*40,CSG*49,FILE*40,  RSQ*4,RSQD*12
        LOGICAL       USE,PREG
        INTEGER       XTITL(10),YTITL(10),IP(3),MSG(13),KACN(50)
        REAL          X(50),Y(50), STAT(12)
        DATA          IP/4,2,3/

1       FORMAT(Q,A)
2       WRITE(*,*)'ENTER X-LABEL (40 CHRS MAX)'
        READ(*,1) NC,XT
        NC = NC + 1
        XT(NC:NC) = '$'
        ENCODE(NC,'(A)',XTITL) XT(1:NC)

        WRITE(*,*)'ENTER Y-LABEL (40 CHRS MAX)'
        READ(*,1) NC,YT
        NC = NC + 1
        YT(NC:NC) = '$'
        ENCODE(NC,'(A)',YTITL) YT(1:NC)

3       WRITE(*,*) 'XMIN,XMAX =',XXMIN,XXMAX
        WRITE(*,*) 'YMIN,YMAX =',YYMIN,YYMAX
        WRITE(*,*) ' '
        IF(L.EQ.3) THEN
          WRITE(*,*)'ENTER XMIN,XMAX AND YMIN,YMAX FOR AXES'
          READ(*,*) XMIN,XMAX,YMIN,YMAX
        ELSE
          XMIN = 0.0
          YMIN = 0.0
          WRITE(*,*)'ENTER XMAX,YMAX FOR AXES'
          READ(*,*) XMAX,YMAX
```

```
      WRITE(*,*)'ENTER THE XINC,YINC  INCREMENTS'
        READ(*,*) XINC,YINC

        IPD = 1
4       CONTINUE
        IF(IPD.EQ.1) THEN
          CALL COMPRS
          CALL NOBRDR
          WRITE(*,*)'ENTER POPFIL NAME <POPFIL.DAT>'
          READ(*,'(A)') FILE
          IF(FILE.EQ.' ') FILE = 'POPFIL.DAT'
          OPEN(UNIT=2,NAME=FILE,STATUS='NEW',FORM='UNFORMATTED')
          CALL SETCPR(2,0,0,0)
        END IF
        IF(IPD.EQ.2) CALL TEKALL(4014,960,2,0,0)

        CALL SETDEV(99,99)
        CALL PHYSOR(2.2,2.7)
        CALL PAGE(8.5,11.)
        CALL AREA2D(5.25,5.25)
        CALL COMPLX

        CSG( 1:40) = '(size of dot relates proximity to Nation'
        CSG(41:41) = CHAR(39)
        CSG(42:49) = 's Draw)$'
        ENCODE(52,'(A)',MSG) CSG
        CALL HEIGHT(0.06)
        XLEN = XMESS(MSG,100)
        XP = 0.5*(5.25-XLEN)
        YP = -.85
C       CALL MESSAG(MSG,100,XP,YP)
        CALL RESET('HEIGHT')

        CALL INTAXS
        CALL XNAME(XTITL,100)
        CALL YNAME(YTITL,100)
        CALL GRAF(XMIN,XINC,XMAX, YMIN,YINC,YMAX)
        CALL THKFRM(0.015)
        CALL FRAME
        CALL GRACE(0.0)

        CALL IPRMPT('PLOT THE REGRESSION LINE <NO> ? ','N',PREG,1,IER)
        IF(PREG) CALL IPRMPT('ENTER ACCESSION NUMBERS TO IGNORE > ',
        1                    KACN,0,NPTS,0,IER)

        REWIND 1
        DO WHILE(.TRUE.)
C         READ COORDINATES (X,Y), SECTOR NUMBER (N), ACCESSION NO, DISTANCE (D)
          READ(1,*,END=99) XX,YY,N,IACN,D
          USE = .TRUE.          ! USE OR EXCLUDE FROM REGRESSION ANALYSIS
          DO 16 I=1,NPTS
16        IF(IACN.EQ.KACN(I)) USE = .FALSE.
          IF(USE) THEN
            NP = NP + 1
            X(NP) = XX
            Y(NP) = YY
          END IF
          IF(PREG .AND. (.NOT.USE)) WRITE(*,17) IACN,'  NOT USED'
17        FORMAT(' ACCESSION NUMBER',I5,A)
          SF = D + 0.5
          IMARK = 15
          CALL SCLPIC(SF)
          CALL MARKER(IMARK)
          CALL CURVE(XX,YY,1,-1)
          IF(.NOT.USE) THEN
            CALL SCLPIC(5.0)
            CALL MARKER(4)
            CALL CURVE(XX,YY,1,-1)
          END IF
        END DO
```

```
 99    IF(PREG) THEN
          CALL LINREG(X,Y,NP,A,B,R2)
          WRITE(*,199) R2,A,B
199       FORMAT(' COEFFICIENT OF DETERMINATION (R**2) = ',F6.4,
     1       /' COEFFICIENTS OF REGRESSION LINE A,B = ',2F10.4)
          X(1) = XMIN
          Y(1) = A + B*X(1)
          X(2) = XMAX
          Y(2) = A + B*X(2)
          CALL THKCRV(0.018)
          CALL CURVE(X,Y,2,0)
          CALL RESET('MIXALF')
          CALL COMPLX
          WRITE(RSQ,19) R2
19        FORMAT(F4.2)
          RSQD = 'R**2 = ' // RSQ // '$'
        END IF

        CALL ENDPL(0)
        CALL DONEPL

        IF(IPD.NE.1) THEN
          WRITE(*,*)'(1) - MAKE A DISK FILE <POPFIL.DAT>'
          WRITE(*,*)'(2) - START AT "ENTER XMIN,XMAX ..."'
          WRITE(*,*)'(3) - START AT "ENTER X-LABEL ..."'
          READ (*,*) IPD
          IF(IPD.EQ.1) GO TO 4
          IF(IPD.EQ.2) GO TO 3
          IF(IPD.EQ.3) GO TO 2
        END IF

        END



        SUBROUTINE LINREG(X,Y,N,A,B,R2)
C-------------------------------------------------------------------------
C       LINEAR REGRESSION: Y = Y(X) AT N POINTS
C       COEFFICIENTS OF REGRESSION LINE A,B RETURNED WHERE Y = A + B*X
C       COEFFICIENT OF DETERMINATION (R**2) ALSO RETURNED

        REAL   X(N), Y(N)


        SUMX = 0.0
        SUMY = 0.0
        SMX2 = 0.0
        SMY2 = 0.0
        SMXY = 0.0

        DO K=1,N
          SUMX = SUMX + X(K)
          SUMY = SUMY + Y(K)
          SMX2 = SMX2 + X(K)*X(K)
          SMY2 = SMY2 + Y(K)*Y(K)
          SMXY = SMXY + X(K)*Y(K)
        END DO

        XBAR = SUMX/FLOAT(N)
        YBAR = SUMY/FLOAT(N)
        YBSQ = YBAR*YBAR

        B = (SMXY-N*XBAR*YBAR)/(SMX2-N*XBAR*XBAR)
        A = YBAR - B*XBAR

        R2 = (A*SUMY + B*SMXY - N*YBSQ) / (SMY2-N*YBSQ)

        RETURN
        END
```

This thesis is accepted on behalf of the faculty of the Institute by the following committee:

John K. MacWilliam

Advisor

Fred M. Phillips

W. J. Stone

December 17, 1987

Date